August 2020

Optogenetic Interrogation of Hippocampal Circuit Stabilization

Laurel Watkins de Jong
University of Wisconsin-Milwaukee

Optogenetic Interrogation of Hippocampal Circuit Stabilization

by

Laurel Watkins de Jong

A Dissertation Submitted in

Partial Fulfillment of the

Requirements for the Degree of

Doctor of Philosophy

in Psychology

at

The University of Wisconsin-Milwaukee

August 2020

Abstract

Optogenetic Interrogation of Hippocampal Circuit Stabilization

by

Laurel Watkins de Jong

The University of Wisconsin-Milwaukee, 2020
Under the Supervision of Dr. Kamran Diba

Understanding the response of excitatory and inhibitory populations to varying input is vital to understanding how a brain region transforms information. Optogenetics - the combined use of optics and genetics to control the activity of proteins, provides neuroscientists with a tool to interrogate neuronal circuits with high spatio-temporal resolution and targeted cell specificity. This thesis examines the effects of optogenetic manipulations on hippocampal circuit responses. The hippocampus is a structure required for the formation and retention of episodic memories and is comprised of anatomically distinct subregions including cornu ammonis 3 (CA3) and cornu ammonis 1 (CA1). Both regions, despite differences in local circuitry, contain excitatory cells that fire in a spatially selective manner as an animal explores an environment. Based on these differences in circuitry, studies have proposed different computational roles of each region. In order to gain insight into how distinct hippocampal networks respond to light-induced external drive we measured the responses of neurons in CA1 and CA3 to optogenetic perturbation.

To date, no work has explored the differences in CA3 and CA1 network responses to acute optogenetic manipulation of the circuits. This thesis uses a combined approach of optogenetic perturbation with simultaneous high-density electrophysiological recordings to answer two fundamental questions related to the computational roles of region CA3 and CA1. The first question asks, what role does region CA3 play in shaping spiking activity in downstream CA1? To address this question, electrophysiological recordings of CA1 were combined with optogenetic silencing of CA3 using the light-driven proton pump ArchT in both freely moving and urethane-anesthetized rodents. Since the major projection from CA3 to CA1 is excitatory, our initial hypothesis predicted an overall decrease in CA1 activity due

to the expected decrease in excitatory drive from CA3. Surprisingly, suppression of CA3 resulted in a robust and consistent increase in interneuron firing in CA1 (awake: 68% increase, 10% decrease, 22% no response n = 87, anesthetized: 59% increase, 26% decrease, 15% no response, n = 96). The second question asks, how do excitatory and inhibitory populations in CA3 and CA1 differentially respond to incoming signals? To address this question, integrated opto-electrode devices were used to simultaneously manipulate and measure the responses of CA3 and CA1 circuits to perturbations. We found that focal suppression of CA3 driven by both ArchT and the light-driven chloride channel stGtACR2 resulted in a paradoxical increase in firing of both inhibitory and excitatory cell at all distances from the site of photoinhibition. In contrast, CA1 cells responded to focal photoinhibition by showing nearly 100% decrease in cell response at the site of illumination. Paradoxical increases in firing in response to external inhibitory input to interneurons can be a feature of networks with highly-recurrent excitatory connections that are unstable in the absence of inhibition (ISNs: inhibitory-stabilized networks. Broad (600 μm diameter) photoinhibition was applied and network responses were measured over a range of laser intensities to test whether differences in responses between CA3 and CA1 can be attributed to CA3 operating in an ISN-regime. Paradoxical increases in pyramidal cell or interneuron firing were not observed when inhibitory opsins were expressed in both pyramidal cells and interneurons. When external input was restricted to interneurons, CA1, and to a smaller extent, CA3 showed increased firing in response to varying intensities of photoinhibition, suggesting both CA1 and CA3 operate as ISNs. Taken together, these results indicate that perturbations of neuronal activity can produce paradoxical effects that affect both local and connected regions. The emerging patterns depend on the detailed interactions between excitatory and inhibitory subpopulations within a region, and can be broadly explained by network models of global stabilization through inhibition. Our results further highlight the need for simultaneous monitoring of cellular responses when using optogenetics or other manipulations that alter neuronal activities.

To my parents -

My mother, whose curiosity of our self and interaction with the world first inspired me to explore the field of Neuroscience.

My father, whose passion for Mathematics extends to all applications from Sculpture to Neuroscience to Genetics. Our collaborations throughout my dissertation are some of my most cherished memories.

TABLE OF CONTENTS

LIST OF FIGURES

Acknowledgements

I would like to thank everyone who has helped me along this journey. First and foremost I would like to thank my advisor, Dr. Kamran Diba. I am honored to have been your first graduate student. Our research project(s) challenged me and pushed me to think of systems neuroscience in ways that were at times uncomfortable but in the end immeasurably rewarding. (Being given the opportunity to travel to 4 continents certainly didn't hurt). Working with you has shaped the scientist I am today.

Thank you to my lab mates both past and present. A very special thank you to Dr. David Lyttle a.k.a. "Mr. Walkway, Mr. Walk-down-me I'm the walkway". There is no one else that could have brought as much laughter to troubleshooting acute recordings at 12 am. Thank you also to Dr. Nat Kinsky, I'm so glad we were able to collaborate this last year but I do feel a little bad that I got you started on opto (see this entire dissertation). I would also be remiss not to thank you for all of your *very early morning* comments and suggestions on this dissertation. To the other grad students, Kourosh Maboudi and Bapun Giri, this journey (both figuratively and literally moving our lab) has been much more enjoyable with the two of you. Finally, thank you to my undergraduate students, Yunchang Zhang and Atissa Rostami. Whenever my own inspiration was lacking, your enthusiasm and fresh perspective re-energized me.

Thank you to all of my friends. Thank you to my NSF GRFP crew: Sarah MacNamee and Clayton Mosher. Sarah, your fierceness and determination are contagious. Whenever I felt discouraged, you were there to snap me out of it. Clayton, your silliness and unconventional perspective on neuroscience always reminded me, even in the hardest of times, that this is supposed to be fun. Thank you to Ursula Basinger, Christine Bootes, and Deborah Hur. You are all some of the strongest, most creative, and all around wonderful women I know. I am grateful for the support each of you have given me throughout the years. Last but absolutely not least, thank you to Skye Robins. You are my person. I could write so much more, but I think that about summarizes it.

Thank you to my family. Thank you to my sister, Emily, for many things but mostly for enabling my unwieldy plant collection and then helping me transport it across the country. Thank you to my mom, Jean for your unconditional emotional support. Thank you to my dad, Joe. I'm not sure I could have finished this without you. Your help and encouragement are reflected in the pages of this thesis.

1 Introduction

Understanding how neural circuits operate locally and interact globally can provide critical insights into how our brain processes incoming information and guides behavior. Neural activity is organized in both spatial and temporal domains. Spatial organization of neural ensembles separates regions based on their computational function. This is most commonly attributed to the neocortex, which has regions dedicated to the processing of specific sensory modalities. Temporal organization coordinates spiking activity at multiple timescales, forming patterned relationships between spiking output that can be translated by downstream structures. The first step in understanding the function of regional circuits is to learn the architectural features of the network. Connectivity patterns between inhibitory and excitatory neurons in a network guide the flow of information from afferent locations and transform those input patterns into output patterns received by downstream targets. Interpreting the rules governing those interactions locally and between neuronal systems can help tackle the extreme complexity of brain wiring leading to a more unifying theory of neural function.

Network activity patterns are difficult to study by recording single cells in isolation or even by measuring the activity of populations of neurons, especially when our interaction with the circuit is only observational. One approach is to simultaneously record and perturb activity of neural populations, which can be achieved through optogenetics - the use of light to control neurons genetically modified to express light-sensitive ion channels. Expression of light-sensitive ion channels can be localized to specific regions and to specific classes of cells within a specific region, allowing for rapid and reversible manipulation of neuronal populations with high spatial and temporal resolution. Optogenetic tools can thus provide neuroscientists with a means to causally test relationships between circuit elements and observed population activity patterns.

The hippocampus, a structure required for episodic memory, is comprised of anatomically distinct subregions. Each region differs in terms on inputs and local circuitry. Subregions CA1 and CA3, despite notable differences in local circuitry, contain excitatory cells that

fire in a spatially selective manner as an animal explores an environment(O'Keefe, 1976). Region CA3 forms highly recurrent excitatory connections. In contrast, excitatory cells in CA1 are not extensively interconnected (Amaral and Witter, 1989). Based on differences in excitatory connectivity, studies have proposed different computational roles for each region (Treves and Rolls, 1994; Lee et al., 2004; Leutgeb et al., 2004). A deeper understanding of the differential processing between regions can be achieved by measuring network responses to targeted manipulations of each circuit.

The introduction can be broken up into five sections. Section 1.1 discusses optogenetics as a method for examining neural circuits. Decisions related to the selection of opsin, light delivery method and cell-specific targeting approach all need to be considered when designing an experiment and can impact the interpretation of results. Confounding effects stemming from each of these parameters will be discussed in this section. Section 1.2 introduces hippocampal circuitry and provides a synopsis of the anatomy and functional properties of structures (CA3 and the entorhinal cortex) that give rise to activity patterns in hippocampal region CA1. Section 1.3 discusses activity patterns in CA1 and how coordination of spiking activity can support memory encoding. Additionally, Section 1.3.1 explores how input from upstream regions CA3 and entorhinal cortex shape activity patterns in CA1. In addition to external input, interneurons play a vital role in modulating the gain and timing of firing with respect to ongoing oscillatory events. Section 1.4 focuses on the contribution of interneurons class (Section 1.4.1) and excitatory-inhibitory circuits (Section 1.4.2) in regulating incoming signal and temporally coordinating CA1 activity (Section 1.4.3). Local changes in activity can result in unexpected network responses as the system rebalances. Section 1.5 focuses on understanding the response of excitatory and inhibitory populations to perturbations driven by incoming signals.

The goal of this introduction is twofold. The first is to understand how optogenetics is used to interrogate neural circuits. The second is to provide a detailed description of the activity patterns within hippocampal area CA1 and how activity within the region is shaped

as a function of input, local excitatory-inhibitory interactions and perturbations in global excitatory-inhibitory balance. Understanding both elements is critical to the interpretation of results presented in Chapter 3. Experiments in this chapter use optogenetic manipulations to dissect circuits in hippocampal regions CA1 and CA3.

1.1 Optogenetic interrogation of neuronal circuits

In the broadest sense, optogenetics refers to the combined use of optics and genetics to control the activity of proteins resulting in optical control of genetically modified cells. Optogenetics provides neuroscientists with a tool to interrogate neuronal circuits with high spatio-temporal resolution and targeted cell specificity. First applied in the mammalian brain in 2005, optogenetic technology uses light to modulate neuronal function by way of light sensitive proteins engineered from naturally occurring forms (Boyden et al., 2005). Prior to the development of optogenetic tools, the most common means to interrogate neuronal circuits were through either electrical stimulation or pharmacological manipulation. Electrical stimulation provides temporal and spatial specificity but cannot be used to silence neurons or target specific cell types (Butovas and Schwarz, 2003). On the other hand, pharamcogenetic manipulations provide targeted spatial and cell specificity but lack a well-defined temporal window (Dong et al., 2010). However, optogenetics is not without its own constraints on experimental design. Three things need to be considered when designing and interpreting results of optogenetic experiments, 1) type of opsin, 2) light delivery method and 3) genetic targeting approach.

The most common class of proteins used in optogenetic experiments are rhodopsins which include light-gated ion channels and pumps (Govorunova et al., 2017). Rhodopsins can be used to elicit excitation and inhibit neurons. Channelrhodopsin (ChR), a light-gated cation channel optimally activated by blue wavelength light (460 nm peak absorption) is the most commonly used excitatory opsin (Boyden et al., 2005). Excitation through ChR results in a pronounced increase in firing upon stimulation which decays with time. In order to

maintain excitation with ChR, pulses of light are often administered which can result in non-physiological synchronization of cell populations. In order to overcome this limitation, mutant variants, such as oCHIEF, have been developed with modified kinetic properties which induce action potential trains that more closely resemble natural spiking patterns (Lin et al., 2009).

Halorhodopsin (eNpHR), an light-driven chloride pump (570 nm peak absorption), and archaerhodopsin (ARCH), an outward directed proton pump (532 nm peak absorption) both inhibit spiking through hyperpolarization (Gradinaru et al., 2008; Chow et al., 2010) The pump mechanics of these inhibitors can cause non-physiological intracellular ion concentrations. Prolonged illumination of eNpHR expressing cells leads to the intracellular accumulation of chloride (Cl^-) which changes the $GABA_A$ receptor reversal potential. Therefore, silencing with eNpHR can result in synchronized neuronal excitation as neurons are released from light-induced inactivation (Raimondo et al., 2012). Illumination of ARCH expressing cells is shown to increase intracellular pH levels, which can induce Ca^{2+} influx. Rather than targeting the cell body, several studies manipulate cell activity by targeting opsins expressed in the axon terminal. Targeting the synaptic terminals of ARCH expressing cells can elicit spontaneous vesicle release in presynaptic terminals resulting in light-induced excitation rather than inhibition (Mahn et al., 2016). Naturally occurring anion-conducting rhodopsins (ACRs), in particular chloride-conducting ChR (GtACR1 and GtACR2) were developed as an alternative to proton-pumping rhodopsins (Wietek et al., 2015; Govorunova et al., 2015), though these are not without their own faults. Since Cl- concentrations are particularly high in synaptic compartments, axonal activation of GtACR variants can still result in somatic depolarization (Malyshev et al., 2017). To address this concern, recent variants of GtACR localize expression of the light-gated ion channel to the soma and proximal dendrites (stGtACR2) (Mahn et al., 2016). Taken together, there are two important considerations when choosing an opsin: 1) the kinetics of a given opsin can require stimulation patterns that artificially entrain populations of cells and 2) the location of illumination can result in

excitation rather than inhibition, further complicating the interpretation of the data.

Light is generated by way of fiber-coupled lasers or light emitting diodes (LEDs) allowing for experimental control of wavelength, intensity and temporal pattern of illumination. Considerations need to be made when deciding on these parameters. In brain tissue, light from the fiber source is both scattered and absorbed to varying degrees depending on the wavelength and brain region; the end result being that shorter wavelength light penetrates more deeply into the brain, allowing for more extensive perturbations (Stujenske et al., 2015). Light delivery can also result in significant heating of brain tissue. Increased light intensity and longer wavelengths, both properties of most inhibitory opsins, produce the most heat (Stujenske et al., 2015). Continuous illumination at powers commonly used for optogenetic experiments (10-15 mW) can increase brain tissue temperature by 1-4°C, which is sufficient to induce physiological and behavioral changes in naive animals. Neurons throughout the brain, including in the hypothalamus, hippocampus and striatum, are sensitive to changes in temperature (Tabarean et al., 2005; Kim and Connors, 2012; Owen et al., 2019). For example, in the striatum, light induced temperature increases activated inwardly rectifying potassium conductances and biased animal behavior. In the prefrontal cortex, increased tissue temperature (>1 deg C) elicited increases in firing rates upwards of 30% (Stujenske et al., 2015). Temperature induced changes seem to vary region by region confounding the interpretation of optogenetic experiments in unpredictable ways.

Cell specificity of opsins is determined by the genetic targeting approach. Promoter based targeting is widely used since neuronal subtypes express unique genes or combinations of genes. For example, inhibitory (GABAergic) neurons uniquely express GABA-synthesizing enzymes (GAD: glutamate acid decarboxylase) allowing for the use of specific promoter sequences to target these neurons. Genetic sequences can either be introduced using a viral vector or, if the sequence is too large, expression can be obtained using a Cre driver line combined with a Cre-dependent viral vector (Dimidschstein et al., 2016). Viral vectors, such as adeno-associated virus (AAV) allow for region specific targeting in non-transgenic

animals but lack cell specificity within a target region. Non-specific neuronal promoters such as hSyn (human synapsin) and CAG (hybrid cytomegalovirus/chicken beta-actin) or cortical excitatory cell promoter CamKII (Ca^{2+} binding protein activated protein kinase) are a few of the most commonly used promoters. Recent work, however, has shown even less specificity in these promoters. hSyn promoters in combination with specific enhancers can result in expression in non-neuronal cells (Thiel et al., 1991). The CamKII promoter has been shown to drive expression in both pyramidal cells and interneurons with AAV-mediated delivery (Nathanson et al., 2009; Watakabe et al., 2015). In dorsal CA1, CamKII mediated delivery of NpHR resulted in 76% of PV+ cells and 65% of SOM+ cells expressing NpHR (Schoenenberger et al., 2016). Lack of specificity can lead to unintended network responses. In experiments by Schoenenberger et al. (2016), expression of NpHR in a subset of inhibitory cells resulted in decreased feed-forward inhibition and increased pyramidal cell firing. One method to achieve sufficient specificity is a combinatorial transgenic/viral approach. With numerous types of viral vectors and mouse/rat transgenic lines available, this approach allows for both region specific and cell type specific expression of optogenetic genes. For example targeted opsin expression in inhibitory neurons can be achieved by using a Cre-dependent viral vector in a knock-in animal expressing Cre-recombinase specifically in inhibitory cells.

Understanding how optogenetics influences network activity is accomplished through the use of integrated optogenetic control with electrophysiology which allows for simultaneous measuring of neuronal outcome to optogenetic manipulations. Most of the unexpected network responses described above were discovered using integrated devices such as optrodes (Royer et al., 2010; Stark et al., 2012) or optotetrodes (Voigts et al., 2013). Optrode recordings have the added advantage of localizing the effect of perturbation in the network while simultaneously capturing the responses of nearby, unaffected neurons. However, the bulky nature of these devices causes significant tissue damage resulting in fewer recorded neurons. Hyper-local control of spiking and fast population oscillations can be achieved with μLED probes allowing for optical manipulation of very specific neuronal circuits without cell loss

(Wu et al., 2015). Integrated devices provide an opportunity to map networks by focally perturbing specific cell classes while simultaneously recording responses in nearby cells.

1.2 Anatomy of the hippocampus

Cellular, oscillatory and coordinated spiking activity observed in region CA1 is far from isolated. Specifics of CA1 activity patterns will be explored in depth in Section 1.3, but understanding the local dynamics of CA1 requires an initial understanding of entorhinal-hippocampal circuitry. Each region within the entorhinal cortex-hippocampus circuit has unique patterns of connectivity that support different neural computations and consequently plays a different role in the overall function of the hippocampus in memory. This section provides a detailed overview of the anatomy of the entorhinal-hippocampal circuit with a special focus on the functional properties of three specific regions: the medial entorhinal cortex (MEC), hippocampal area CA3 and hippocampal area CA1. For reference, a detailed diagram of this circuit can be found in Figure 1 a/b.

The hippocampus is one of a group of structures in the limbic system. Generally, the *hippocampal formation* can be divided into three main areas: the dentate gyrus (DG), the subicular complex (SC; consisting of the subiculum, presubiculum and parasubiculum) and the *hippocampus proper*, which consists of three subfields known as the *cornu ammonis* regions CA3, CA2 and CA1 (Witter and Amaral, 2004).

The primary input to the hippocampus originates in the superficial layers of the entorhinal cortex (layer II and layer III), which receives highly processed, multimodal sensory information from several regions of the association cortex, including the parahippocampal gyrus (perirhinal and postrhinal cortices), and the parietal, inferotemporal and frontal cortices. Accordingly, the hippocampus receives highly integrated sensory information compared to other brain regions (Shepherd, 2003). The primary output of the hippocampus varies along its long-axis with the ventral pole sending efferents to frontal cortices and ventromedial entorhinal cortex and the dorsal pole projecting to parietal and retrosplenial cortex and

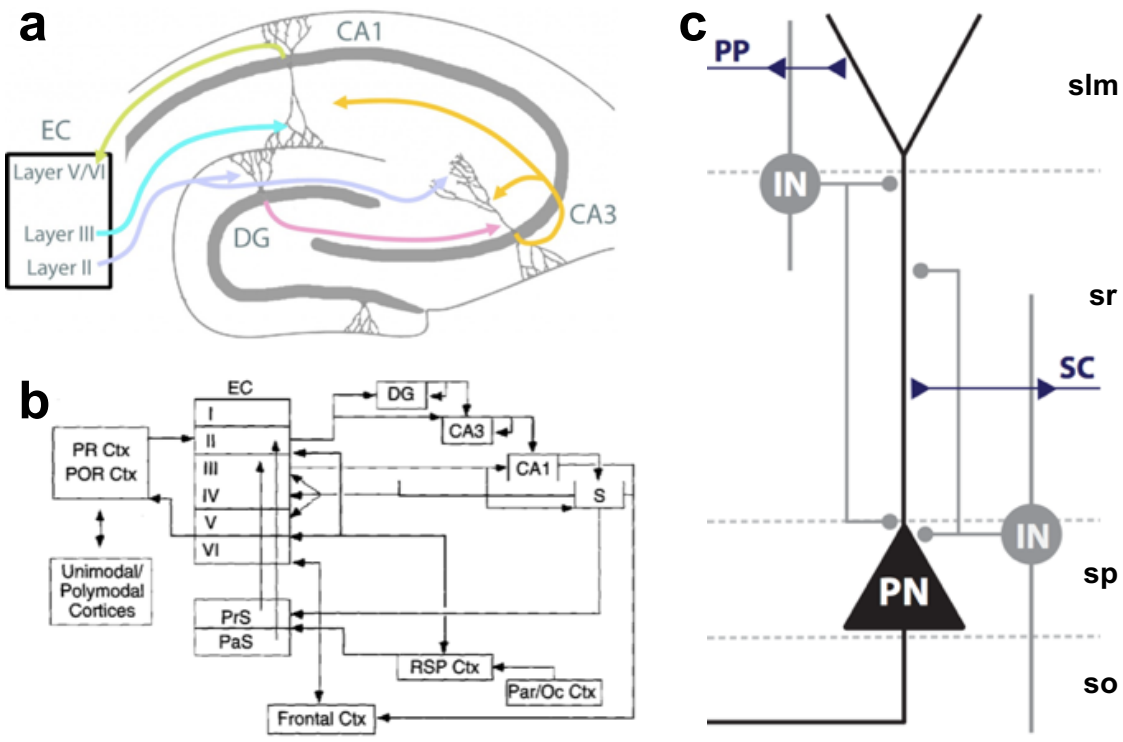

Figure 1: Hippocampal anatomy.

a) Basic neural circuitry of the hippocampal complex. b) Hippocampal circuit diagram detailing the major intrinsic connections and external cortical inputs (figure borrowed from Shepherd (2003)). c) Simplified diagram of CA1 microcircuit. This figure highlights inputs from the perforant path (PP) target distal dendrites of principal cells in the stratum lacunosum moleculare (slm) while inputs from the Schaffer collateral pathway (SC) target proximal dendrites in the primarily in the stratum radiatum (sr) (sp: stratum pyramidal, so: stratum oriens).

dorsolateral parts of the entorhinal cortex (Witter and Amaral, 2004).

The most well characterized hippocampal circuit is the *trisynaptic loop* where information advances from DG to CA3 to CA1 in an almost exclusively feedforward manner. Glutamatergic neurons from layer II of the entorhinal cortex give rise to this pathway (via the perforant pathway) and project to both the DG and region CA3. The next step in this pathway is the DG, which gives rise to granule cell axons, known as mossy fibers which terminate on CA3 pyramidal cells. CA3 cells, in turn, project to other CA3 cells and to CA1 via excitatory Schaffer collateral projections. CA1 projects to the subiculum and to deep layers of the EC

(layer V), which projects to many of the same cortical regions that originally projected to the entorhinal cortex. CA1 also receives direct input from layer III of the entorhinal cortex via the temporoammonic, or perforant pathway, (Witter et al., 1989; Amaral and Witter, 1989).

Differences in connectivity within hippocampal regions increases the complexity of information processing within the hippocampus. Studies of these differences lead to the hypothesis that microcircuits in each region may provide a substrate for parallel processing streams within the aforementioned trisynaptic circuit. Some of these microcircuits will be described in more detail below (de la Prida, 2020; Lee et al., 2020).

1.2.1 Cornu Ammonis 3

CA3 pyramidal cells (PCs) receive two parallel inputs; direct input from the entorhinal cortex and from the dentate gyrus via the trisynaptic pathway. Inputs from EC and DG to CA3 are highly organized and spatially distributed, with input from DG and EC terminating on different dendritic layers of the CA3 pyramidal cells and interneurons within those layers.

CA3 is classically divided into three subregions along the proximodistal axis: CA3a, CA3b and CA3c, with proximal CA3c lying closest to DG and distal CA3a lying closest to CA2 (Lorente de Nó, 1934). Each subegion consists of four distinct layers: 1) stratum lacunosum moleculare (SLM), 2) stratum radiatum (SR), 3) stratum pyramidale (SP) and 4) stratum oriens (SO). The SLM, while lacking in excitatory cells, contains direct input from the entorhinal cortex. The SR receives direct input from the DG via mossy fibers in addition to recurrent collateral axons from both ipsilateral and contralateral CA3. The SP, as suggested by its name, contains densely packed excitatory pyramidal cells bodies as well as a large number of paravalbumin (PV), cholecytokinin (CCK) and vasoactive intestinal polypeptide (VIP) expressing neurons. Finally the SO contains somatostatin (SOM) and oriens-lacunosum moleculare (O-LM) interneurons (Witter and Amaral, 2004). A more expansive discussion of interneuron classes can be found in Section 1.4.

CA3 PCs form two primary connections. As mentioned previously, CA3 sends axons to CA1 via Shaffer collaterals. Additionally, CA3 forms associational connections with other CA3 neurons. These recurrent projections from CA3 neurons to other CA3 neurons are a unique feature of the subregion, which led to the postulation that CA3 plays a key role in performing memory computations (Treves and Rolls, 1994). In this framework, sparse input from DG activates a population of CA3 neurons. The extensive recurrent connectivity within CA3 then acts as an *autoassociative* network to further amplify the incoming signal, allowing neuronal assemblies in CA3 to be reactivated even when presented with a degraded or partial input from DG through a process called *pattern competition* (Rolls, 2013).

CA3 was classically modeled as a homogeneous network. However, recent studies have uncovered notable differences in both the cytoarchitecture and connectivity between distal and proximal subregions suggesting CA3 is composed of at least two distinct microcircuits. Strength of input from mossy fibers degrades along the proximodistal axis and is mirrored by an increase of direct synaptic excitation by EC (Thompson et al., 2008; Sun et al., 2017). The end result being that CA3a (proximal) receives stronger input from DG while CA3c (distal) receives stronger EC inputs. Heterogeneity in synaptic connectivity likely contributes to the differences observed in both behavioral and spatial encoding properties of CA3 subregions. Electrophysiological recordings show activity in proximal CA3 behaves similarly to DG in response to mismatch inputs while distal CA3 maintains coherent representations in conflict situations, closely resembling a classic attractor network system (Lee et al., 2015; Lu et al., 2015). Lesion and immediate-early gene studies show spatial information is preferentially processed by distal CA3 (Hunsaker et al., 2008; Nakamura et al., 2013; Beer et al., 2018). Together these studies suggest that proximal CA3 likely works as a functional unit with DG while distal CA3 functions as an autoassociative network.

1.2.2 Entorhinal Cortex

The focus of this thesis is on local hippocampal circuits and the relative contribution of region CA3 to activity patterns in CA1. In the absence of CA3 drive, the primary input to CA1 is the entorhinal cortex (EC). In order to understand the contribution of CA3 to CA1 activity, it is also necessary to consider the influence of EC input. The entorhinal cortex (EC) is the major input and output structure of the hippocampal formation. Functionally the EC can be divided into two components, the medial EC (MEC) and lateral EC (LEC). The MEC receives afferents from the presubiculum, parasubiculum, retrosplenial cortex and postrhinal cortex, all of which are involved in processing spatial information. In contrast, the LEC receives input from olfactory areas, insular cortex, medial-and orbitofronal areas and the perirhinal cortex. These areas are thought to be involved in processing sensory information relevant to encoding episodic memories such as object information, attention and motivation. Within CA1, input from EC varies along the transverse axis with direct inputs from MEC concentrated in the proximal portion of CA1 (adjacent to CA2) and inputs from LEC terminating on dendrites in the distal portion of CA1 (closer to the subiculum) (Witter et al., 2017).

Cells in MEC are predominantly spatially modulated. Due to the spatial modulation of cells in both the MEC and hippocampus, significantly more focus has been spent studying the MEC and its subsequent role as a primary input to multiple hippocampal regions. MEC layer II provides direct excitatory input to DG and CA3, while MEC layer III provides direct input to layer SLM of CA1. Recently studies have also found clusters of MEC layer II neurons, *island cells*, that project directly to CA1, which highlights the complexity of various entorhinal-hippocampal circuits and their respective roles in shaping activity within CA1 .

Functionally, MEC is defined by its large population of spatially modulated cells, most notable of which is the grid cell. Discovered in 2004, grid cells fire in a two-dimensional hexagonal pattern in an open field environment (Fyhn et al., 2004). Additionally, grid cells

in deep layers of the MEC integrate information related to the animal's head orientation and movement speed (Sargolini et al., 2006). Theoretical studies supported by recent experimental findings have demonstrated that the MEC network is the core of a path integration system, which allows an animal to track progress through space in the absence of visual information and support spatial firing in downstream hippocampal regions (McNaughton et al., 2006; Gil et al., 2018). Additionally, lesions to the entire MEC result in less stable spatial representations in the hippocampus (Schlesiger et al., 2018). More targeted disruption of MEC layer III projections to CA1 results in a degradation of spatial information in CA1, but not CA3 which receives input from MEC layer II, suggesting multiple inputs from MEC support spatial representations in the hippocampus (Brun et al., 2008).

1.2.3 Cornu Ammonis 1

CA1 is the most widely studied hippocampal region since it is the primary output structure of the hippocampus - sending processed information out to other brain structures. CA1 is positioned between CA3 and the subiculum and has a radial organization nearly identical to CA3. CA1 pyramidal neurons receive signals from CA3 Schaffer collaterals projecting to proximal dendrites in SR and from layer III of the EC via the temporoammonic pathway terminating on distal dendrites located in the SLM.

Like CA3, inputs to CA1 are heterogenous along the transverse axis. Presynaptic axons from MEC predominantly target dendrites in the SLM of proximal CA1 (adjacent to CA2) while distal CA1 (adjacent to subiculum) primarily receives input from LEC (Igarashi et al., 2014; Masurkar et al., 2017). Additionally, recent studies provide evidence for radial deep-superficial organization in the CA1 pyramidal layer, where neurons located more superficially in SP receive input from CA3 and deep neurons receive input from ECIII (Fernández-Ruiz et al., 2017). In addition to input from EC and CA3 being spatially separated, evidence shows inputs are temporally segregated during various oscillations. The function of temporal segregation of input will be further discussed in Section 1.3.1.

1.3 Activity patterns in CA1

The notion that the hippocampal formation plays a role in spatial representation began with the discovery of the place cell (O'Keefe and Dostrovsky, 1971). Excitatory pyramidal cells, *place cells*, recorded from area CA1 fire at specific locations in the environment *place fields*. Place fields pattern space such that the entire environment is represented in the activity of the local cell population: this configuration of place cells is commonly referred to as a place field map (O'Keefe and Nadel, 1978). Given enough place cells, an animal's trajectory in an environment can easily be decoded from the activity of a population of place cells (Zhang et al., 1998). Studies have shown that although the same cells participate in different environments, every environment is represented by an independent subset of place cells (Bostock et al., 1991; Kubie and Muller, 1991). Each representation is unique and stable, even across sessions separated by months (Muller and Kubie, 1987; Thompson and Best, 1989), suggesting that these representations are stored rather than randomly generated with each subsequent exposure. Learning new environments does not destabilize representations of previously learned spaces, such that, if you return an animal to a previously learned environment the place code for that environment is the same (Wilson and McNaughton, 1993). Hippocampal place cells thus vary their firing rate based on an animal's position, which is commonly referred to as *rate coding* (O'Keefe, 1976; Huxter et al., 2003). The hippocampus is therefore capable of storing multiple representations without interference.

In addition to forming representations of the environment using rate coding, hippocampal networks can display sequences of neuronal activation at various temporal resolutions. The sequential organization of activity is thought to underlie numerous fundamental operations of the hippocampus. At the behavioral time scale, animals traverse place fields during active exploration (Figure 2a). The trajectory of the animal determines the sequence of activation of place specific cells. Remarkably, this sequence of activation is preserved on two compressed timescales (theta sequences and replay). A proposed mechanism of both theta sequences and replay is to facilitate encoding of information through spike-timing dependent

plasticity mechanisms (Mehta, 2015). This sequential organization of firing activity is commonly referred to as *temporal coding* (O'Keefe and Recce, 1993; Skaggs et al., 1996; Jensen and Lisman, 2000; Harris et al., 2003; Dragoi and Buzsáki, 2006).

Theta sequences refer to the compressed, ordered spiking activity that accompanies theta oscillations, a prominent feature of the hippocampal local field potential. Theta oscillations (4-12 Hz) emerge when the animal is actively exploring the environment and during REM sleep (Vanderwolf, 1969; Buzsáki et al., 1983). During active exploration, a unique correlation emerges between place cells and the ongoing rhythm. A given place cell fires towards the peak of theta cycle when an animal enters that cell's place field. As the animal moves through the place field the cell fires at earlier phases of the cycle (O'Keefe and Recce, 1993; Skaggs et al., 1996)). The relationship between the firing of the place cell and phase of the ongoing oscillation was termed *theta phase precession* (Figure 2a, lower inset). Incorporating information about the phase of spiking improves decoding of the animal's position (Jensen and Lisman, 2000; Harris et al., 2003). One prediction of phase precession is that the hippocampus is not representing the animal's position at each point in time, but rather a short trajectory during each theta cycle that begins slightly behind the animal and ends slightly ahead of the animal (Foster and Wilson, 2007). As an animal moves through space, the order of place cells activated during a single theta cycle reflects the local trajectory of the animal. However, theta sequences are not simply an emergent property of hippocampal phase precession. Within a theta cycle, temporal coordination between pairs of neurons is stronger than predicted by independent phase precession, suggesting a role for synaptic plasticity in the emergence of theta sequences (Dragoi and Buzsáki, 2006) (Figure 2b). In support of this hypothesis, Feng et al. (2015) show that in a novel environment, theta sequences, but not phase precession were absent during initial exploration but emerged quickly after and remained stable once established.

A second type of compressed, ordered spiking activity occurs during quiet wakefulness and slow wave sleep. Bursts of spiking activity known as *population bursts* are accompanied by

large amplitude negative polarity deflections (40-100 ms) in the CA1 stratum radiatum and coincide with a high frequency (140-220 Hz) oscillation in the CA1 pyramidal layer known as a sharp wave ripple complex (SWR) (Suzuki and Smith, 1988). SWRs propagate throughout the entorhinal-hippocampal output pathway synchronizing neuronal networks that connect the hippocampus to the neocortex (Chrobak and Buzsáki, 1996; Ólafsdóttir et al., 2016). As first observed by Wilson and McNaughton (1994), pairs of neurons that fire together during behavior preferentially reactivate during SWR events in slow wave sleep. Subsequent discoveries revealed that not only did these cells coactivate, the order of activation reflected the firing order observed during behavior. The ordered reactivation events are termed *replay*.

Replay events occur in both forward and reverse direction to the trajectory of the animal. During sleep, reverse replay events dominate (Foster and Wilson, 2006), however during quiet waking both forward and reverse replay events are observed (Diba and Buzsáki, 2007). Forward replay events occur just prior to an animal's movement and reflect the future trajectory of the animal while reverse replay events replay the animal's last experience (Figure 2a, left and right panels). Awake replay is not restricted to beginning at the animal's position on the maze and can reflect never experienced novel path sequences (Gupta et al., 2010). Some recent experiments have suggested SWR driven sequences exist prior to experience and provide a structure on which later experiences are imprinted (Dragoi and Tonegawa, 2011, 2013), while other research has supported the notion that these sequences are experience-dependent (Feng et al., 2015). Whether these sequences reflect preconfigured internally-generated dynamics, unique patterns driven by recent experience or some combination of the two (Grosmark and Buzsáki, 2016) is still up for debate, however all evidence supports the notion that the hippocampal area CA1 encodes episodes as ordinal structures.

1.3.1 Role of CA3 and MEC in shaping CA1 activity

As described in the previous subsection, activity in CA1 can accurately represent space through both a place cell rate code and a temporal code. Since MEC and CA3 comprise the

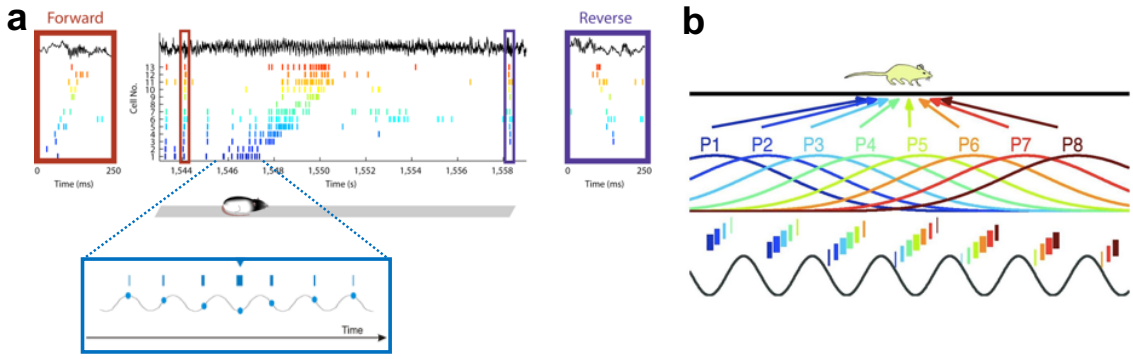

Figure 2: CA1 activity patterns.

a) The top panel describes hippocampal activity patterns as a rat runs along a linear track. The black trace is the raw local field potential. Note the state transitions in the LFP clearly changes to a persistent theta oscillation as the rat starts begins to move. Below the trace, cells recorded simultaneously from a silicon probe are shown ordered by their place cell location on the track. The red and blue insets to the left and right are magnified to show firing activity during detected sharp wave ripple (SWR) events. Notice the preserved order between the place-cell sequence and ripple sequence. Sequences during ripples (replay) can occur in a forward or reverse direction. The inset below is a cartoon illustration describing phase precession. As the animal enters the place field the cell fires at the peak of the ongoing theta oscillation, as the animal moves through the field, the cell fires earlier in the theta cycle (borrowed from Diba and Buzsáki (2007)). b) Cartoon describing theta sequences. As the animal traverses through hypothetical place fields P1-P8, each place field precesses in time, maintaining a temporal ordered relationship within each cycle so that the first cell firing within a given cycle represents the first place field traversed by the animal (borrowed from Buzsáki (2010)).

primary inputs to CA1, it is important to understand how each input contributes to the firing patterns observed in CA1. Many studies have attempted to disentangle the contribution of internally generated CA3 input from extrinsic EC input in the expression of place cell responses though no clear consensus has been reached.

MEC and CA3 both provide positional information to CA1 circuitry; MEC in the form of grid cells and CA3 in the form of place cells. Physical, pharmacological and genetic methods depriving CA1 of input from either CA3 or MEC fail to abolish CA1 place cell activity in familiar environments. Following MEC lesioning, a reduction in the percentage of active place cells as well as spatial information content and stability of place cells was observed (Schlesiger et al., 2018) while lesions of the entire EC reduce CA1 place field firing and induce global remapping in familiar environments (Brun et al., 2008; Van Cauter et al., 2008; Hales et al., 2014). In line with these findings, transient silencing of MEC results in non-reversible global

remapping in a subset of CA1 place cells (Miao et al., 2015; Rueckemann et al., 2016). CA3 lesions and genetic manipulations to block Schaffer collateral transmission do not change the field properties of CA1 pyramidal cells (Nakazawa et al., 2002, 2003; Nakashiba et al., 2008; Middleton and McHugh, 2016). These findings are in conflict with recent studies by Davoudi and Foster (2019) which show abolishment of CA1 place cells under reversible optogenetic silencing of CA3. One explanation for incongruous results is a difference in inactivation techniques. Chronic inactivation methods like lesions and genetic manipulations could allow for a variety of compensatory mechanisms to develop and rescue hippocampal function. Another explanation for incongruous results is a difference in experimental design. A recent study by Sharif et al. (2020) found place cells located in deep SP are more active in cue-rich environments and are driven by EC inputs while place cells in superficial SP are more active in cue-poor environments and are driven by intra-hippocampal inputs. Removal of EC or CA3 input to CA1 pyramidal cells may have varying consequences depending on task demands.

Input from EC and CA3 to CA1 is temporally segregated. During active exploration precise spike timing is organized by theta and gamma oscillations. The amplitude of hippocampal gamma oscillations (30-120Hz) is the greatest when they are nested within slower theta oscillations and can function as a synchronization mechanism between EC/CA1 or CA3/CA1 (Colgin et al., 2009). CA3 and EC inputs to CA1 preferentially occur at different theta phases and are associated with distinct but overlapping layer-specific frequencies of CA1 gamma oscillations. Slow gamma (gamma_{S}: 30-80 Hz) is localized in the SR and reflects input from CA3 while mid-frequency gamma (gamma_{M}: 60-120 Hz) is localized in the SLM and reflects input from EC (Colgin et al., 2009; Schomburg et al., 2014). A third frequency, originally classified as fast gamma ($\text{gamma}_{\text{F}} > 100$ Hz) is thought to reflect spiking output of the CA1 pyramidal cell populations (Belluscio et al., 2012; Schomburg et al., 2014). Gamma_{S} emerges during the descending phase of CA1 theta oscillations and corresponds to peak firing of CA3 neurons while gamma_{M} occurs at the peak of theta and corresponds to

maximal firing of EC neurons (Mizuseki et al., 2009; Schomburg et al., 2014). Timing of CA1 spiking is in turn tuned by the relative strength of input from CA3 and EC, reflected by both gamma power and spike-gamma coupling (Fernández-Ruiz et al., 2017). During active exploration, place cell activity is initiated by EC input at the peak of theta and is associated with gamma_{M} bursts in the SLM. As the animal moves across the field, EC drive decreases and activity is driven predominantly by CA3, reflected by increased gamma_{S} power in the SR (Fernández-Ruiz et al., 2017). Together these data suggest gamma oscillations provide a mechanism to temporally organize neural activity especially in conjunction with theta oscillations.

While temporal segregation of EC/CA3 inputs to CA1 is well established, the influence of these inputs in organizing spike timing in CA1 is less understood. Lesions of both MEC and CA3 seem to disrupt temporal organization of CA1 firing patterns during theta oscillations. MEC lesions result in disruption of CA1 theta phase precession but also lead to place field instability while pharmacogenetic lesions and optogenetic silencing of Schaffer collaterals (SCs) preserve CA1 phase precession (Schlesiger et al., 2015; Middleton and McHugh, 2016; Davoudi and Foster, 2019). Furthermore, pharmacogenetic lesions of SCs abolish temporal coding at the ensemble level, suggesting a dissociation between temporal coding at single cell and population levels (Middleton and McHugh, 2016). MEC and CA3 also appear to play different roles in the generation of CA1 replay. Pharmaco- and opto-genetic silencing of SCs abolishes high frequency ripples and ripple associated reactivation in CA1 suggesting replay content is driven primarily by input from CA3 (Nakashiba et al., 2009; Middleton and McHugh, 2016; Yamamoto and Tonegawa, 2017; Davoudi and Foster, 2019). Several studies have established that replay of long spatial trajectories can be represented by multiple concatenated ripple events (Davidson et al., 2009; Yamamoto and Tonegawa, 2017). During awake replay, ripples in MEC alternated with mutli-ripple events in CA1, suggesting a recurrent loop of activity between CA1 and MEC. Silencing MEC activity reduced the number of multi-ripple events without altering total ripple number (Yamamoto and Tonegawa, 2017).

Together these data suggest CA3 input to CA1 may regulate the content of replay while MEC coordinates extended replay events.

1.4 Influence of Interneurons in Coding

The previous section characterized the temporal and spatial organization of ongoing CA1 activity which is primarily distinguished by firing patterns of principal cells and their relationship to local oscillations. The shaping of this activity is due, in large part, to the activity and interactions between local interneuron populations which play a significant role in circuit dynamics. This section describes the role of interneurons in local dynamics and shaping input/output response of neural circuits through changes in excitatory-inhibitory balance. Our understanding of the role of interneurons in coding has gained significant insight through optogenetic experiments targeted generally or at a specific genetic class of interneurons.

During pharmacological blockade of inhibition, principal cells lose most of their distinguishing features such as spatial tuning (Rao et al., 2000). At the single cell level, synaptic inhibition filters synaptic excitation by countering excitation and modulating timing, tuning, gain and bursting properties of pyramidal cells (Freund and Buzsáki, 1996). At the network level coherent activation of interneurons coordinates interactions among pyramidal cells aiding in the formation of cell assemblies and routing of excitatory activity at various time scales (Isaacson and Scanziani, 2011). The following section will characterize the types of interneurons, and their role in circuit dynamics within the hippocampal formation, focusing on the computational role of classes of interneurons and their coordination in organizing network events.

In the hippocampus, there are over two dozen types of inhibitory neurons, which make up only 10-15% of total cell population yet regulate nearly all aspects of hippocampal function (Klausberger and Somogyi, 2008). The diversity of interneurons in the region dramatically expands the computational ability in hippocampal circuits (Buzsáki et al., 2004). Based on their inhibitory target, interneurons can eliminate synaptic integration across entire den-

dritic regions, shunt signals between dendrites and the soma or the soma and axon effectively changing the morphological properties of the principal cell (Roux and Buzsáki, 2015). Classifying interneurons into functional categories can help us understand the role of different classes of interneurons in circuit function. While many types of classification strategies exist, I will focus on morphology, molecular, and electrophysiological characterization which are the most relevant for interpretation of later explored experimental findings.

1.4.1 Classification of interneurons

Morphological classification

While none of these labels is sufficient on its own, neuroanatomical profiling provides a basis for understanding interneuron diversity and predicting circuit function (Klausberger and Somogyi, 2008; Freund and Buzsáki, 1996). Interneuron subtypes can be defined based on their morphological characteristics, displaying distinct axonal branching patterns and innervating different membrane compartments along the somato-dendritic axis (Figure 3a). Classification based on this schema separates interneurons into the following categories: perisomatic targeting, dendrite-targeting, interneuron specific, and long-range. Perisomatic-targeting interneurons preferentially target the soma and axon initial segment of principal cells. Their innervation proximal to the location of spike integration and initiation suggests these cells play a role in controlling the precise timing and output of efferent spikes (Mann and Paulsen, 2007; Buzsáki, 2001). Dendritic-targeting interneurons target the distal dendritic portions of pyramidal cells and function to control kinetic properties of target domain, such as shunting excitatory inputs, regulating generation of Ca^{2+} action potentials and synaptic plasticity (Isaacson and Scanziani, 2011; Miles et al., 1996). Members of this class are highly diverse, each innervating one or more dendritic regions and are at minimum associated with each incoming excitatory pathway (Buzsáki, 1984). Interneuron-specific interneurons specifically target other interneurons while avoiding connections with principal cells. Through this reciprocal inhibitory connectivity, this family of interneurons can exert strong inhibition on

principal cells, facilitating network synchronization (Gulyás et al., 1996; Pi et al., 2013). Long range interneurons have axons spanning two or more anatomical brain regions. These neurons are the most morphologically diverse and possibly least understood of the classes. Their long-range GABAergic afferents preferentially target local inhibitory interneurons, potentially facilitating precise temporal coordination of neuronal activity at distant locations through disinhibition (Caputi et al., 2013). The anatomical specialization of interneuron subtypes grants inhibitory networks refined spatio-temporal control over principal cell activity, rather than just providing non-specific global inhibition. However, while each interneuron class targets a specific domain, multiple subtypes of interneurons target the same domain, each potentially contributing to different circuit functions.

Genetic classification

Genetic expression of calcium binding proteins allows for the categorization of interneurons based on molecular markers. Three groups of particular importance to contemporary research methods are parvalbumin-positive (PV+), somatostatin-positive (SOM+) and vasoactive intestinal polypeptide positive (VIP+) interneurons. A general role of parvalbumin positive interneurons is to provide fast-spiking, perisomatic inhibition. Two main interneuron subtypes expressing parvalbumin are PV+ basket cells (PVBCs) and axo-axonic/chandelier cells (AACs). The most ubiquitous of these PV+ interneuron types are PV+ basket cells, comprising approximately 60% of all PV+ interneurons and 14% of CA1 interneurons (Bezaire and Soltesz, 2013). The soma of PVBCs are situated adjacent to the pyramidal layer in the SR and the SO. These cells receive input from all excitatory afferent projections in CA1 and send large axon collaterals to the soma and proximal dendrites of pyramidal cells. The somatic location and dendritic arborization is similar in AACs. The main difference between these cell groups is in their axonal targets. AACs selectively innervate the axonal initial segment, providing strong control over principal cell spike generation (Pelkey et al., 2017). Current genetic targeting techniques and spike properties fail to differentiate among

PV-expressing cohorts, so caution is required when interpreting whole animal/circuit level experiments.

A wide variety of cortical interneurons express somatostatin. These cells are generally classified as non-fast-spiking and target apical dendrites. The largest percentage of SOM+ cells are O-LM interneurons. O-LM cells are named for their distinct anatomy, with the soma and dendrites restricted to the oriens and the axon ascending and terminating on dendrites in the SLM (Freund and Buzsáki, 1996; Sik et al., 1995). These cells receive excitatory recruitment from principal cells and in turn send inhibition back to the apical dendrites of principal cells, performing the role of gating excitatory input from the entorhinal cortex (Leão et al., 2012). A wide range of interneuron subtypes express VIP+, most of which are inhibitory selective interneurons associated with disinhibition in cortical circuits (Tyan et al., 2014; Pi et al., 2013). Transgenic mouse lines take advantage of these genetic markers to optically manipulate different interneuron groups. It is important to recognize that current genetic targeting techniques may provide an oversimplification of the role of interneuron subtypes in circuit functions, with multiple subtypes incorporated in each transgenic model and keep this in mind when interpreting results using genetic manipulations.

Electrophysiological classification

Electrophysiological classification can be used in conjunction with genetic markers to potentially further disambiguate subtypes of interneurons. Classification based on electrophysiological profiles has been performed largely in anesthetized rats using juxtacellular recording techniques. Following the recordings, cells were labeled and traced to identify them based on their morphological profiles and genetic expression profile (Klausberger et al., 2003, 2004, 2005; Tukker et al., 2007). These experiments were labor intensive with maximally one interneuron characterized per recording, but provided a basis for identification of interneuron types in high density recordings where large heterogeneous populations of cells are simultaneously recorded. The main feature distinguishing interneurons is their distinct temporal firing

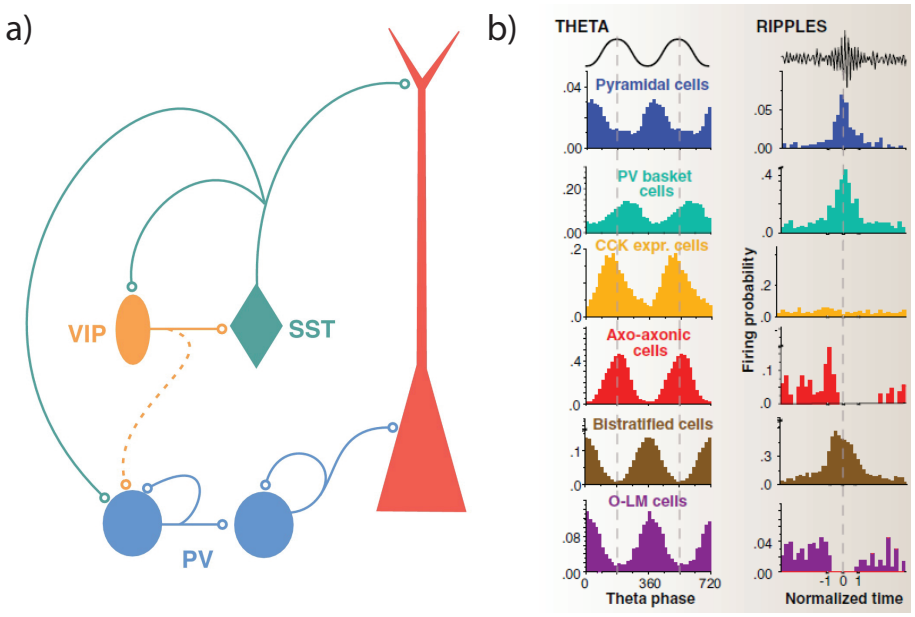

Figure 3: Connectivity and firing patterns of CA1 interneurons.

a) Simplified schematic of stereotyped interneuron connectivity based on various interneuron subtypes and their main synaptic connections (borrowed from Deleuze et al. (2014)). b) Firing pattern probability histograms show that interneurons innervating different domains on principal cells fire with distinct temporal patterns during theta oscillations and sharp wave ripples (borrowed from Klausberger and Somogyi (2008)).

patterns during different local field rhythms (for example, theta, gamma and ripple) and with distinct phase relationships (Figure 3b). This suggests that different types of interneurons differentially contribute to network dynamics (Klausberger and Somogyi, 2008).

1.4.2 Excitatory-Inhibitory Circuits

Interneurons do not operate in isolation but rather in circuits, coordinating with the activity of multiple inhibitory and excitatory neurons at multiple time scales. The following section will describe two ways in which interneurons elicit control in circuits. These canonical circuits provide a framework to understand how inhibition operates to regulate excitatory neural activity at multiple time scales.

The anatomical arrangement of excitatory afferents and local inhibitory interneurons provides the functional basis for feedforward inhibition in neural networks and plays a role

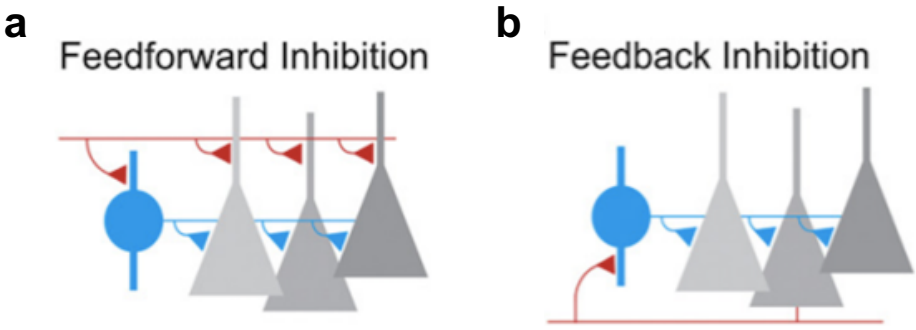

Figure 4: Feedforward and feedback circuits

Cartoon diagram of a) feedforward and b) feedback inhibition. Inhibitory cells and projections are in blue. Excitatory cells are in grey and their projections in red (borrowed from Isaacson and Scanziani (2011)).

in the shaping of excitatory events (Figure 4a). Excitatory afferents from EC and CA3 target both inhibitory and excitatory neurons in CA1, so that any input that provides monosynaptic excitement on principal cells will also trigger disynaptic inhibition, primarily through CCK+ basket cells, onto those same cells, creating an excitatory-inhibitory sequence of input onto the postsynaptic cell (Basu et al., 2013). Feed forward inhibition can target the dendrites, soma or axonal initial segment of principal cells (Freund and Buzsáki, 1996). Two temporal windows of integration emerge depending on the excitatory synaptic target. For inputs to the perisomatic regions feed forward inhibition enforces a narrow time window for spiking activity with rapid, early inhibition of the somatic and axon initial segment domains. Dendritic inputs, in contrast, facilitate a broader integration window (Pouille and Scanziani, 2001). Feedforward disinhibitory circuits have also been discovered, with VIP+ interneurons acting as the primary conduit. These interneurons are recruited by long-range inputs and in turn inhibit local interneuron populations (Pi et al., 2013). One circuit function of this disinhibition may be to provide transient activation of precise, selective circuits under conditions of blanket inhibition.

In contrast to feed forward inhibition, feedback inhibition is generated through initial activation of the principal cell (Figure 4b). Discharge from the principal cell recruits post-synaptic interneurons which feedback onto the principal cell, preventing any further spiking

activity. The recurrent excitatory-inhibitory loop regulates the spike frequency and timing of principal cells. Two temporal windows also exist for feedback inhibitory circuits depending on the type of interneuron recruited. Onset inhibition recruits primarily PV+ interneurons, resulting in rapid reduction in firing of the primary principal cells and ensuring a brief window of excitation, while late persistent inhibition is driven by O-LM interneurons and drives distal inhibition more proportional to the level of excitatory input (Pouille and Scanziani, 2004).

Feedforward and feedback circuits provide the building blocks through which much more complex networks are built. Dynamics within these circuits are based on the intrinsic connectivity between populations of inhibitory and excitatory cells and the relative weights of those connections. Adding further complexity, synaptic weights can change slowly or rapidly depending on behavioral states or learning. Even within the hippocampus, neural architecture from one region is unique and depends on the computational role of the region. For example, CA3 is a recurrent network, with high connectivity both within and between populations of excitatory and inhibitory cells yet the laminar organization of local interneurons is highly similar to CA1.

1.4.3 Role of interneurons in shaping activity patterns in CA1

Within the hippocampal formation, the bulk of experimental research has focused on the role of local and long-range interneurons in shaping spatial and temporal coding in CA1. Within CA1, input from CA3 contacts the basal and proximal dendrites of pyramidal cells and input from ECIII innervates distal apical tuft dendrites (Kajiwara et al., 2008; Takahashi and Magee, 2009). ECIII/CA3 inputs activate multiple classes of local inhibitory interneurons. These CA1 interneurons target specific domains of other local interneurons and principal cells that in turn serve as afferents to downstream regions (Takács et al., 2012). The coordination amongst these cell populations has been shown to be involved in shaping CA1 activity patterns and dynamically routing information from various input locations.

Early evidence for the involvement of interneurons in regulating hippocampal excitatory output came from studies measuring hippocampal spiking patterns during active exploration. Originally it was believed that spatial information was carried in the output patterns of pyramidal cells (Chrobak and Buzsáki, 1998). However, hippocampal interneurons also have spatially localized increases and decreases in activity, with information content comparable to principal cells (Wilent and Nitz, 2007; Ego-Stengel and Wilson, 2007). High positive and negative correlations are found between pyramidal cell-interneuron pairs. Negative correlations in firing indicate that not all interneuron activity is a product of excitation of a pyramidal cell with a similarly positioned firing field. These correlations suggest that location-specific firing of place cells is partially determined by location-specific decreases in interneuron activity that release place cells from inhibition (Hangya et al., 2010). Though these studies suggest a strong role of inhibition in regulating spatial representations, the types of interneurons and circuitry involved remain unclear.

Studies employing targeted optogenetic silencing combined with high density electrophysiology reveal dynamic interactions between multiple interneuron subtypes during place cell firing. Silencing either PV+ or SOM+ interneurons while a mouse was running on a linear treadmill caused increased firing rates of pyramidal cells but only within their place field. Silencing PV+ cells increased firing preferentially during the ascending phase of the field while silencing SOM+ cells increased firing during the descending phase (Royer et al., 2012). While PV and SOM expressing cells contain multiple subtypes of interneurons, PV+ cells can roughly be associated with input from CA3 since they are located primarily in the stratum radiatum, whereas the majority of SOM+ cells are O-LM interneurons which receive input from EC afferents. These finding suggest that under normal conditions, PV+ activity is higher at the onset of place cell firing, suppressing input from CA3, while SOM+ activity in higher towards the end of a place field, suppressing input from EC. This interpretation is supported by findings showing spike transmission probability between CA1 place cells and PV-like and SOM-like interneurons was either depressing or potentiating, respectively. As

an animal entered a place field, O-LM-type interneurons increased activity corresponding to increased inhibition of EC input. Conversely, decreased recruitment of PV-like interneurons from the beginning to end of the place field could signify an increase of CA3 input on place cell firing (Fernández-Ruiz et al., 2017).

Inputs from ECIII and CA3 are segregated anatomically and temporally in CA1, suggesting this separation in critical for information processing within the CA1 circuit (Colgin et al., 2009; Hasselmo et al., 2002; Belluscio et al., 2012; Schomburg et al., 2014). Interneurons play a significant role in dynamically gating and rerouting input between the two main afferents. Much of the gating appears to be accomplished through local neuron interactions. Increases in dendritic excitation causes increased perisomatic inhibition, suggesting that strong input from EC shunts incoming signal from CA3 (Losonczy et al., 2010). In contrast, increased firing of O-LM interneurons suppresses inputs to the distal dendrites, indirectly disinhibiting dendritic segments in the stratum oriens and radiatum, resulting in increased effectiveness of CA3 input on CA1 principal cells (Leão et al., 2012). Another potential mechanism of gating comes from neurogliaform cells (NGFC), located within the SLM and spanning over the distal dendrites of principal cells (Tricoire et al., 2011). These cells release GABA synchronously and through volume transmission, which could subject large areas of dendrites to indiscriminate inhibition, shunting EC input in favor of activity arising through the Schaffer collateral pathway (Pelkey et al., 2017). This type of "blanket inhibition" has previously been reported in neocortical regions where PV+ and SOM+ interneurons target all principal cells within a 200-um radius from their cell body (Packer and Yuste, 2011).

Long-range interneurons may also contribute to gating and facilitation functions within CA1. Long-range inhibitory projections (LRIPs) are found in nearly all cortical regions, including reciprocal projections between EC and CA1 and from CA1 to output structures (Germroth et al., 1989; Jinno et al., 2007; Melzer et al., 2012; Caputi et al., 2013). While not technically long-range, evidence also exists for direct inhibitory projections from CA3 to CA1 (Buzsáki, 2015). Little research has been conducted on the circuit effects of these

projections. However the majority target local interneuron populations, so LRIPs likely play a role in disinhibition of excitatory cells. Recent studies from Basu et al. (2013, 2016) found LRIPs from LEC to CA1 preferentially target CA1 CCK+ inhibitory neurons that border the SR and SLM. Under normal conditions, these interneurons are activated by Schaffer collateral input and target distal pyramidal cell dendrites (Basu et al., 2013; Cope et al., 2002; Klausberger and Somogyi, 2008). Long-range inhibition of CCK+ cells acts as a disinhibitory gate, promoting the excitation of CA1 principal neurons by suppressing feedforward inhibition. This inhibition subsequently enhances excitatory signals from CA3 arriving within a 20-ms window of LRIP activation signals, facilitating input timing–dependent plasticity with coincident CA1 and LEC input (Basu et al., 2013, 2016). This mechanism may explain why conjunctive input from EC and CA3 induces new place field formation (Bittner et al., 2015). LRIPs from a given input may also act to shunt input from competing sources (Fuchs et al., 2016). LRIPs from a subset of cells in the LEC known as "island cells" inhibit CA1 pyramidal cell dendrites and suppress the impact of excitatory input from MECIII (Kitamura et al., 2014). Since LRIPs originating from other sources to CA1 have not been studied, it is difficult to determine their postsynaptic effects and role in regulating CA1 excitatory output. However, based on these findings it is clear that long-range inhibition plays a crucial role in temporal coordination of neuronal activity in distant brain areas.

1.5 Balance of excitation and inhibition

The interactions between excitatory and inhibitory cells shape the spatial and temporal features observed across neural networks. Proper dynamics can only be maintained if excitatory forces are balanced by inhibition. Precise balance in an excitatory-inhibitory (EI) network is achieved when balanced responses are received from all subsets of presynaptic inputs at fast (<10 ms) timescales (Denève and Machens, 2016). Precisely balanced networks are well suited for input gating, which occurs when the E/I ratios at specific neuronal inputs are shifted while other inputs remain balanced in the background. In contrast, the

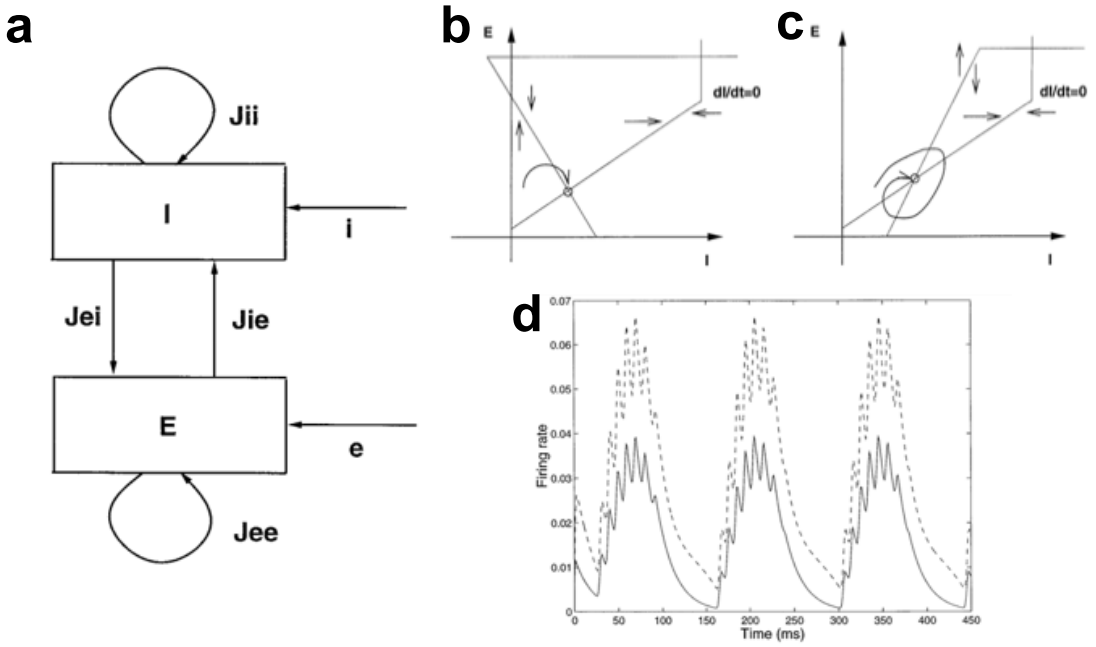

Figure 5: Dynamics in inhibitory-stabilizing models

All subfigures borrowed from Tsodyks et al. (1997). a) Schematic of network model. The excitatory (E) population is connected to itself through recurrent connections (J_{ee}) and to the inhibitory (I) population through connections (J_{ie}). I is connected to itself through recurrent connections (J_{ii}) and to E through connections (J_{ei}). E receives external excitatory input e (for all simulations $e = 0$) and I receives external inhibitory input i. Phase plane analysis of the dynamic population. Stable state of the network is indicated by a point at the intersection of the E and I nullclines. Arrows indicate the direction of motion proximal to the nullclines b) Phase plane for weak recurrent excitation ($4\beta J_{ee} < 1$). c) Phase plane for strong recurrent excitation ($\beta J_{ee} > 1$). d) Network response to periodic input provided to the inhibitory population in the parameter regime corresponding to strong recurrent excitation.

absence of balanced cortical activity shifts network activity to a hyperexcitable (decreasing inhibition) or silent (decrease excitation) state (Dudek and Sutula, 2007). Depending on the connectivity of the network, balance between excitation and inhibition can result in very different network dynamics including sustained responses to transient stimuli and oscillatory network activity (Vogels et al., 2005). Models of network connectivity can provide insights and testable predictions into how various neural architectures can respond to perturbations in the system. These models can also explain seemingly contradictory responses observed in experimental data (Ozeki et al., 2009; Rubin et al., 2015; Li et al., 2019; Sanzeni et al., 2020).

Networks with strong recurrent connectivity are found in area CA3 of the hippocampus

and across various cortical regions. In CA3 recurrent excitation appears to be strong but balanced by similarly strong feedback inhibition (Andersen et al., 1963). Seminal modeling of these systems was performed by Tsodyks et al. (1997). A schematic of their network model is illustrated in Figure 5a. Briefly, two populations, excitatory (E) and inhibitory (I), have recurrent connections within each cell population with synaptic weights J_{ee} and J_{ii}, and across cell populations with synaptic weights with synaptic weights J_{ei} and J_{ie}. The hippocampal theta rhythm was modeled as an external inhibitory input $i(t)$ to the inhibitory population. Initial tests of this model revealed a paradoxical response of inhibitory neurons to increased inhibitory input. Increased inhibitory input to the network resulted in an increased firing rate of interneurons. Conditions for this response were that recurrent connections amongst the excitatory population were strong enough to make the excitatory network unstable when feedback inhibition was removed. In general, a stable solution to this system always exists if recurrent excitation is small enough ($J_{ee} < 1$) or recurrent inhibition is sufficiently large. Phase analysis of these two conditions shows this paradoxical response is a general feature of the network (Figure 5b,c). The nullclines in the I, E phase plane are shown for a case of weak recurrent excitation ($J_{ee} < 1$, Figure 5b) and strong recurrent excitation ($J_{ee} \gg 1$, Figure 5c). The sign of the corresponding derivative (dE/dt or dI/dt) is indicated by arrows on both sides of the nullclines. In the case of weak recurrent excitation, excitatory connections are stable (Figure 5b, arrows point towards the nullcline) for any fixed level of inhibition. Under conditions of strong excitatory feedback, excitatory connections are unstable (Figure 5c, arrows facing away from the nullcline), and for any fixed level of inhibition, the excitatory population will either explode or decline, depending on the initial conditions. However, a locally stable solution can still exist given the appropriate weights are provided for all inhibitory connections. In both conditions, increasing external input $i(t)$ results in a downward shift in the I nullcline. In the case of weak recurrent excitation, an increase $i(t)$ leads to a downward right shift in the stable point. As external input increases, excitatory activity decreases and inhibitory input increases, resulting in

out-of-phase modulation between the cell populations. For networks with strong recurrent excitation, increased external inputs shifts the stable point down and to the left, resulting in in-phase modulation between the cell populations that is out of phase with the external input. In networks where J_{ee} is stronger that J_{ii}, the stable solution becomes a limit cycle and fast oscillations emerge (Figure 5c,d). Taken together, this model demonstrates that non-intuitive firing patterns within a given region can emerge depending on the structure and strength of recurrent inhibition.

This model provides a circuit mechanism and testable predictions of excitatory-inhibitory balancing under conditions of weak and strong intrinsic excitatory connections. For networks with sufficiently strong intrinsic excitatory connections, external input to inhibitory interneurons will modulate their activity in the direction opposite to the change in input. For oscillatory inputs, a phase difference emerges between excitatory and inhibitory populations that varies depending on the strength of internal interactions. If the weight of recurrent excitation is stronger than that of inhibition, gamma oscillations emerge at phases of the oscillatory input, indicating decreases in $i(t)$ could result in fast oscillatory increases in both inhibitory and excitatory activity.

Experimental perturbation of cortical circuits, using paradoxical firing responses as a proxy for inhibitory stabilized networks, have found conflicting results as to whether these circuits operate in an ISN regime. Earlier studies found stimulation or suppression of PV+ inhibitory neurons did not elicit a paradoxical responses in mouse V1 (Atallah et al., 2012). More recent work by Sanzeni et al. (2020) found widespread stimulation or stimulation of PV+ interneurons resulted in a paradoxical increase in inhibitory firing in multiple cortical regions, suggesting ISNs are a general propery of cortical circuits. Interpretation of experimental results can be due to a lack of biological realism in models, which do not capture the complexity of responses in networks with multiple inhibitory populations and a diversity of connectivity patterns between excitatory and inhibitory populations. The Tsodyks et al. (1997) model of recurrent networks is constrained by the assumption that inhibitory

neurons can be grouped into a single homogeneous population. Modeling work by Litwin-Kumar et al. (2016) investigated the impact of heterogeneous inhibitory subpopulations in both strong (ISN) and weak (non-ISN) recurrent networks. Their model found responses of inhibitory cells depended largely on the population receiving external input. Non-stimulated inhibitory classes did not necessarily respond paradoxically to external drive. These findings suggest that using firing rate responses to detect ISNs may lead to inconclusive results when only a subpopulation of inhibitory cells are stimulated. Additionally the method of perturbation can constrain tests of ISNs. Modeling work by Sadeh et al. (2017) explored what parameters of perturbation could successfully detect ISN-regimes. They found that eliciting a paradoxical response required a large fraction, in spatial size and proportion of cells, of the inhibitory population to be perturbed. These models will be discussed extensively in both Chapter 3 and Chapter 4 as predictions from each model influenced both our experimental design and interpretation of our results. Taken together these results indicate that rebalancing dynamics and the response of inhibitory and excitatory cells to varying external drive is highly dependent on the local network architecture, especially in relation to the the diversity and connectivity of local interneurons and the extent of recurrent excitation. Insights from computational models combined with optogenetic manipulations and electrophysiological recordings within local circuits can provide insights into how inhibitory and excitatory cells coordinate to process information.

1.6 Open Questions

Proceeding from this background, the work described in this dissertation addresses two main questions. First, what is the role of CA3 in shaping spiking activity in downstream CA1? Transient optogenetic silencing of area CA3 combined with electrophysiological recording in CA1 allows for a comparison of firing properties of CA1 neurons with and in the absence of CA3 input. Second, how do excitatory and inhibitory populations respond to incoming signal? CA3 and CA1 have remarkably similar architecture with the caveat that CA3 contains

highly-recurrent associational connections. Activity in hippocampal subregions CA1 and CA3 can be locally manipulated and measured using a combination of optogenetic and electrophysiological techniques to provide insight into how strong and weak recurrent networks differentially absorb large external perturbations.

2 Methods

In this chapter, general methodologies for experiments covered in Chapter 3 will be discussed.

2.1 Animals

Subjects for the majority of experiments were wild type (WT) male Long-Evans rats (300-400g) obtained from either Envigo or Charles River. Male transgenic rats (LE-Tg(Gad1-iCre)3Ottc expressing Cre recombinase in cells where GAD1 promoter is active were originally obtained through the Rat Resource and Research Center (RRRC #751) and were bred with female WT Long-Evans rats. A colony was maintained by the Unit for Laboratory Animal Medicine (ULAM) Breeding Colony at the University of Michigan. Both male and female transgenic animals were used in experiments localizing stGtACR2 opsin to inhibitory cells. All experiments were approved by the Institution of Animal Care and Use Committee (IACUC) and followed US National Institutes of Health animal use guidelines.

2.2 Animal Training and Behavior

For experiments combining chronic recording methods and behavior, subjects were male WT Long-Evans rats. Prior to virus surgery and electrode implantation, animals were habituated to daily handling and placed on water restriction, having ad libitum access to water during training periods where they learned to associate plastic water wells with water reward. Animals were not exposed to the experimental room or linear track until after surgery to ensure novelty of the task during the first recording session. Following surgery, animals were introduced to the recording room and a sleep box for 7 days prior to recording. During this time, electrodes were slowly lowered towards hippocampal area CA1. Starting on the first recording day, and all subsequent recording days, population activity in the hippocampus was recorded while the rats ran on an 1.75-m elevated linear track for water reward at each end. The track was equipped with two photosensors that detected entry into a selected

"trigger zone" segment on the track. During one block of 20 trials, a laser connected to the optical fibers was triggered by the photosensors and cells illuminated by the fiber were reversibly silenced while the rat was running in the trigger zone. Another block of 20 laps were used as a control to verify the firing fields of neurons on the center portion of the track. On the second day of recording, the linear track was kept in the same position, but the silencing protocol was changed so that the silencing block occurred between laps 16-30 sandwiched between two sets of 15 control laps. These two silencing protocols were interleaved for multiple days. For each block, the linear track was repositioned in the room to record from different place cell populations. At the end of each session, the animal was returned to his sleep box and allowed to sleep uninterrupted for $\sim$ 2 hrs, during which time light was pulsed (2 s ON/8 s OFF) long enough to quantify which cells were affected by the stimulation.

2.3 Fiber-based optoelectronic design ('optrodes')

Optrode design was based on Royer et al. (2010). Briefly, 125-μm multimodal fibers were either cleaved to create a perfectly flat endface or cone-etched using hydrofluoric acid to allow for easier penetration of brain tissue. The optic fiber was placed on the shank of a silicon probe (Buz32 or Buz64; Neuronexus Inc, Masmanidis-128; (Yang et al., 2020)) with help of a micromanipulator. The silicon probe was placed horizontally and the fiber was placed parallel to the probe with the tip 50-μm above the highest electrode (Masmanidis-128) or at a slight angle ($\sim$ 15°) with the tip 400-μm above the highest electrode (Buz32 or Buz64). The fiber was secured to the bonding area of the probe using either epoxy (Resinlab EP965 Black, Masmanidis-128) or UV light-curable glue, followed by dental acrylic (Buz32 or Buz 64). This process was repeated so two (Buz 32 or Buz64) or four (Masmanidis128) shanks were equipped with optic fibers (Figure 6a,b).

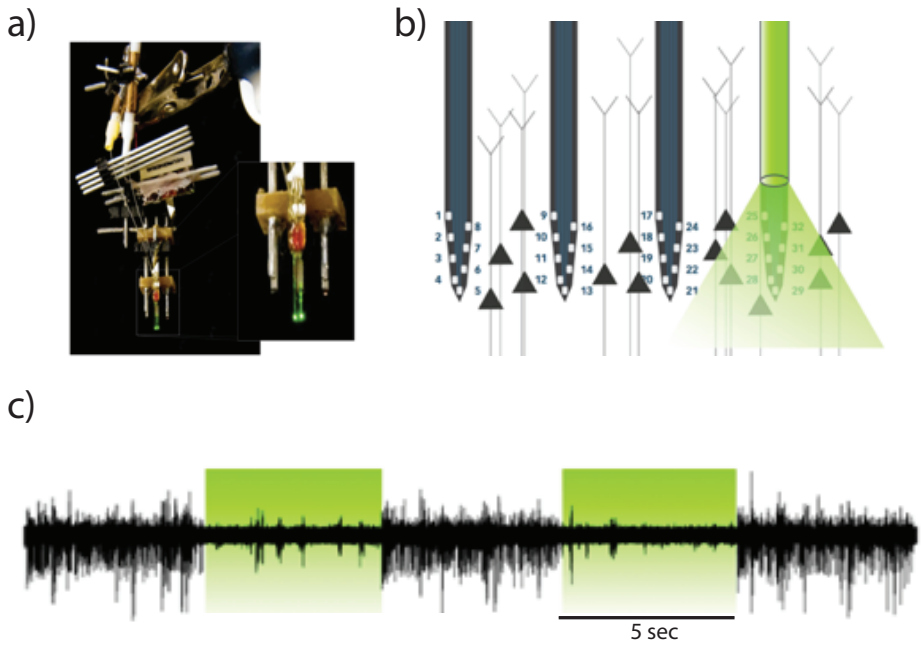

Figure 6: Optrode design and sample recording.

a) Custom made optrode. A 32-channel buzsaki probe (4 shanks, 8 channels/shank) fit with two independently illuminated 125-um cone etched optic fibers. b) Illustration of optrode design and electrode arrangement. c) Multiunit activity recorded on one electrode during light stimulation. Note how firing decreases during stimulation epochs.

2.4 Surgery

2.4.1 Virus Surgery

Animals were anesthetized with isoflurane (induction at 5%, maintained at 1.2% during surgery) and placed in ear bars on a stereotaxic stage. Rats were placed on a heating pad to prevent loss of body temperature and vitals, including temperature, heart rate and oxygen saturation were monitored throughout the procedure. Prior to incision the scalp was sterilized using betadine and alcohol wipes and a bupivacaine/lidocaine cocktail (1 ml/kg) was administered subcutaneously at the injection site. The virus delivery protocol and location were optimized in 11 animals.The final target coordinates were adjusted -0.3 mm from bregma and 0.25 mm ventral from stereotaxic coordinates. Bregma-lambda distance was measured and final coordinates were scaled from the atlas distance of 8.7 mm (Paxinos and Watson,

1986). The final coordinates for CA1 were, AP: $-3.3/-3.54$ mm, ML: 2.2/2.6 mm, DV: 2.35 mm. The final coordinates for CA3b were, AP: $-3.3/-3.54$ mm, ML: 3.0/3.4 mm, DV: 3.45 mm. Virus was loaded into a 10 μ l injection syringe equipped with a 35 gauge beveled needle(NANOFIL$^{\text{TM}}$, World Precision Instruments) and lowered to the target coordinate. Total virus amount was divided and delivered at three depths, DV depth ± 0.2 mm at a rate of 0.05 μl/min. All viruses were diluted to $\sim \times 10^{12}$ vg/ml except for SIO-stGtACR2 which was $\sim 1 \times 10^{13}$ vg/ml. The following volumes were used for each virus: AAV2/CamKIIα-ARCHT-GFP (0.5μl/site, UNC Vector Core), AAV5/hSyn-oCHIEF-dtTomato (0.3μl/site, Duke Viral Vector Core), AAV1/CamKIIα-stGtACR2-fusionRed (0.4μl/site, Addgene), AAV1/hSyn-SIO-stGtACR2-FusionRed (0.45μ/site, Addgene). pAAV/CamKIIα-stGtACR2 (Addgene viral prep #105677-AAV1) and pAAV/hSyn1-SIO-stGtACR2-FusionRed (Addgene viral prep #105677-AAV1) were gifts from Ofer Yizhar (Mahn et al., 2018). Acute recordings or chronic implantation were performed a minimum of two weeks following virus injection to ensure expression.

2.4.2 Anesthetized Recordings

Animals were anesthetized with 1.3 mg/kg urethane (1.3 g diluted into 10 mL saline) plus a supplemental dose of ketamine and xylazine (20 and 2 mg/kg respectively). Additional urethane was administered if signs of inadequate depth of anesthesia persisted, including pedal reflex response. A circular craniotomy was made over dorsal CA1 centered on coordinates, AP: -3.06 mm, ML: 2.0 mm using a 3.7-mm diameter trephine drill bit. For recordings with detached fibers targeting CA3, fibers were attached bilaterally and secured to the skull at coordinates, AP: -4.34 mm, ML: ± 3.50 mm, DV: 3.45 mm angled $\sim 15^{\circ}$ anterior to target dorsal CA3b. Electrodes were slowly advanced to the target location (either CA1 or CA3) and allowed 30 minutes to stabilize prior to recording. Recordings lasted for ~ 30 min during which time light was pulsed at a cycle of either 2-s ON/ 8-s OFF, 500-ms ON/ 2-s OFF, or 250-ms ON/ 1-s OFF.

2.4.3 Chronic Recordings

A minimum of two weeks following virus surgery, rats were implanted unilaterally with high-density silicon probes (32 or 64 sites; Buz32 or P-Series; Neuronexus or Cambridge NeuroTech). Probes were attached to a microdrive (modified, see Chung et al. (2017) for basic design) and implanted with a 15° angle along the hippocampal long axis at the following coordinates, AP: −3.06 mm, ML: 2.0 mm. During surgery the tips of the electrodes were lowered to the neocortex at a depth of 1.3 mm. Ground and reference screws were placed in the bone above the cerebellum. Craniotomies were sealed with silicone gel (Dow Corning 3-4680) and wax. To provide physical and electrical shielding, the crown of copper mesh was built around the probe and reinforced with dental acrylic.

2.5 Data acquisition

All data, unless otherwise specified, were collected using either Neuralynx Digital Lynx SX data acquisition system with Cheetah software or InTan RHD recording controller with openEphys software (Siegle et al., 2017). Analogue neural signals were amplified and recorded at 32 kHz or amplified and digitized on the headstage at 30kHz. LFP was downsampled to 1250 Hz for additional analysis. For chronic recordings, rat's position was tracked using two LED diodes (red and green), mounted to the headstage and detected by an overhead digital video camera at 30 frames/s. For experiments using detached optic fibers, laser power was measured and set to 10 mW at the end of the cable prior to acquisition. For experiments using either optrodes or uLEDs, output intensity was set low and gradually increased until changes in cell activity were visually observed. For detached fiber and optrode experiments, light was delivered via a laser (wavelength: 445 nm, oCHIEF/stGtACR2 opsins and 523 nm, ARCHT opsin) and output power was controlled using an variable reflective mirror attenuator. For μLED experiments, current was controlled using a customized OSC1-LITE μDriver provided by the Yoon lab.

2.6 Histology

For chronic recordings, a small DC current (2 μA for 10 sec) was passed through the deepest electrodes on each shank of the probe prior to sacrificing the animal in order to identify the depth location of a specific recording site. This procedure was not performed for acute recordings since multiple passes were made through both CA1 and CA3 in the same animal. These recordings relied on the depth of electrodes, LFP patterns characteristic to certain layers and responsivity of cells to identify the recording location. The rats were deeply anesthetized using ketamine/xylazine and perfused through the heart first with 0.9% saline solution followed by 4% paraformaldehyde solution. The brains were sectioned by a Vibratome (Leica, Germany) at 75 um in the coronal plane for hippocampus. Sections were mounted on slides, cover-slipped and imaged to verify appropriate location of both electrodes and virus expression (Figure 7a).

2.7 Data processing and cell classification

Raw signal was high-pass filtered and waveform extraction and initial clustering was conducted using SpikeDetekt and KlustaKwik (Rossant et al., 2016). Further manual adjustment of the waveforms was then performed using Klusters (Hazan et al., 2006). Only well isolated units, defined by clear refractory periods and well-defined cluster boundaries were included in analysis. A subset ($\sim$25%, 815/3019 recorded cells) of putative pyramidal and putative interneuron cell types were initially categorized visually using firing rate and features of the autocorrelograms (Figure 8a). Quadratic discriminant analysis was then used to classify the remaining cells as either putative pyramidal or putative interneurons. Four variables were used for classification: waveform asymmetry, waveform trough to peak, cell burstiness and firing rate (Mizuseki et al., 2009; Royer et al., 2012) (Figure 8b). The discriminant analysis perfectly separated the training group. 93 cells did not meet our criterion of having a posterior probability between 0.1 and 0.9 were excluded from future analysis (Figure 9). Pyramidal cells in CA1 and CA3 had significantly different waveform and firing

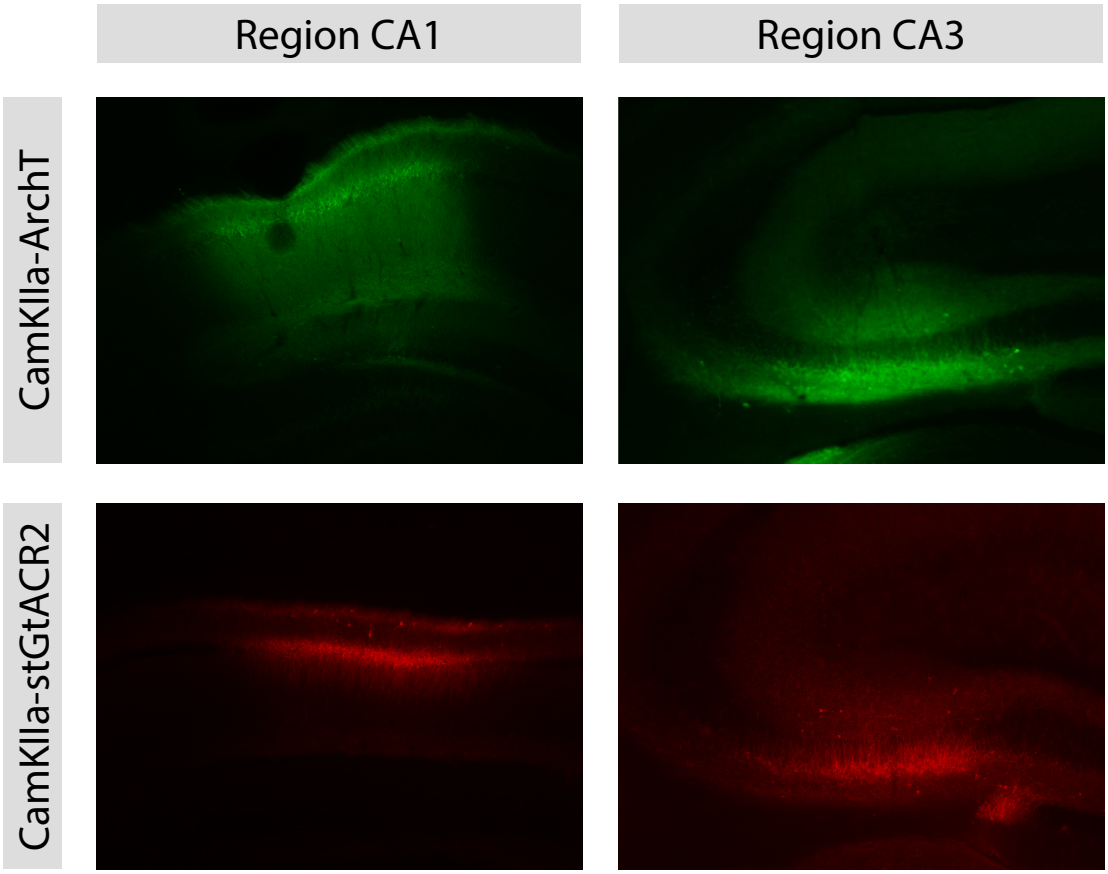

Figure 7: Viral expression in CA1 and CA3.

Expression of AAV2/CamKIIα-ArchT-GFP (top) and AAV1/CamKIIα-stGtACR2-fusionRed (bottom) in hippocampal subregions CA1 (left) and CA3 (right).

properties (Figure 10), however the classifier did not perform any better when regions were considered separately (data not shown).

2.8 Cell response classification

Laser pulse epochs either following behavior or during the anesthetized recording were used for cell response classification. For each cell, spiking activity organized into 100-ms bins and aligned to the onset of the laser. In order to account for neuron instability especially during anesthetized recordings analysis was restricted to trials with a firing rate > 0 . Baseline (OFF) was considered to be the window of time in the middle of the laser off epoch with

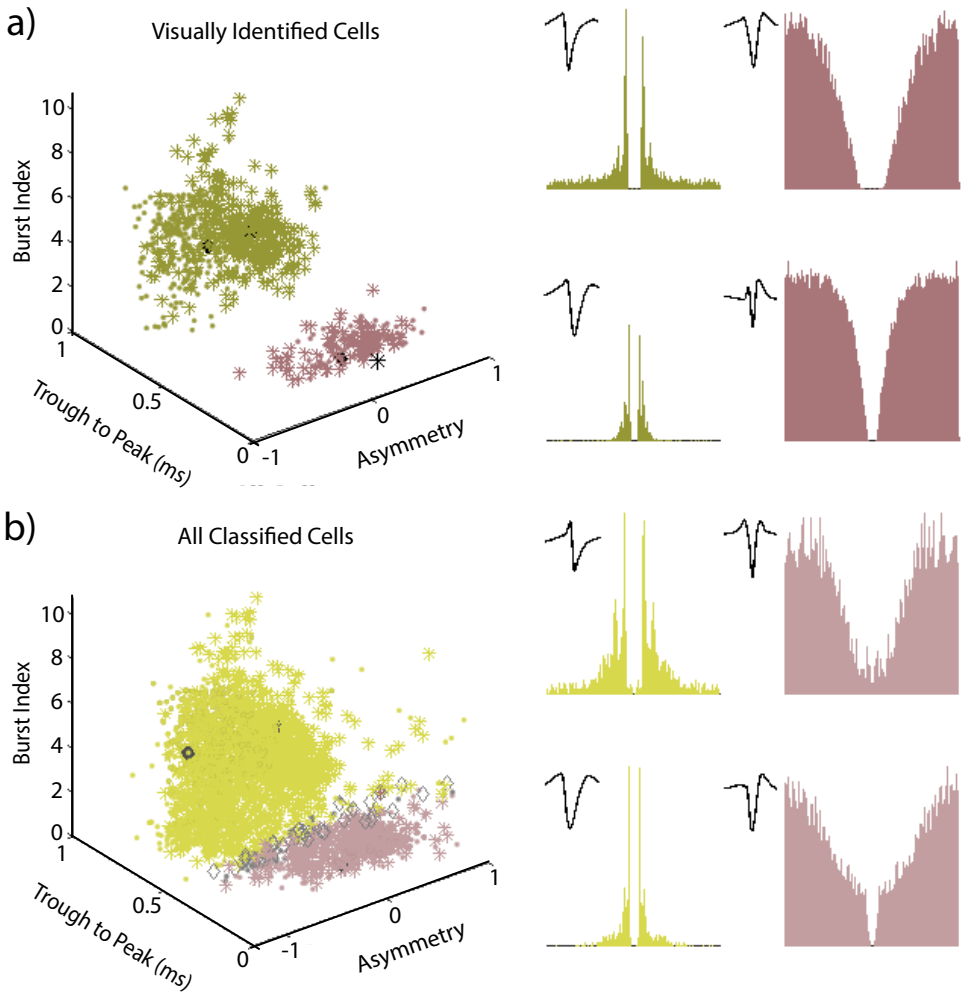

Figure 8: Cell classification.

a) (*left*) Spiking and waveshape features of visually classified cells (pyramidal: green, interneuron: pink). (*right*) Examples of the autocorrelogram and waveshape of two visually classified pyramidal cells and two visually classified interneurons. b) (*left*) Classification of all cells using quadratic discriminant analysis and visually identified neurons as the training set. Cells with posterior probability between 0.1 and 0.9 (grey) were excluded from analysis. (*right*) Example of the autocorrelogram and waveshape of two pyramidal cells and two interneurons identified by the classifier.

duration equal to duration of illumination (for example, if laser duration was *dur* ms, ON = 0 to *dur* ms and OFF = -2*dur* to -*dur* ms). A permutation test was used to determine whether individual cells responded significantly to optogenetic perturbation. Briefly, for each cell, spike times were jitter randomized across a window of -2**dur* to 3*dur* (laser on a t = 0),

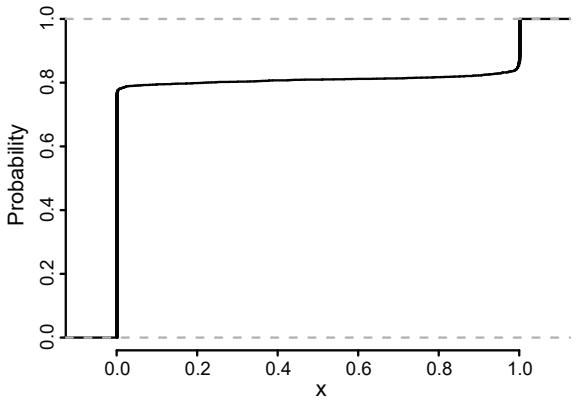

Figure 9: Performance of cell classifier.

Cumulative distribution x is the posterior probability of the cell classifier. $x = 0$ corresponds with identification as a pyramidal cell. $x = 1$ corresponds with identification as an interneuron. 93 cells fell between $x > 0.1$ and $x < 0.9$. Those cells were excluded from all future analyses.

keeping the total number of spikes on each trial fixed. Mean ΔFR (ON-OFF) was compared to 1000 permutations. The p-value was taken as the ratio of the number of permutation values exceeded the test statistic over the number of permutations (min p-value = 0.001). Cells with $p < 0.05$ were considered responsive. Mean ΔFR was used to determine the direction and degree of responsiveness. Group responses were taken as the summed activity of significantly classified pyramidal cells and interneurons for each session.

2.9 Sharp-wave ripple detection

For each shank located in CA1, one electrode with maximum average power in the ripple-band frequency (130-230 Hz) was selected. The signal on each of the selected electrodes was bandpass filtered. Theta-epochs excluded from analysis. Ripple events were triggered when bandpass signal exceeded 5 SD above the mean. The duration of the ripple event was measured as the time before and after this event when the signal dropped below 1 SD from the mean. Ripples $<$ 35-ms or $>$ 500-ms were excluded and ripples with inter-ripple intervals $<$ 50-ms were merged.

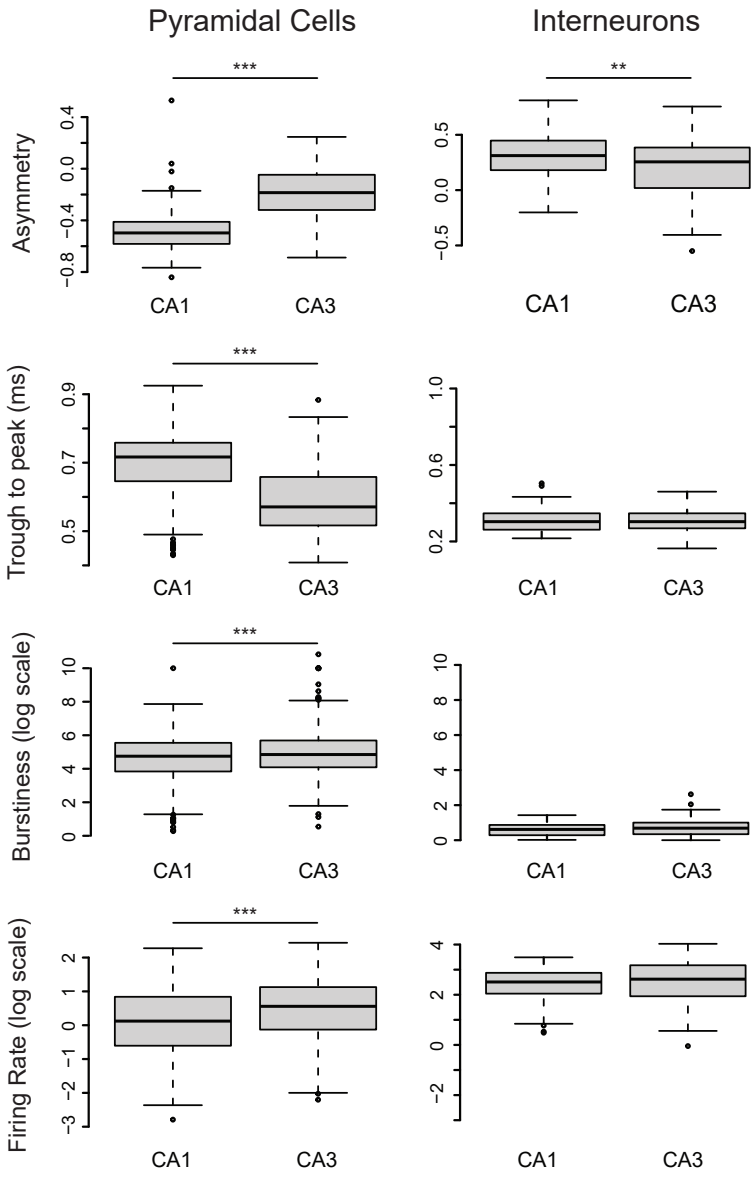

Figure 10: Comparison of cell features between CA1 and CA3.

All measured features of pyramidal cells were significantly different between CA1 and CA3. Interneurons had slight differences in waveform asymmetry between CA1 and CA3 but all other features were not significantly different (Key above boxplot: $^{***}p < 0.001$, $^{**}p < 0.01$ on t test for different in means).

2.10 Statistics

For all ΔFR figures, significant changes in firing rate were determined by a two-tailed paired t-test with the null hypothesis, H_0. Symbols for stats reported in ΔFR figures are as follows:

ˆ: $p < 0.05$, *: $p < 0.01$, **: $p < 0.001$, ***: $p < 0.0001$. For all proportion figures, Pearson's chi-squared test was used when appropriate. In most cases either the total number of observations were small or there were too few observations in too many cells. In these cases, Fisher exact test was used. Fisher tests were initially run on 2000 simulations, if the p-value was too small, simulations were run on 2,000,000 simulations to better estimate the p-value. Binomial tests were used to compare between categories in proportion figures.

3 Optogenetic probe of CA3 and CA1 hippocampal networks

3.1 Introduction

One goal of neuroscience is to link cell types and brain regions to the organization of neural activity patterns, such as spiking and local field oscillations. Classically, surgical and pharmacological lesions were used to inactivate small brain regions, allowing scientists to causally explore relationships between brain regions and neural activity. Loss-of-function studies provide much of what we know about localization of brain function but lack the specificity to dissect circuits at a finer resolution. These techniques are also irreversible and neural circuits can compensate for the loss of particular inputs (Otchy et al., 2015; Goshen et al., 2011). The advent of optogenetics provided a means to manipulate circuits with high spatio-temporal resolution and targeted cell specificity. A widespread use of optogenetics has been to rapidly and reversibly inactivate neuronal populations during specific phases of brain activity in attempts to establish causal links between genetically identified cell types and specific neural activities and functions.

Finding a direct link between optogenetic manipulations and circuit responses is not straight forward. Optogenetic manipulations often have unexpected spatial and temporal effects on activity patterns. These effects can depend on brain state, connectivity of neuronal circuits, different classes of neurons stimulated or the strength and duration of light manipulation (Fröhlich et al., 2010; Mateo et al., 2011; Moore et al., 2018; Stujenske et al., 2015). Some of these unexpected responses can be used to our advantage to better understand the actions of complex circuits. Networks with extensive recurrent connectivity are a feature of many cortical regions. Strong recurrent coupling allows networks to perform operations such as signal amplification and generation of spatiotemporal activity patterns (Rubin et al., 2017). The strong recurrent coupling in these networks results in unstable dynamics unless stabilized by inhibition. Detection of networks operating under inhibitory

stabilization can provide information on the computational role of the system. A consistent feature of inhibitory stabilized networks (ISNs) is a paradoxical decrease in firing of excitatory and inhibitory cells when external drive is applied to interneurons (Ozeki et al., 2009; Sanzeni et al., 2020). Detection of ISNs is well suited for optogenetic techniques since it requires brief, cell-type specific perturbations at degrees of external drive. In ISN networks, optogenetic stimulation of interneurons results in a net decrease in activity of the same population of interneurons. This paradoxical response can arise from the interactions between recurrent excitation and inhibition (Tsodyks et al., 1997; Litwin-Kumar et al., 2016; Sadeh et al., 2017).

Measuring the optogenetic effects on neural populations can provide valuable information about circuit properties and how different circuits respond to perturbation. In the following experiments we study the effects of optogenetic manipulation on hippocampal circuit responses. The hippocampus plays a critical role in spatial and episodic memory with hippocampal subregions proposed to play distinct but complementary roles in memory processes (Kesner and Rolls, 2015). Regions CA3 and CA1 display different connectivity patterns despite forming similar representations of the environment (Lee et al., 2004; Leutgeb et al., 2004). CA3 forms highly recurrent excitatory connections similar to various cortical regions, while lateral projections in CA1 are significantly more sparse (Bernard and Wheal, 1994). One suggestions is that differences in connectivity enable CA3 to perform nonlinear transformations of input while CA1 transforms input in a more linear fashion (Guzowski et al., 2004). Comparison of responses to optogenetic perturbation in these regions can provide insight into how different hippocampal networks respond to light-induced external drive.

We designed three types of experiments to address various common optogenetic experimental paradigms. First, we examined how photoinhibition of area CA3 changes activity patterns in downstream region CA1. These experiments provided information on how "silencing" a primary input can result in non-intuitive responses by the target region. Next we measured local responses of CA1 and CA3 networks to focal perturbations to examine "off

target" responses in networks with different connectivity. Lastly, we investigated how CA1 and CA3 networks responded to broad inhibition at varying light intensities and to specific cell populations to examine network responses to varying degrees of external drive.

3.2 Results

Silencing CA3 results in disinhibition of CA1 interneurons

In order to assess the contribution of CA3 inputs in shaping activity in area CA1, we combined high-density electrophysiological recordings of CA1 with optogenetic silencing of CA3 freely-moving rodents ($n = 4$ rats, 8 sessions). Rapid and reversible silencing was achieved using ArchT, a light activated outward proton pump (Chow et al., 2010). Briefly, animals were infused with CamKIIα-AAV2-ARCHT-GFP in dorsal CA3b (dCA3b). Dorsal CA3b was chosen for the site of expression since the majority of projections from this region target dorsal CA1 (Witter 1989, Kesner 2013). After allowing a minimum of two weeks for sufficient opsin expression, a second surgery was performed to chronically implant bilateral optical fibers targeting CA3 and recording electrodes in dorsal CA1 (See Methods Section 2.4.3 , Figure 7). During quiet waking/sleep periods in the homecage, light was pulsed in a 2-sec ON / 8-sec OFF cycle to measure the effect of silencing CA3 on spiking activity in CA1.

Since the major projection from CA3 to CA1 - the Schaffer collateral pathway - is excitatory, our initial hypothesis predicted an overall decrease in activity in CA1 due to decreased excitatory drive from CA3. Surprisingly, few CA1 cells showed decreased firing (Figure 11c). We classified cells as excitatory or inhibitory using quadratic discriminant analysis based on properties of the waveshape and autocorrelogram statistics (see Methods Section 2.7, Figures 8, 9, 10). Responses of cells to inactivation of CA3 were measured as the ratio of response between stimulation window (laser ON) and baseline (laser OFF). Significance was determined by a comparison to 1000 surrogate data sets where spike times were ran-

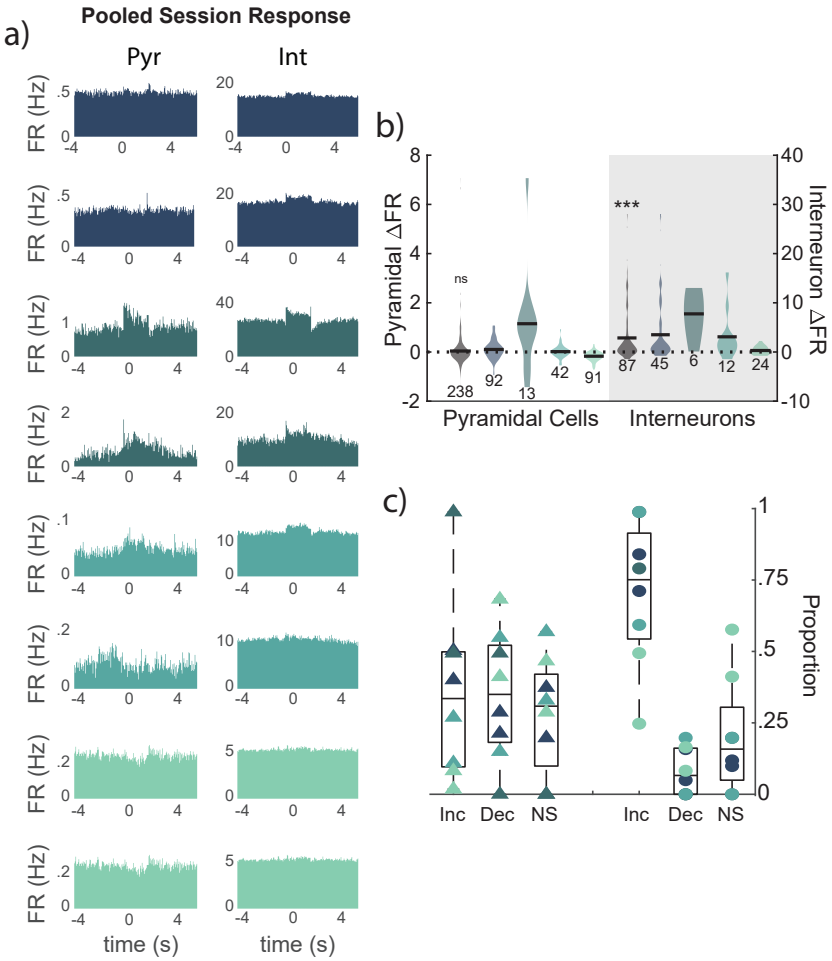

Figure 11: Responses of CA1 cells to CA3 silencing in awake animals.

a) Pooled firing rate responses for all significant cells ($p > 0.05$) recorded in each session. Each row shows pooled responses for a single session. Data from different animals corresponds to different colors. The left column shows pooled pyramidal cell responses. Pooled interneuron responses are on the right. b) Difference in firing rate during pulsed illumination (ON-OFF) for all recorded cells. The number below each colored violin plot shows number of recorded cells for each animal. Grouped data for all sessions across animals shown in black. Stats were only performed on data grouped across sessions. CA1 pyramidal cells showed no significant changes in firing rate during acute silencing of CA3 (paired t-test,mean = 0.0397 Hz, n = 238 cells, $p = 0.32$). CA1 interneurons increased firing during acute silencing of CA3 (paired t-test, mean = 2.86 Hz, n = 87 cells, $p = 7.42 \times 10^{-7}$). c) Data shown as the proportion of pyramidal and interneurons that increased firing, decreased firing, or showed no significant change during illumination. Pyramidal cells showed no significant difference in the proportion of cells that increased or decreased response (binomial test, $p = 0.078$). The proportion of interneurons showing increased firing response was significantly higher than the proportion that decreased firing (binomial test, $p = 3.914 \times 10^{-10}$).

domly redistributed across the baseline and stimulation window while total number of spikes per trial was preserved ($p < 0.05$). Surprisingly, suppression of excitatory drive from CA3 resulted in a strong, consistent disinhibition of interneurons in CA1 (Figure 11c). Of the

87 recorded CA1 interneurons (4 rats, 8 sessions), 68% showed a paradoxical increase in firing, 10% decreased firing and 22% had no response to light stimulation in CA3 (Figure 11c). The proportion of disinhibited CA1 interneurons compared to inhibited CA1 interneurons was significantly higher than the proportion of disinhibited to inhibited CA1 pyramidal cells, which showed a largely heterogeneous response to inactivation of CA3 (interneurons: binomial test, n = $p < 10^{-10}$, pyramidal: $p = 0.078$).

To understand how silencing CA3 changed the overall balance of excitation and inhibition in CA1, pooled responses were measured for the population of pyramidal cells and interneurons. Degree of responsivity of cells was measured as the mean change in firing rate between photoillumination and baseline epochs (ΔFR = FR(ON)-FR(OFF)). A ΔFR > 0 corresponds to an increase in firing to optogenetic perturbation while an ΔFR < 0 corresponds to a decrease in firing. Overall, the population response of pyramidal cells showed no overall increase in firing, implying a net neutral effect of stimulation (paired t-test, $p = 0.32$). Individual cells responded heterogeneously with similar proportions increasing (28%) and decreasing (38%) firing in response to upstream silencing. Interneurons, on the other hand, displayed a mean firing increase of 2.6 Hz (paired t-test, n = 87, $p < 10^{-7}$). These data imply that silencing CA3 input to CA1 results in a net increase of inhibition through disinhibition of interneurons in CA1.

A local feedforward inhibitory circuit within CA1 could potentially explain these results. Decreased drive from CA3 could preferentially target a subset of interneurons, which decrease firing resulting feedforward disinhibition of other classes of CA1 interneurons. In order for that to be true, two other changes in firing rate would be observed. First, if feedforward inhibition emerged via local excitatory-inhibitory interactions, we would expect to observe a decrease in pyramidal cell firing in response to increased inhibition. We found no increases in overall pyramidal cell firing rate as a result of CA3 silencing (Figure 11b and proportional response of CA1 pyramidal cells was not biased toward increased firing (11c). Second, since feedforward disinhibition is localized in CA1 we would expect to see a subset of CA1

interneurons decrease firing. Our recordings predominantly targeted the pyramidal layer and the adjacent stratum radiatum (SR) and stratum oriens (SO). PV+ interneurons located in the stratum pyramidale (SP) and oriens respond robustly to CA3 input (Wierenga and Wadman, 2003; Milstein et al., 2015). Decreased excitatory input from CA3 would likely be reflected in a decreased firing of interneurons radially adjacent to the SP, which we did not observe. Since different classes of interneurons are anatomically segregated along the hippocampal radial axis, we cannot rule out that another class of interneurons, located at further radial distanced from the pyramidal layer decrease firing. In order to test this hypothesis, we measured the response of interneurons as a function of radial distance from the pyramidal layer. Maximal sharp-wave ripple amplitude was used to locate the pyramidal layer (see Methods Section 2.9, Mizuseki et al. (2011); Oliva et al. (2016)). No patterns emerged in relation to interneuron response as a function of distance from the pyramidal layer (data not shown) suggesting feedforward disinhibition was not localized to CA1.

These results suggest that feed-forward disinhibition of CA1 interneurons may arise from changes in CA3 activity inherited by CA1 during periods of CA3 silencing. In order to test this hypothesis, we performed to a series of experiments conducted with the animals under a urethane-ketamine cocktail anesthesia (see Methods section 2.4.2). Anesthetized recordings allowed for a simplified experimental setup where we could test multiple electrode and fiber configurations during a single session. Furthermore, robust and diverse network activity can be observed under a combined urethane-ketamine dosage, including spontaneous high-frequency ripple events and theta oscillations, allowing us to capture neural firing patterns during behaviorally realistic network states (Klausberger and Somogyi, 2008).

Before local network experiments were performed, we first verified our initial findings were preserved under an anesthetized preparation. Similar to the chronic experiments, anesthetized animals ($n = 4$ rats, 7 sessions) were implanted with bilateral fibers targeting dCA3 and recording electrodes were lowered to CA1. Inhibitory cells in CA1 showed the same strong increase in firing during disruption of CA3 as in chronic recordings (Figure 12a-c). Of

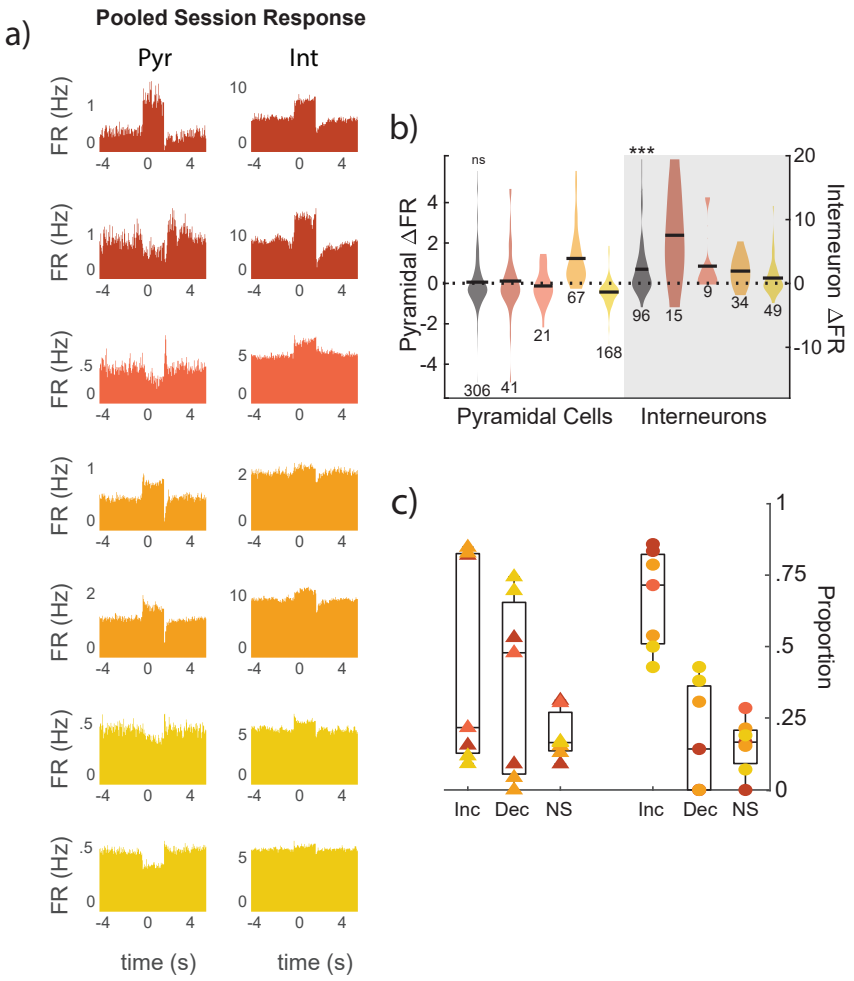

Figure 12: Responses of CA1 cells to CA3 silencing in anesthetized animals.

a-c) Data collected from anesthetized animals a) Pooled session responses as in Figure 11a. b) Firing rate differences. CA1 pyramidal cells showed no significant changes in firing rate during acute silencing of CA3 (paired t-test, mean = 0.06, n = 306, $p = 0.38$). CA1 interneurons increased firing during acute silencing of CA3 (paired t-test, mean = 2.23 Hz, n = 96, $p = 1.4 \times 10^{-6}$). c) Proportion increasing, decreasing and unresponsive pyramidal cells and interneurons to acute silencing of CA1. Pyramidal cells showed a significant number of cells decreased response compared to increase (binomial test, $p = 0.0004$). Significantly more interneurons increased response in CA3 silencing (binomial test, $p = 0.0005$).

the 96 recorded interneurons, 59% showed increases in firing, 26% showed decreases in firing and 15% had no response to light stimulation (Figure 12c). Similar proportions of pyramidal cells showed an increase in firing (31% in acute recordings compared to 28% in chronic recordings, proportion test, $\chi^2 = 0.52$, $p = 0.472$), however a larger proportion of pyramidal cells showed decreased firing (50% in acute recordings compared to 38% in chronic recordings). Together these data indicate that in both awake and anesthetized animals, pyramidal

cell responses were heterogenous while interneurons were consistently disinhibited.

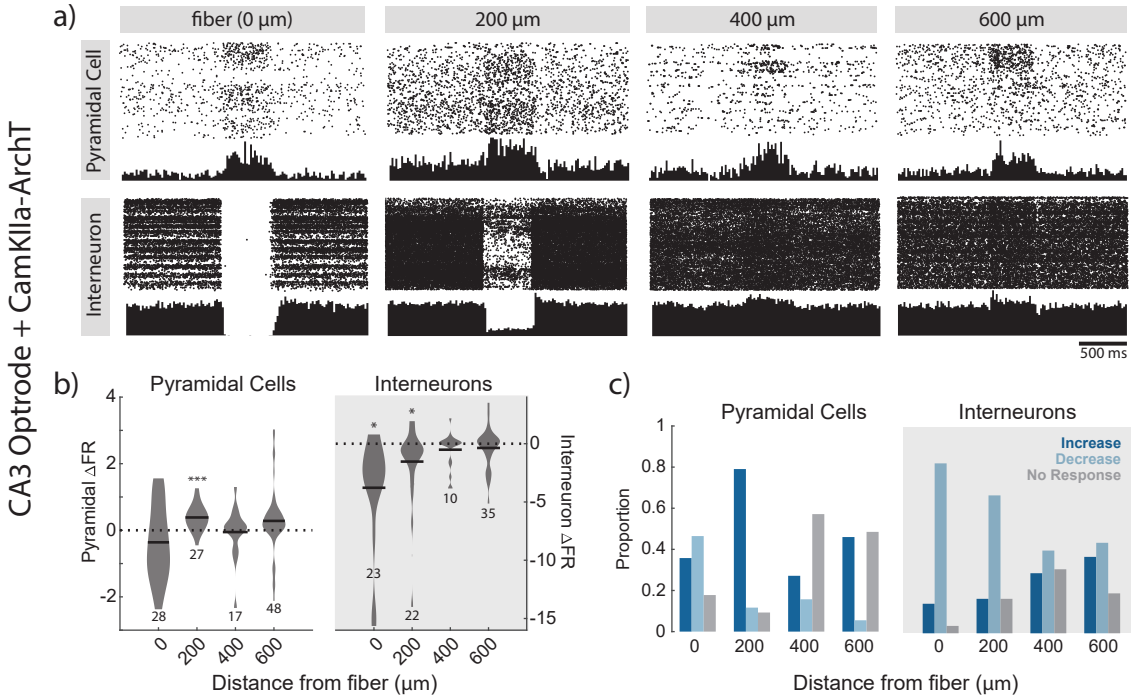

Figure 13: Spatial profile of direct photoinhibition in CA3.

Optrode silencing of CA3 in animals expressing CamKIIα-ArchT. a) Example responses of pyramidal cells (top) and interneurons (bottom) at the location of the fiber and at increasing distances from the site of illumination. b) Population firing rate changes for pyramidal cells (left) and interneurons (right) as a function of distance from the optic fiber. Pyramidal cells 200-μm away from the optic fiber showed a significant increase in firing (mean = 0.38 Hz, n = 27, $p = 2.04 \times 10^{-5}$). Interneurons significantly decreased firing at the site of illumination (mean = -3.78 Hz, n = 17, $p = 0.005$) and 200-μm away (mean = -1.53 Hz, n = 24, $p = 0.03$). c) Proportion of pyramidal cells (left) and interneurons (right) increasing, decreasing, or showing no significant response as a function of distance from the site of illumination. The distribution of responses were different for both cell types as a function of depth (Fisher's exact test, PYR: $p = 0.0006$ INT: $p = 4.7 \times 10^{-5}$).

3.3 Focal silencing of CA3 cells results in disinhibition of CA3 interneurons

To determine whether dCA1 interneurons inherit inhibition from CA3 during optogenetic silencing, recordings ($n = 4$ rats, 8 sessions) were performed in CA3 using integrated opto-electrode devices (Figure 6, (Royer et al., 2010)). Optrodes allow for focused illumination

directed at a subpopulation of cells while simultaneously recording from unaffected cells adjacent to the site of illumination (see Methods, Figure 6b,c). At the site of the fiber, a higher proportion of pyramidal cells decreased firing than decreased firing during photoinhibition (28% increase, 54% decrease, Figure 13c). Pooled firing responses of pyramidal cells revealed net increases in firing 200-μm distant from the site of inhibition. Unexpected, or "paradoxical" population increases were also observed but at a further distance (600-μm) from the site of illumination (Figure 2b). These changes are reflected in the proportion of cells showing increased firing in response to focal silencing. A proportion of pyramidal cells exhibit increased firing at all distances relative to the location of the fiber. This is reflected in the pooled firing rate response, which shows net decreases in excitation but high variability in cell response (Figure 13b). At distances greater than or equal to 200-μm, however, the proportion of cells showing increased firing dominates. Inhibitory cells show a more linear progression of response as a function of distance from the fiber. Locally, the majority of cells show inhibitory responses in line with stimulation. As distance from the fiber increases the proportion of cells exhibiting decreased firing growss while the proportion of excited cells shrinks.

In these data it is difficult to disentangle cells that respond primarily to illumination versus secondary network responses. Two potential confounds in the interpretation are due to the choice of opsin and the opto-electrode design. First, expression of ArchT is not restricted to the cell soma. Studies have reported illumination of axons expressing ArchT can lead to an increase in frequency of synaptic events (Mahn et al., 2016). Even though our illumination window is relatively short, we could inadvertently be increasing firing of distal cells through paradoxical excitation of axons. To examine whether these issues are unique to ArchT suppression, we repeated the experiments using a soma-targeted anion-conducting channelrhodopsin (stGtACR2). Since expression is restricted to the soma and proximal dendrites, confounding effects of axonal stimulation are eliminated. Second, even using our optrode design, it is difficult to restrict light to $< 200 - \mu$m. Combined with variability in

expression levels, it is challenging to disambiguate the immediate and secondary responses at intermediate distances (200-400μm). To restrict illumination further, we used integrated-μLEDs on silicon neural probes for simultaneous optogenetic manipulation and recording (Wu et al., 2015). These probes have the advantage of highly localized targeting. Each shank is equipped with three independently controlled-μLEDs. Power can be adjusted so illumination of one LED can only affect activity on proximal electrodes on the same shank, restricting manipulations to neurons even within a single electrode array.

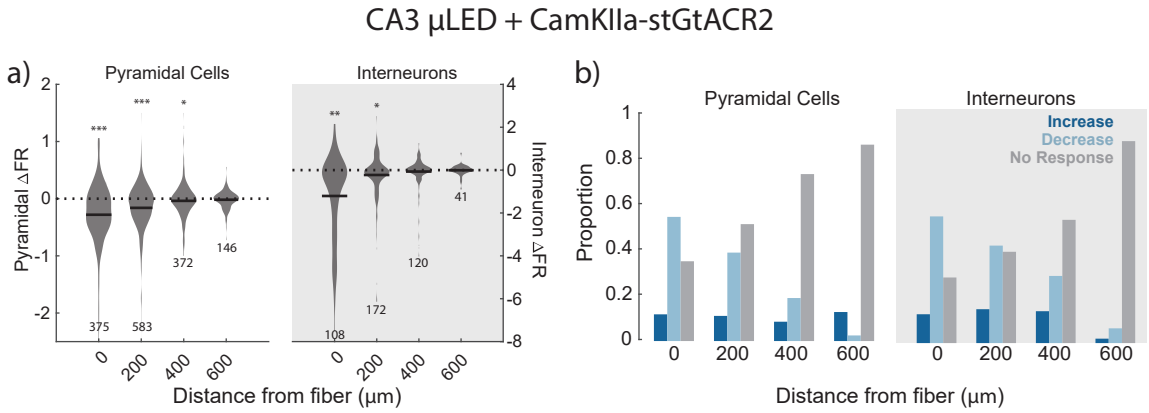

Figure 14: Spatial profile of hyper-focal photoinhibition in CA3.

μLED silencing of CA3 in animals expressing CamKIIα-stGtACR2. a) Both pyramidal cells and interneurons showed significant decreases in firing rate at the site of illumination (paired t-test, PYR: mean = -0.28 Hz, n = 375, $p = 6.79 \times 10^{-18}$ INT: mean = -1.21 Hz, n = 108, $p = 7.12 \times 10^{-9}$) and 200-μm distance (paired t-test, PYR: mean = -0.16 Hz, n = 583, $p = 1.97 \times 10^{-15}$ INT: mean = -0.23 Hz, n = 172, $p = 0.004$). b) The distribution of responses were different for both cell types as a function of depth (Pearson's chi-squared test, PYR: $\chi^2 = 141.8$, df = 6, $p = 2.2 \times 10^{-16}$ INT: $\chi^2 = 68.88$, df = 6, $p = 6.9 \times 10^{-13}$).

Population responses to-μLED silencing (n = 3 rats, 9 sessions) revealed a paradoxical response in a small proportion of both pyramidal cells and interneurons cells at all distances. (Figure 14c). Interestingly a subset of both interneurons and pyramidal cells showed a robust increase in firing on the same shank as the illuminated μLED indicating a subset cells show opposing responses external drive, even under direct illumination (Figure 14b). These data suggest that even under direct illumination, pyramidal cells and interneurons in CA3 do not necessarily respond in line with the direction of external drive. Data from stGtACR2-μLED experiments were consistent, albeit weaker, than data from ArchT-optrode

experiments suggesting increases in stimulation intensity may cause increases in both the proportion and spatial extent of increased excitation due to optogenetic silencing.

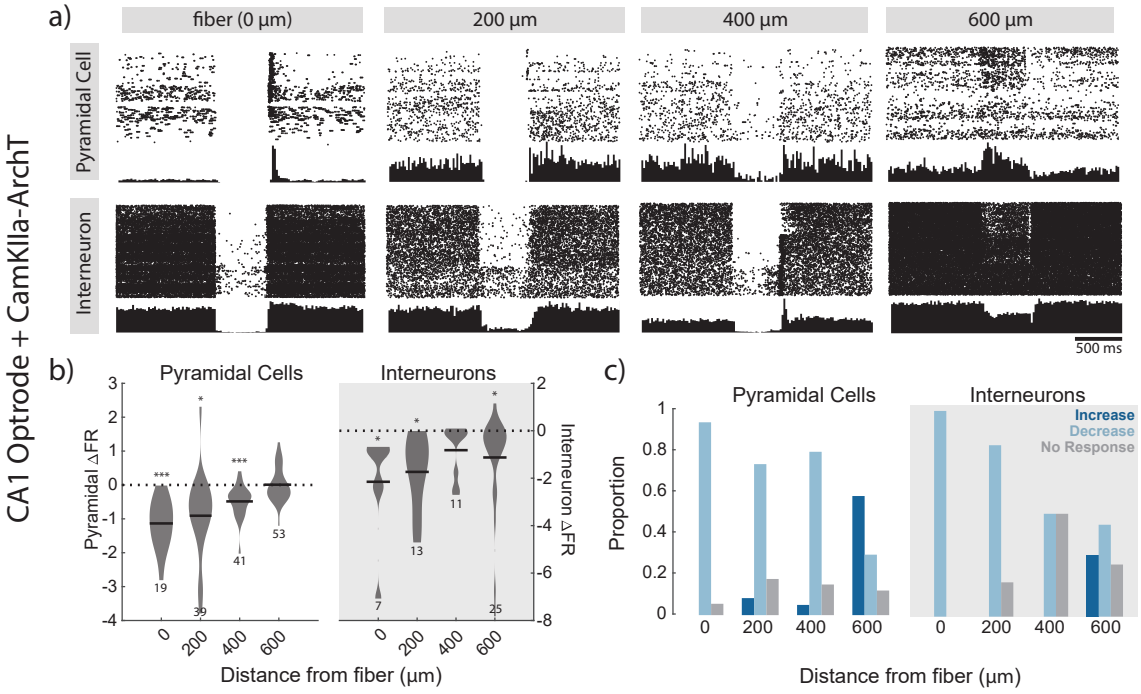

Figure 15: Spatial profile of direct photoinhibition in CA1.

Optrode silencing of CA1 in animals expressing CamKIIα-ArchT. a) Example responses of pyramidal cells (top) and interneurons (bottom) at the location of the fiber and at increasing distances from the site of illumination. b) Population firing rate changes for pyramidal cells (left) and interneurons (right) as a function of distance from the optic fiber. Pyramidal cells showed decreased firing at the site of the illumination (paired t-test, mean = -1.14 Hz, n = 19, $p = 3.25 \times 10^{-5}$) and at 200-μm (paired t-test, mean = 0.91 Hz, n = 39, $p = 0.003$) and 400-μm (paired t-test, mean = 0.49 Hz, n = 41, $p = 4 \times 10^{-5}$) distance. Interneurons showed decreased firing at the site of illumination (paired t-test, mean = -2.15 Hz, n = 7, $p = 0.047$), 200-μm (paired t-test, mean = -1.73 Hz, n = 13, $p = 0.005$), and 600-μm (paired t-test, mean = -1.11, n = 25, $p = 0.002$) distance. b) The distribution of responses were different for both cell types as a function of depth (Fisher's exact test, PYR: $p = 0.04$ INT: $p = 0.04$).

3.4 CA3 and CA1 networks respond differentially to focal perturbations

These results suggest that in highly recurrent networks, such as CA3, focal inhibition results in non-local disinhibition of interneurons. It is currently unknown how networks with weaker intrinsic excitatory connections respond to strong, focal inhibition. To test responses to

external input in regions with weaker excitatory connections, we performed both ArchT-optrode and stGtACR2-μLED experiments in CA1, which has sparse lateral connectivity compared to CA3 (Guzowski et al., 2004).

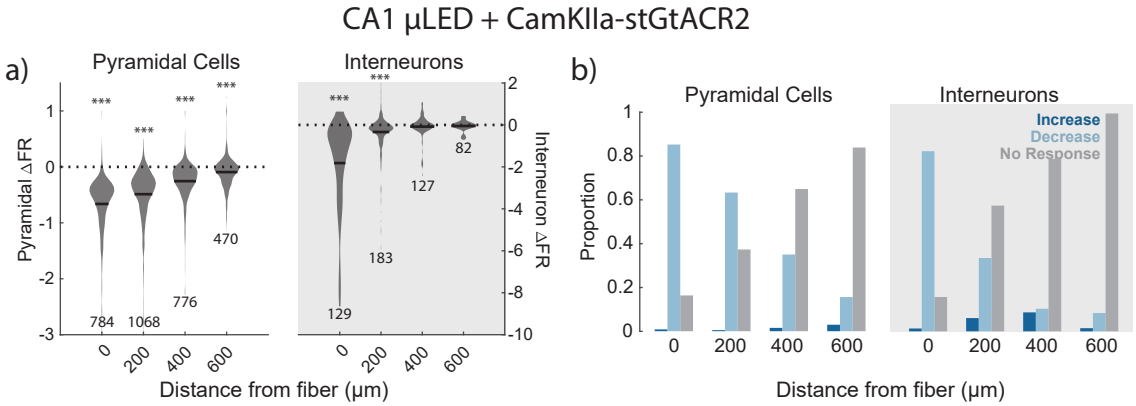

Figure 16: Spatial profile of hyper-focal photoinhibition in CA1.

μLED silencing of CA3 in animals expressing CamKIIα-stGtACR2. a) Pyramidal cells show significant decreased in firing rate at all distances (paired t-test, 0-μm: mean = -0.66 Hz, n = 784, $p = 4.48 \times 10^{-139}$, 200-$\mu$m: mean = -0.19 Hz, n = 1068 , $p = 8.33 \times 10^{-142}$, 400-$\mu$m: mean = -0.25 Hz, n = 776 , $p = 2.34 \times 10^{-66}$, 600-μm: mean = -0.09 Hz, n = 470, $p = 5.2 \times 10^{-11}$). Interneurons showed decreased firing at the site of illumination (paired t-test, mean = -1.82 Hz, n = 129, $p = 3.3 \times 10^{-16}$) and at 200-μm distance (paired t-test, mean = -0.34 Hz, n = 183, $p = 4.58 \times 10^{-7}$). b) The distribution of responses were different for both cell types as a function of depth (Pearson's chi-squared test, PYR: $\chi^2 = 532.05$, df = 6, $p = 2.2 \times 10^{-16}$ INT: $\chi^2 = 116.26$, df = 6, $p = 2.2 \times 10^{-16}$).

In contrast to responses observed in CA3, cell responses ($n = 3$ rats, 6 sessions) to photoinhibition in CA1 using an optrode were roughly linear as a function of distance from the optical fiber. These data are reflected in the population firing rate responses, where firing rates in both pyramidal cell and interneuron populations is significantly suppressed and distances up to 400-μm from the site of illumination (Figure 15b). At a distance of 600-μm from the optical fiber a subset of both pyramidal and interneurons increased firing (Figure 15c). In the case of pyramidal cells, the proportion of cells increasing firing was sufficient to offset the proportion of cells decreasing firing, resulting in no net firing rate changes (Figure 15b). Together these data suggest that in CA1, primary effects of photoinhibition can be observed up to 400-μm from the site of illumination. At distances beyond 400-μm, responses are likely capturing the re-balanced excitation and inhibition within the circuit. Silencing

CA1 in CamKIIα-stGtACR2 rats (n = 3 rats, 7 sessions) resulted in strong silencing of both pyramidal cells and interneurons at the site of illumination (Figure 16c). A negligible number of pyramidal cells showed increased firing in response to silencing at all distances. Interneurons 400-μm away from the site of illumination show a small but equal proportion of cells increasing and decreasing firing. Interestingly CA1 silencing with either technique resulted in nearly complete silencing of both pyramidal cells and interneurons at the site of illumination, perhaps the most stark contrast between responses in CA1 and CA3 to focal silencing where a subset of cells, even under direct illumination, increased their firing.

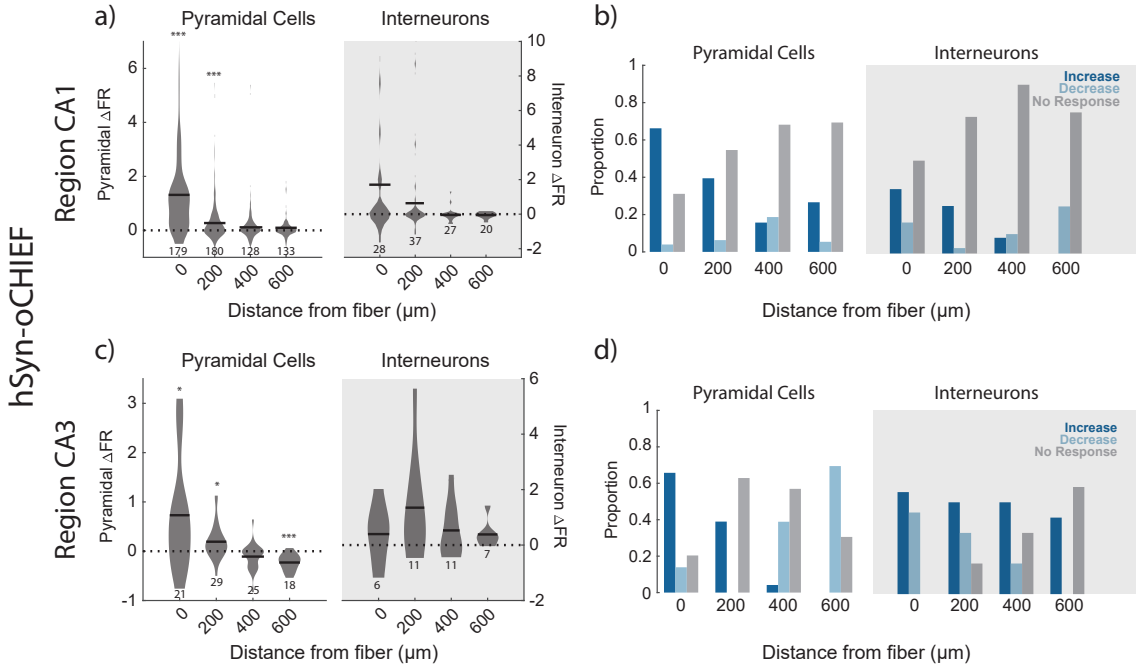

Figure 17: Spatial profile of hyper-focal photostimulation in CA1 and CA3.

Focal stimulation in CA1 and CA3 in animals expressing hSyn-oCHIEF. a-b) Cell responses to focal stimulation in region CA1. a) Pyramidal cell show significant increases in firing up to 400-μm distance from the site of stimulation (paired t-test, 0-μm: mean = 1.31 Hz, n = 179, $p = 1.04^{-23}$ 200-μm: mean = 0.27 Hz, n = 180, $p = 3.75 \times 10^{-7}$ 400-μm: mean = 0.11 Hz, n = 128, $p = 0.03$). Interneurons show no significant changes in firing at any distance. b) The distribution of responses were different for both cell types as a function of depth (PYR: Pearson's chi-squared test, $\chi^2 = 162.17$, df = 6, $p = 2.2 \times 10^{-16}$ INT: Fisher's exact test, $p = 0.003$). c-d) Cell responses to focal stimulation in region CA3. c) Pyramidal cells show significant increases in firing up to 200-μm distance from the site of stimulation (paired t-test, 0-μm: mean = 0.73 Hz, n = 21, $p = 0.008$ 200-μm: mean = 0.19 Hz, n = 29, $p = 0.007$). At 600-μm distance pyramidal cells show a significant decrease in firing rate (paired t-test, mean = -0.23 Hz, n = 18, $p = 1.68 \times 10^{-5}$). Interneurons show no significant changes in firing at any distance. d) The distribution of responses were different only pyramidal cells as a function of depth (Fisher's exact test, PYR: $p = 1.52 \times 10^{-7}$ INT: $p = 0.57$).

Bidirectional manipulations are often used to identify specific cell functions in circuits, however, cell responses to activation and inactivation can produce asymmetric network responses (Phillips and Hasenstaub, 2016). To examine whether external excitatory drive would lead to similar paradoxical responses we infused oCHIEF, an excitatory channelrhodopsin with modified kinetics, in dorsal CA1 and CA3 (Lin et al., 2009). Since networks were stimulated instead of silenced, increases in firing rate at the site of stimulation (ΔFR > 0), are expected. Interestingly, many CA1 cells showed a net decrease in firing to CA1 stimulation ($n = 4$ rats, 9 sessions), with maximal proportions of cells showing decreased firing at 400-μm distance from the LED light for pyramidal cells and 600-μm for interneurons. At 400-μm distance the proportion of pyramidal cells and interneurons showing decreased firing balanced the proportion of cells showing increased firing (Figure 17a). Interneurons exhibited a no significant change in firing at distances greater than or equal to 400-μm (Figure 17a). In CA3, pyramidal cells showed stronger paradoxical inhibition as distance from the site of stimulation increased. At distances 400-μm and 600-μm distance from the site of illumination, net firing rate of pyramidal cells was significantly suppressed (Figure 17c). In contrast to pyramidal cell response, inhibitory cells showed the greatest decrease at the site of stimulation and no differences in proportion of cells increasing response as a function of distance from the site of stimulation (Figure 17d). Differences in response to activation and inhibition are most apparent in CA1. Stimulation resulted in a greater number of cells exhibiting a paradoxical decreased response compared to inhibition, which elicited minimal paradoxical excitation. Consistent in both activation and inhibition experiments was the heterogeneous response of both pyramidal and interneurons at the site of illumination. Together these data suggest that network responses to activation are not necessarily symmetric to network responses to inhibition.

3.5 CA3 and CA1 are inhibitory-stabilized networks

In our experiments measuring network responses in CA3 and CA1 as a function of distance from the site of illumination, we found a large proportion of inhibitory cell response opposed the direction of external drive even under direct illumination. The large proportion of paradoxical responses in CA3 networks compared to CA1 led to the question of whether these effects could be explained by region CA3 operating as an inhibitory stabilized network (ISN, (Tsodyks et al., 1997)). In the case of external inhibitory drive, paradoxical inhibitory responses arise because external drive to inhibitory cells disinhibits excitatory cells. Increased excitation in turn drives the suppressed inhibitory cells. Since more excitatory input from recurrent sources is driving inhibitory cells than suppression from optogenetic silencing the net response of inhibitory cells is increased firing. As external drive is gradually increased, through an increase in laser intensity, stronger inhibition eventually suppresses excitatory cells until they reach a firing rate where the excitatory network is stable in the absence of inhibition. At this point, increasing inhibitory drive to inhibitory cells produces a decrease in firing rates as the network transitions into a non-ISN regime. The net result is an "inverted-U" response inhibitory cells to increases in external optogenetic suppression (Figure 18). At low intensity levels, interneurons are unresponsive to illumination. As the intensity of illumination increases inhibitory cells respond by increasing firing (ISN-regime). At maximal intensity levels, inhibitory cells respond in the direction of external stimulation.

Recent modeling work by Sadeh et al. (2017) explored parameters by which an ISN network would respond paradoxically. The authors found that for a stable ISN, global perturbation of the inhibitory population resulted in a paradoxical response of the network. Since global perturbation is unrealistic under most experimental conditions, the authors considered experimental parameters under which paradoxical responses are still observed. In their model, for an ISN regime to be detected three things must be true; 1) the minimum spatial diameter of 250-μm is required to evoke a paradoxical inhibitory effect, 2) perturbation must target a large proportion of the inhibitory population and 3) optogenetic suppression

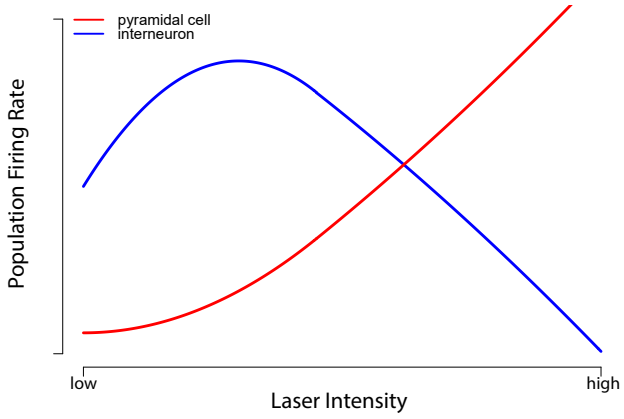

Figure 18: Model of ISN network response to varying intensity of photoinhibition.

Prediction for average neural responses with strong coupling when inhibitory cells are externally suppressed. At low light intensities suppression of interneurons results in a paradoxical inhibitory activation - a counterintuitive increase in firing rate as inhibitory cells receive direct suppression. Due to strong excitatory recurrent coupling, acute suppression of inhibition results in increases in recurrent excitation which ultimately overrides external optogenetic suppression, leading to a net increase in input to inhibitory cells. As external drive increases, the network moves into a non-ISN regime and results in decreases in interneuron firing rates.

is more powerful than optogenetic stimulation at revealing ISNs. This is because inhibitory activation can lead to decreases in excitation. In order for a network to operate as an ISN, a minimal number of excitatory cells must be active (Sadeh and Clopath, 2020). Thus, reduced excitation resulting from inhibitory activation could inadvertently mask an ISN-regime. Controlling for these parameters resulted in unambiguous detection of ISN regimes. Keeping these predictions in mind, we designed an experiment to test whether CA3 operated under an ISN regime. To maximize the spatial size we designed a specialized opto-electrode device integrating fibers with a high-density 4-shank, 128-channel probe (Masmanidis-128, see Methods section 2.3). Fibers were positioned 50-μm above the highest electrode on all four shanks, allowing for even light delivery to an area $\sim$ 600-μm in diameter. To selectively target inhibitory cells, GAD-Cre rats were used to restrict opsin expression to GABAergic expressing interneurons(Sharpe et al., 2017). GAD animals were selected over interneuron subtype specific lines, such as PV+ or SOM+, to maximize the number of interneurons

perturbed. Finally, inhibitory opsin stGtACR2 driven by a Cre promoter was selected to suppress activity. Experiments were conducted in both non-transgenic animals, driven by CamKIIα promoter, and GAD-Cre animals to compare responses of cells to indiscriminate external drive and selective external drive to inhibitory cells respectively. Finally, external drive was varied through laser output power to capture the population response in ISN and non-ISN regimes.

For CA1 CamKIIα experiments (n = 3 rats, 5 sessions), a subset of cells were optogenetically silenced even at light intensities < 0.001 mW. In excitatory cells, a larger proportion of cells decreased firing in response to increases in light intensity(Figure 19a-c). Net pyramidal cell firing decreased at all intensity levels, with nearly all excitation shunted at maximal delivered intensity (~ 0.3 mW). At maximal intensity levels, firing was suppressed in 100% of CA1 interneurons. At lower intensities a proportion of interneurons increased firing rate, with maximal proportion responding at the lowest intensities and shifting to decreased response to illumination as intensity increased (Figure 19b). Still, at the population level, inhibitory cells decreased firing at all intensity levels (Figure 19a). The result was a net decrease in excitation and inhibition in CA1 at all intensity levels with maximal intensity resulting in nearly 100% decrease in cell response.

For CA3 CamKIIα experiments (n = 3 rats, 7 sessions), pyramidal cells displayed similar proportional increases compared to interneurons at maximal intensity levels (Figure 19f, PYR: 28% increase, INT: 21% increase). At lower intensity levels the majority of pyramidal cells either were unresponsive or decreased firing in response to illumination. CA3 interneurons increased firing in response to photoinhibition over a wide range of light intensities. Roughly one-quarter of interneurons increased firing at all intensity levels (Figure 19f, 0.001mW:27% 0.05mW: 28% 0.1mW: 25% 0.15mW: 15% 0.25mW: 21%). As intensity increased a larger proportion of cells displayed a decreased response while a smaller proportion of cells were unresponsive. The population of pyramidal cells decreased firing at all intensity levels while the population of interneurons decreased firing only at higher laser intensity

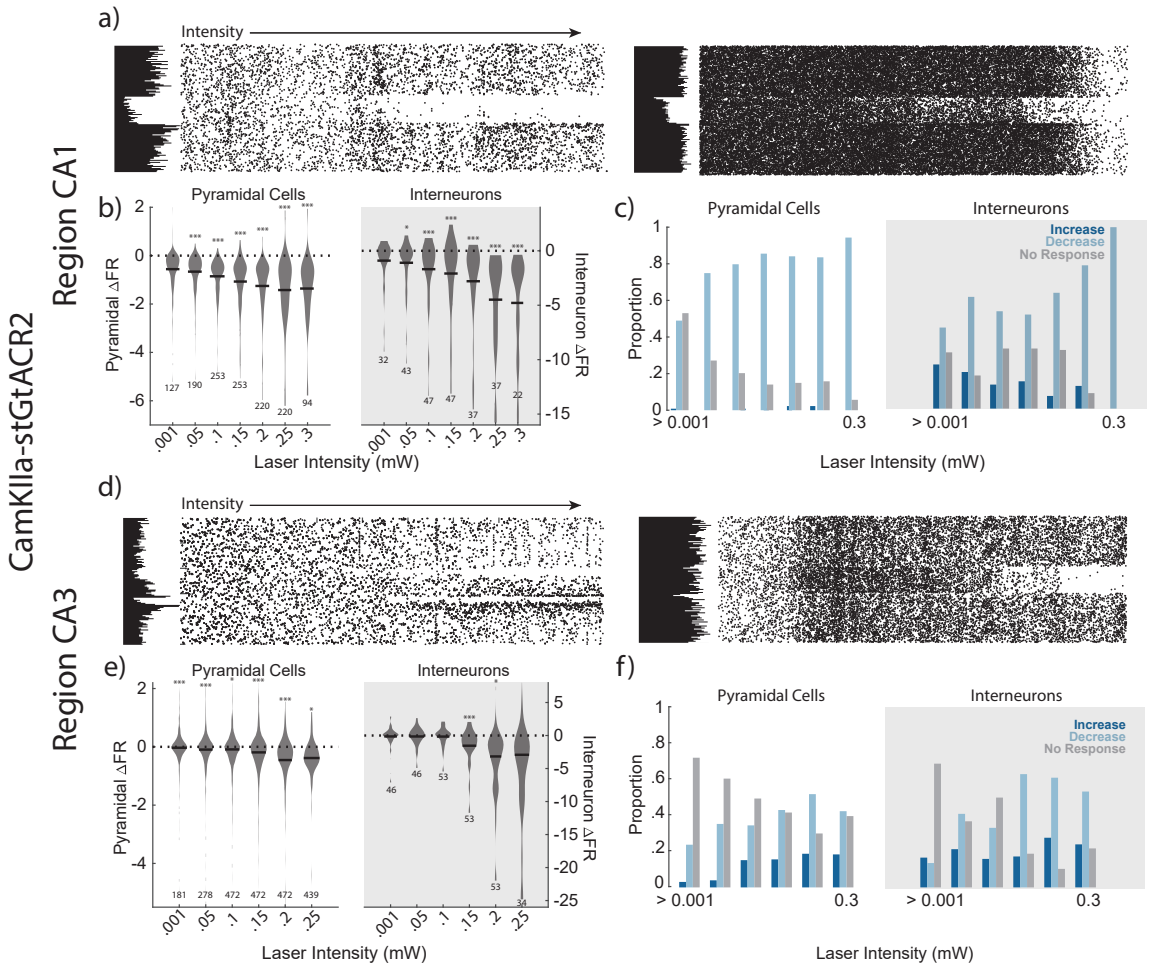

Figure 19: CA1 and CA3 responses to varying external drive.

Broad silencing in CA1 and CA3 in animals expressing CamKIIα-stGtACR2. a-c). Responses of pyramidal cells and interneurons in CA1 to varying intensities of illumination. a) Example response of a pyramidal cell (left) and interneuron (right) as light intensity increases from <0.001 mW to 0.3 mW. b) Firing rate of both pyramidal cells and interneurons decrease as light intensity increases with significant decreases at all intensity levels (paired t-test, PYR: 0.001mW: mean = -1.66 Hz n = 127 p = 1.55×10^{-15} 0.3mW: mean = -0.15 Hz, n = 94, $p = 1.88 \times 10^{-18}$, INT: 0.001mW: mean = -0.1 Hz, n = 32, $p = 0.01$ 0.3mW: mean = -0.9, n = 22, $p = 2.07 \times 10^{-18}$). c) The distribution of responses were different for both cell types as a function of laser intensity (Fisher's exact test, PYR: $p < 5^{-7}$ INT: $p = 0.0002$). d-f) Responses of pyramidal cells and interneurons in CA3 to varying intensities of illumination. d) Example response of a pyramidal cell (left) and interneuron (right) as light intensity increases from <0.001 mW to 0.3 mW. e) Pyramidal cell firing rate decrease as light intensity increases with significant decreases at all intensity levels (paired t-test, 0.001mW: mean = -0.15 Hz, n = 181 p = 1.67×10^{-4} 0.25mW: mean = -0.2 Hz, n = 439, $p = 1.88 \times 10^{-18}$). Interneurons show significant decreases in firing rate at intermediate intensity levels (paired t-test, 0.15mW: mean = -1.76 Hz, n = 53, $p = 5.52 \times 10^{-5}$ 0.2mW: mean = -2.64, n = 53, $p = 0.013$). f) The distribution of responses were different for both cell types as a function of laser intensity (Pearson's chi-squared test, PYR: $\chi^2 = 153.65$, df = 10, $p < 5^{-7}$ INT: $\chi^2 = 55.703$, df = 10, $p = 2.3 \times 10^{-8}$).

levels (Figure 19e). At lower intensity levels, the majority of cells either showed no response or decreases in firing to illumination (Figure 19f. In these experiments, both excitatory and inhibitory cells were directly inhibited so we cannotmake any conclusions as to whether CA1 or CA3 were operating as an ISN. At maximal intensities, responses in both CA1 and CA3 were similar to responses in our focal regime photoinhibition experiments at the site of illumination. CA1 pyramidal cells and interneurons both showed nearly complete silencing, while CA3 cells responded heterogeneously. To expand on our focal manipulation experiments, these results suggest lower intensity levels might result in heterogenous responses of interneurons in CA1 while CA3 interneuron responses were remarkably consistent across a wide range in intensities.

For CA1 GAD experiments (n = 3 rats, 5 sessions), a higher proportion of pyramidal cells increased firing than decreased firing at all intensity levels which is reflected in the mean population response. The proportion of cells with increased firing increased with light intensity. Interneurons responded in an "inverted U" shape as a function of intensity with the highest proportion of cells increasing firing at mid-intensity levels. These data suggest that at high intensities the CA1 network is operating in a non-ISN regime, where inhibitory cells show decreased firing and excitatory cells show predominantly increases in firing. At mid-range intensities, the network is responding as an ISN with paradoxical responses elicited from both pyramidal cells and interneurons.

For CA3 GAD experiments (n = 2 rats, 3 sessions), at mid-range intensity levels interneurons show a weak but significant increase in firing in response to external input (Figure 20e, paired t-test, mean = 0.19 Hz, n = 43, $p = 0.047$). As intensity increases, the inhibitory population shows a higher proportion of cells with decreased responses, though this increase was not reflected in the change in interneuron firing (Figure 20e-f). A shift from increased activity to decreased activity as external drive increases is reflective of a network transitioning from an ISN to non-ISN regime. Pyramidal cells showed minimal responses at lower intensity levels and responded heterogeneously at high intensity levels with small decreases

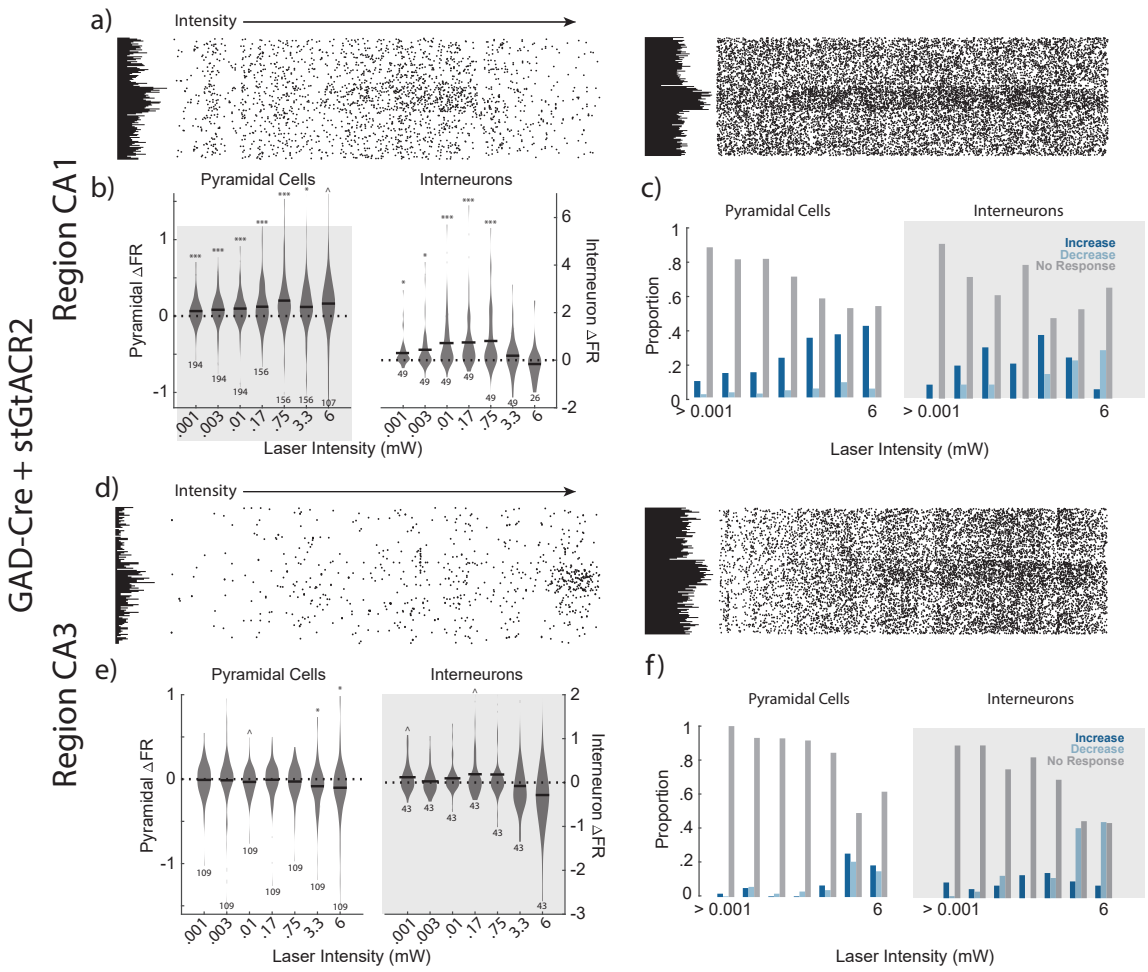

Figure 20: CA1 and CA3 responses to interneuron-specific varying external drive.

Broad silencing in CA1 and CA3 in GAD-Cre rodents expressing stGtACR2. a-c). Responses of pyramidal cells and interneurons in CA1 to varying intensities of illumination. a) Example response of a pyramidal cell (left) and interneuron (right) as light intensity increases from <0.001 mW to 6 mW. b) Pyramidal cells show increased firing at all light intensities (paired t-test, 0.001mW: mean = 0.06 Hz n = 194 p = 3.77×10^{-6} 6mW: mean = 1.16 Hz, n = 107, $p = 0.03$). Interneurons show increased firing rates at low and intermediate but not high intensity light (paired t-test, 0.001mW: mean = 0.3 Hz, n = 49, $p = 0.001$ 0.75mW: mean = 0.81, n = 49, $p = 1.05 \times 10^{-4}$). c) The distribution of responses were different for both cell types as a function of laser intensity (Fisher's exact test, PYR: $p < 5^{-7}$ INT: $p < 5 \times 10^{-7}$). d-f). Responses of pyramidal cells and interneurons in CA3 to varying intensities of illumination. d) Example response of a pyramidal cell (left) and interneuron (right) as light intensity increases from <0.001 mW to 6 mW. e) Pyramidal cells show moderate firing rate decreases at high intensity levels (paired t-test, 3.3mW: mean = -0.08 Hz, n = 109 p = 0.002 6mW: mean = -0.1 Hz, n = 109, 0.0045). Interneurons show small but significant increases in firing at 0.001mW (paired t-test, mean = -0.12 Hz, n = 43, $p = 0.02$) and 0.17mW (mean = 0.19 Hz, n = 43, $p = 0.047$).f) The distribution of responses were different for both cell types as a function of laser intensity (PYR: Pearson's chi-squared test, $\chi^2 = 92.816$, df = 12, $p = 1.4^{-14}$ INT: Fisher's exact test, $p < 5 \times 10^{-7}$).

in net firing rate (Figure 20c-d). Taken together, these experiments suggest that both CA1 and CA3 operate as an ISN under physiological parameters.

3.6 Discussion

We optogenetically disrupted hippocampal circuits to examine the effect of photoinhibition on projections from CA3 to CA1 and local short-range projections in networks with varying degrees of reciprocal excitation. Results of these experiments provide valuable information on how networks respond to acute optogenetic perturbations. Suppression of CA3 resulted in an unexpected increase in inhibitory firing in CA1. Since no evidence was found for disinhibitory circuits in the CA1 network, increased disinhibition was likely a reflection of increased firing inherited from CA3. Local perturbations of CA3 revealed heterogeneous responses of both pyramidal and interneurons at the site of illumination. The proportion of interneurons with increased firing increased as a function of distance from the site of illumination and was dependent on the spatial spread and intensity of illumination. In contrast, cells in CA1 responded strongly and in line with the external drive. The proportion of responsive cells decreased as a function of distance from the site of illumination. Broad illumination at varying intensities in CA3 and CA1 regions revealed CA1 to be operating as an ISN. While evidence was weaker in CA3, interneurons showed increased responses at intermediate intensities, both in firing rate and proportion of the total population. Together these data show a disconnect between whether networks operate as ISNs and local off-target responses of networks to focal perturbations. This disconnect is likely the reflection of local circuits and can provide insights into how networks with varying connectivity respond to acute perturbations of excitatory-inhibitory balance.

ISNs in hippocampal subregions CA1 and CA3

When pyramidal cells are sufficiently silenced, networks move into a non-ISN regime(Tsodyks et al., 1997). Consistent with this prediction, paradoxical responses were not observed when opsins were expressed in both pyramidal cells and interneurons. When external input was restricted to interneurons, CA1, and to a smaller extent, CA3 operated as an ISN. While this finding seemed counterintuitive because of differences in circuit architecture between

the regions, it agrees with work showing that sparsity in local recurrent connectivity can still produce ISN responses as long as the average total of inhibitory and excitatory synaptic strength is maintained (Sadeh et al., 2017). While reciprocal pyramidal cell connectivity in CA3 is stronger than CA1, both networks responded paradoxically to mid-range levels of illumination.

Differences in response to broad perturbations in CA1 and CA3 could be due to a number of technical factors. Modeling work has proposed that a large proportion of interneurons must be manipulated in order to successfully detect of ISNs (Sadeh et al., 2017). To maximize the number of light-sensitive interneurons, we used a GAD-Cre transgenic rodent model in combination with a Cre-dependent AAV virus encoding the light sensitive, anion-conducting channelrhopsin stGtACR2. Indiscriminate targeting of interneurons has been shown to amplify paradoxical responses in ISN networks, though it is still necessary to stimulate a sufficient number of interneurons. Previous work by (Sanzeni et al., 2020) showed viral methods for opsin expression were insufficient to produce a paradoxical response, even in ISN networks. In their study, paradoxical responses were evoked using a transgenic but not viral opsin expression. Discrepancies in their finding were attributed to reduced expression of light-sensitive proteins and thus insufficient numbers of stimulated cells when viral expression methods were used. Even at high intensity levels, the majority of interneurons remained unresponsive to light, suggesting lack of expression may play a factor in our weak light-evoked responses.

Another possibility is our silencing only targeted one type of interneuron since the fibers were all located at a single depth relative to the pyramidal layer. In ISN networks with multiple inhibitory populations, perturbation of only one subtype of interneuron can result in mixed responses in non-perturbed populations (Litwin-Kumar et al., 2016). Focused silencing on one particular interneuron subtype could mask detection of ISNs by eliciting heterogeneous responses across the interneuron population. Thus, we cannotrule out that lack of sufficient expression or interactions between interneuron populations contributed to

our experimental findings. However, whether a network acts as an ISN does not predict the response of the network to focal perturbations, which likely capture connectivity motifs specific to the region.

Intraregional off-target effects of focal perturbations

Focal silencing of CA1 resulted in strong inhibition of both pyramidal cell and interneurons at the fiber. The large proportion of interneurons suppressed by photoinhibition is likely due to non-specificity in CamKIIα promoter which has been shown to drive expression in both pyramidal cell and interneuron populations (Nathanson et al., 2009; Schoenenberger et al., 2016). Assuming local responses in both excitation and inhibition were driven by opsin expression and not secondary network responses, the effect of photoinhibition extended laterally beyond the spatial spread of light (Li et al., 2019). Restricting both the intensity and size of illumination reduced both the spread of photoinhibition and the emergence of off-target disinhibitory effects.

Focal photoinhibition of CA3 produced off target increases in both pyramidal and interneuron firing, with greatest gain in pyramidal cells adjacent to the fiber. Restricting the area and intensity of photoinhibition reduced the proportion of both pyramidal cells and interneurons with paradoxical increases in firing, resulting in decreases in population firing across all distances. Compared to CA1, focal silencing and stimulation of CA3 resulted in high variability in response at the site of illumination. This suggests that focal manipulations under specific network architectures result in non-intuitive responses even at the fiber. These data were consistent with CA3 responses under broad illumination, which showed increased interneurons firing over a wide range of intensities (Figure 19. Together these data suggest that highly reciprocal networks are more likely to respond paradoxically to external drive. Decreasing the range and intensity of illumination reduced off-target responses in both CA3 and CA1 networks.

Interregional off-target effects of photoinhibition

Photoinhibition of area CA3 results in a paradoxical increase in interneuron firing in CA1. These responses appear to be inherited from increased CA3 excitation, though local interneuron interactions cannot be entirely ruled out. Recent studies suggest that cortical circuits can exhibit paradoxical effects due to disinhibition rather than inhibitory-stabilization mechanisms (Moore et al., 2018; Mahrach et al., 2020). Inadvertent suppression of CA3 interneurons could result in feedforward excitation to CA1 outweighing local CA3 suppression. The net result would be an observed increase in downstream interneuron firing. Our recordings predominantly targeted interneurons adjacent to the pyramidal layer. Local disinhibition of PV+ interneurons can only arise from pyramidal cell, SOM+, PV+ circuit, where by decreased firing of SOM+ cells would result in increased PV+ firing (Pfeffer et al., 2013). In CA1, PV+ interneurons have somas situated in the stratum radiatum adjacent to pyramidal cell bodies while SOM+ interneurons are predominantly found in the stratum oriens. If disinhibition of interneurons were due to feed-forward mechanisms, measurement of interneuron responses in different layers of CA1 would reveal layer dependent firing rate changes. This pattern was not observed in our data, however this effect may be due to under sampling of non-PV interneurons.

Photostimulation has been shown to produce effects as far away as 2.5 mm, impacting the responses of cells in nearby regions (Li et al., 2019). The spatial spread of inactivation is largely dependent on the structure of long-range feedforward and feedback connectivity. Strong feed-forward input between CA3 and CA1, and inhibitory feedback from CA1 to CA3 supports the idea that CA1 responses to CA3 inactivation could also be explained through photo-manipulation (Sik et al., 1994). Strong feedback inhibition from CA1 to CA3 has been proposed to act as a synchronization mechanism between regions. In our case, increased inhibition in CA1 may serve as a feedback mechanism to further suppress firing in CA3 through feedback inhibitory mechanisms.

Effects of anesthesia on firing rate and E/I balance

The majority of these experiments were performed under anesthesia and it is reasonable to question whether these results are translatable to awake states. Many anesthetics reduce overall excitability which effectively leads to a reduction in both excitatory and inhibitory synaptics weights(Campagna et al., 2003). The outcome is networks are more stable under anesthesia resulting in weak expression of ISNs. Some studies report a reduction in firing rate of hippocampal units under urethane anesthesia (Mercer Jr et al., 1978) while others find no changes in spontaneous firing rate (Stewart et al., 1992). In our own recordings no differences were observed in firing between awake and anesthetized states. Similar levels of excitation explain similarities in our responses of CA1 interneurons to CA3 inactivation in awake and anesthetized states. Furthermore, recent studies from Sanzeni et al. (2020) found no transition out of inhibition during anesthesia, even at lower network states. Together with our findings, these data suggest urethane anesthesia preserves the excitatory-inhibitory balance in hippocampal and cortical circuits.

3.7 Conclusions

Optogenetic manipulations produce network responses both in local and downstream circuits. Responses of networks to optogenetic interrogation depend on a multitude of parameters including but not limited to, brain region, intensity of illumination, and spatial scale of illumination. Off-target responses are common, often non-intuitive and can affect not only local network activity but downstream brain regions. Taking into consideration not only the primary effects of perturbation but the secondary network responses is crucial to appropriately interpreting experimental findings.

4 Discussion

This dissertation adds to an important body of literature examining the role of optogenetics as a method to interrogate circuit function especially in relation to unique hippocampal circuits which support learning and memory. This discussion, in three parts, will revisit several topics from Chapter 1 in the context of our experimental findings in Chapter 3. The first section, Section 4.1 examines how optogenetics can be used to evaluate the computational role of CA3 and CA1 hippocampal circuits by considering both the network regime and the contribution of local excitatory-inhibitory circuits in shaping activity patterns. Section 4.2 then asks, how experimental design impacts the interpretation of our results. Further, are we able to tease apart network responses to acute perturbation from the confounding effect of optogenetic techniques? Lastly, the methods used in this dissertation were focused on disruption of ongoing activity through optogenetic intervention, however this is not the only method available for circuit manipulations. Section 4.3 examines the best way to genetically manipulate neuronal activity depending on the scientific question.

4.1 Optogenetics as a way to understand circuit function

4.1.1 Detection of network regimes

We can reframe viewing unexpected responses to optogenetic perturbations by instead understanding that these phenomena reflect the action of complex physiological circuits. Understanding network effects can be difficult if our interaction with the circuitry is only observational.

Simultaneous recording and manipulation of neural activity can elucidate regimes of operation in networks, especially contrasting the role of feedforward versus recurrent networks. Previous chapters extensively explored the use of optogenetics to examine whether networks are operating in an inhibitory-stabilized network (ISN) or non-ISN regime, which can be identified through selective perturbation and measured responses of local interneurons. The

main predictions for ISN are 1) strong recurrent excitatory connections result in network instability in the absence of inhibition and 2) interneurons respond out of phase with weak but not strong levels of external drive. The majority of theoretical and experimental work examining the implications of ISNs in circuit computation has been focused on cortical regions. ISNs are well suited for computations such as balanced amplification which allows certain inputs to produce large outputs while suppressing other inputs or amplifying them to a smaller degree (Miller, 2016). These dynamics can explain why spontaneous activity in the cat primary visual cortex has structure resembling evoked responses to orientation stimuli (Murphy and Miller, 2009). To our knowledge, no previous experiments have been performed to address whether hippocampal networks are inhibitory stabilized and the computational benefit of hippocampal ISNs, despite region CA1 serving as the inspiration for the original model (Tsodyks et al., 1997). However, models of cortical networks suggest ISNs are capable of stabilizing memory states in associated memory networks (Rubin et al., 2017). Taken together, ISNs likely support functions of the CA3 autoassociative network, such as pattern completion. Causal identification of various circuit architectures can help generate hypotheses on what computations are performed in different brain regions, though a consensus has still not been reached on how to best identify networks in various regimes.

Recent work by Sanzeni et al. (2020) provides a convincing argument that inhibitory stabilization is a widespread property of cortical circuits. They find robust paradoxical inhibitory responses to optogenetic inhibitory stimulation in mouse visual, somatosensory, and motor cortices. Previous models have predicted ISNs are state dependent and only emerge with increasingly strong external drive (Ahmadian et al., 2013). However, Sanzeni et al. (2020) found ISN effects in paradigms restricting external sensory stimulation and during light isoflurane anesthesia suggesting ISNs can be detected in states with a range of E/I balances. Interestingly, paradoxical effects were only observed in transgenic, not viral, opsin expression in PV interneurons, likely due to insufficient interneuron expression in viral transduced animals. These data support modelling work suggesting that the role of

inhibition in stabilizing networks requires a large proportion ($> 70\%$) of interneurons to be perturbed in order to evoke a paradoxical response (Sadeh et al., 2017). Lower expression levels in inhibitory cells due to viral opsin rather than transgenic expression can potentially account for low proportion of light-responsive cells in our experiments, even at high light intensities (Figure 20).

Most models of ISNs treat inhibitory cells as a homogenous population. As described in Chapter 1 Section 1.3, cortical and hippocampal interneurons have substantial heterogeneity in the connectivity, function and dynamics of different inhibitory neuron subtypes. In the visual cortex, SOM+ neurons are strongly inhibited by VIP+ neurons. VIP neurons disinhibit excitatory pyramidal neurons through suppression of SOM+, while activation of PV+ and SOM+ shapes excitatory response to external stimuli (Pfeffer et al., 2013). In the hippocampus PV+ and SOM+ potentially play a similar role shaping activity and turning cell responses but in spatial rather visual receptive fields (Royer et al., 2012; Fernández-Ruiz et al., 2017). O-LM type cells make up the largest percentage of SOM+ cells in the hippocampus. These cells receive input from principle cells and in turn inhibit apical dendrites which receive input primarily from the entorhinal cortex (Leão et al., 2012). From the beginning to the end the place field, sustained firing of pyramidal cells results in the increased recruitment of SOM+ interneurons targeting distal dendrites resulting in decreased influence of ECIII input (Katona et al., 1999). Increased recruitment of SOM+ interneurons is mirrored with decreased recruitment of PV+ neurons that target the proximal dendrites and somatic region of pyramidal cells, resulting in an increased influence of CA3 input on place fields as the animal traverses the place field (Klausberger and Somogyi, 2008; Fernández-Ruiz et al., 2017).

To address whether networks with heterogeneous inhibitory neuron populations produce responses out of phase with the direction of external drive, Litwin-Kumar et al. (2016) modeled cortical (V1) network dynamics in ISN and non-ISN networks with three classes of inhibitory neurons: PV+, SOM+ and VIP+. These three interneuron classes comprise

80-90% of inhibitory neurons in cortical area V1 (Rudy et al., 2011). Each class of interneuron was modeled as a single population and coupling parameters were based on findings by Pfeffer et al. (2013) (Figure 21a). Unsurprisingly, modeling circuits with multiple interneuron subtypes paints a significantly more complicated picture. In their model, activation of VIP+ neurons increased the gain of excitatory neurons through disinhibitory mechanisms. Depolarization of VIP neurons in both non-ISN and ISNs resulted in the suppression of SOM+ and activation of excitatory cells. Differences in ISN and non-ISN networks were only apparent through measurement of relative inhibitory current to excitatory cells (Figure 21 b-c (bottom)). In an ISN, measuring the inhibitory current revealed a decrease in inhibition and excitation but the response is not visible in the firing rates of the inhibitory population. Stimulated inhibitory cells responded non-paradoxically while non-stimulated interneurons exhibited paradoxical decreases in firing. When networks contain only one inhibitory population, the inhibitory firing rates can thus be used as a proxy for current. This assumption does not hold up when multiple inhibitory subpopulations are present. In these networks, recurrent interactions can dissociate the firing rate of particular subpopulations with the total level of inhibition received by excitatory neurons. Together these data show detection of ISNs is more complicated in biologically realistic scenarios when intracellular current measurements are not feasible.

More recent modelling work by Sadeh et al. (2017) and experimental results of Sanzeni et al. (2020) found paradoxical responses by stimulating either PV+ alone or indiscriminate stimulation of all interneurons. The main difference in these results from the proposed response by Litwin-Kumar et al. (2016) stems from which interneuron populations are perturbed. In Litwin-Kumar et al. (2016) perturbation was restricted to only one subtype of interneuron while responses were measured in non-manipulated interneurons and excitatory cells. In the Sadeh et al. (2017) model and experiments by Sanzeni et al. (2020) external input was provided either to PV+ interneurons or to all interneurons simultaneously. Stimulating PV+ interneurons alone may be sufficient to evoke paradoxical responses in the

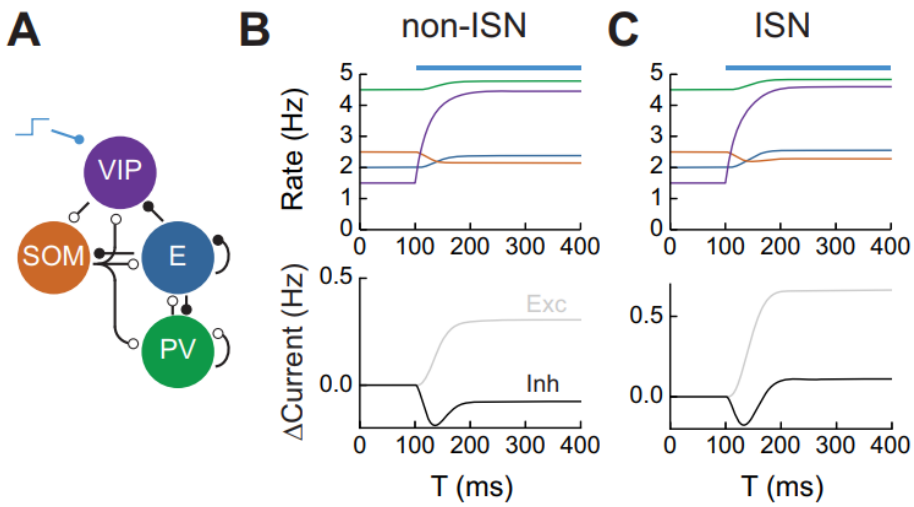

Figure 21: Litwin-Kumar et al. (2016) Model.

Connectivity of interneuron populations and stimulation response in an ISN and non-ISN network. a) connectivity between neuronal subtypes. Open circles represent inhibitory synapses and closed circles represent excitatory synapses. b) *top:* firing rates of neuronal subpopulations in a non-ISN in response to VIP activation at $T = 100ms$. *bottom:* change in magnitude of total excitatory and inhibitory current recieved by the excitatory population. c) same as in b but for ISN. Figure borrowed from Litwin-Kumar et al. (2016).

network since PV+ cells receive input from many excitatory cells and in turn target nearby excitatory cells with strong per-somatic synapses (Bock et al., 2011; Fino and Yuste, 2011). These data suggest inhibitory cells may show a paradoxical effect based on the strength of synaptic influence on other neurons in the network. Other inhibitory classes may contribute but are unable to produce paradoxical network responses when stimulated alone since no single population contributes enough inhibition to satisfy the requirements of ISN detection (Mahrach et al., 2020). Additionally, brain states can modulate dynamical regimes, varying the degree of inhibitory stabilization during behaviors such as locomotion or under anesthesia (Fu et al., 2014).

Our own experiments found that CA1 operates in an ISN regime, though data were inconclusive as the whether CA3 was inhibitory stabilized. In CA1, suppression of interneurons resulted in a gradual increase in the population response of pyramidal cells as a function of increased intensity. In contrast, at low laser intensity levels, interneurons showed no response to external drive. As external drive increased, a higher proportion of interneurons showed

paradoxical increases in firing rate response. At the highest laser intensity levels, paradoxical increases in firing were replaced with decreased responses congruent with the external drive (Figure 20). These results are in line with our predictions for network response to interneuron suppression in an ISN-regime (Figure 18). Similar dynamics in response to increases in laser intensity were observed in CA3, however at all intensity levels, only a small subset of cells showed any significant modulation. The low proportion of responsive cells in CA3 was likely due to low expression levels in the inhibitory population (as reported in Sanzeni et al. (2020)). Silencing only a subset of interneurons may result in insufficient increases in excitation which in turn prevents paradoxical increases in interneuron firing. While a subset of interneurons may still respond paradoxically to external input, heterogeneity in the response of other cells makes it difficult to conclude whether the network is responding as an ISN or due to other mechanisms.

Despite evidence that both CA1 and likely CA3 operate in an ISN-regime, focal perturbations result in drastically different network responses. The most striking difference between these regions is the high variability of response of CA3 cells under direct illumination. An expectation of optogenetic manipulations is cells expressing excitatory (inhibitory) opsins and receiving direct stimulation (suppression) will respond with an increase (decrease) in firing rate. While cells under direct illumination in CA1 responded in line with the external drive, cells in CA3 responded heterogeneously. At the site of the fiber, cells in CA3 showed mixed responses regardless of the opsin expressed or the light delivery method.

Differences in response between CA3 and CA1 could be due to differences in the strength of synaptic connections between excitatory and inhibitory populations. Stronger coupling from excitatory to inhibitory cells, (equivalent to J_{ei} in Figure 5a), would result in amplified inhibitory responses to smaller changes in excitatory firing. Removal of excitatory input in networks with strong J_{ei} would therefore result in robust disinhibition of inhibitory cells. This interpretation is in line with the function of CA3 as an autoassociative network. If strong recurrent connections are designed to amplify weak input, increases in inhibition

combined with decreases in excitation further amplify the response of excitatory cells within the circuit.

4.1.2 The role of CA3 in shaping activity patterns in CA1

A more comprehensive examination of previous studies investigating the role of CA3 in shaping CA1 activity patterns can be found in Chapter 1 Section 1.3.1. For the purposes of this discussion, I will focus on previous findings in the context of our finding that silencing CA3 input to CA1 resulted in a robust firing rate increase in CA1 interneurons.

Schaffer collateral projections synapse preferentially on interneurons located adjacent to the pyramidal cell layer. Perisomatic inhibition, in contrast to dendritic inhibition, is highly effective at regulating spike timing. One consistent finding across studies silencing CA3 input to CA1 is a disruption in the spike timing of pyramidal cells which may be due to dysregulation of perisomatic CA1 interneurons in the absence of CA3 input. Pharmacogenetic block of Schaffer collateral synaptic transmission abolished theta sequences, but not single cell phase precession in CA1 (Middleton and McHugh, 2016). Stimulation of PV+ interneurons during theta oscillations disrupts within-theta timing of spikes, resulting in a shift in phase preference to the trough of theta (Royer et al., 2012). These data suggest that increased perisomatic interneuron firing is a likely mechanism for disrupting coordinated spiking activity during theta oscillations. During offline states, pharmacogenetic blockade of CA3 synaptic transmission reduces CA1 ripple frequency and disrupts ripple-associated coordinated reactivation of CA1 cell pairs (Nakashiba et al., 2009). Tonic activation of PV+ interneurons cannot induce LFP ripples, however it can organize ripple frequency spike-timing of both pyramidal cells and interneurons (Stark et al., 2014) . If spike timing during ripples is set by interneuron-interneuron interactions, dysregulation of CA1 interneuron firing in the absence of CA3 is likely to disrupt coordinated ripple firing and thus replay content. Acute silencing, in contrast to long-term manipulations of CA3 synaptic terminals drastically reduced place cell firing during active exploration and abolished SWRs (Davoudi and Foster, 2019). These

results were surprising given that other studies have reported only minimal changes in place field response under chronic removal of CA3 input to CA1 (Nakashiba et al., 2008; Middleton and McHugh, 2016). Furthermore, CA1 receives multiple excitatory inputs, which should provide redundancy in the absence of CA3 (Nakashiba et al., 2008). One explanation of these findings would be inadvertent direct suppression of CA1 pyramidal cells. Since the fiber was targeted at ArchT-expressing Schaffer collateral synaptic terminals in CA1, expression of ArchT in any CA1 pyramidal cells would result in direct silencing of place cells. Assuming the measured response is in fact due to effective silencing of CA3 input to CA1, suppression of place fields could be due to an increase in local CA1 interneuron activity, similar to the responses observed in our experiments (Figure 11 and Figure 12). In our experiments, silencing CA3 resulted in increased firing of CA1 perisomatic interneurons, including PV+ cells. PV+ cells consist of two subtypes: PV+ basket cells and axo-axonic/chandelier cells (AACs). AACs selectively terminate on the axonal initial segment of pyramidal cells. Increased firing of AACs, in the absence of CA3 input, would result in shunting of any spiking from the post synaptic pyramidal cell and suppression of place field expression.

None of these studies report changes in interneuron firing in response to CA3 inactivation, so with the exception of our study, the role of interneurons in shaping activity in the absence of CA3 is only speculative. However, studies of CA1 circuits in response to changes in excitatory-inhibitory balance support the role of PV+ interneurons in spike-timing and ensemble coordination. Therefore, dysregulation of perisomatic interneurons can account for the disruption of temporal coding during theta and sharp-wave ripples and even the silencing of active place cells. The degree of CA1 network response in the absence of CA3 input is likely due to differences in silencing technique. Chronic silencing methods likely shifts the E/I balance producing tonic changes in interneuron firing rate while optogenetic methods can produce robust, transient changes in firing capable of shunting the activity of cells.

4.1.3 Local excitatory-inhibitory circuits

Silencing CA3 through pharmacogenetic blockade of synaptic transmission, or through optogenetic silencing at the cell body not only disrupts CA3 output to CA1 but also the auto-associative synapses in the local recurrent network. To avoid the confounds of terminal illumination, we chose to silence activity at the cell body, which has the added potential consequence of disrupting not only the output of CA3 but the activity within the CA3 network. Since our optogenetic perturbations of CA3 directly relate to activity inherited by CA1 we needed to understand how silencing CA3 shapes local network responses.

Our results closely examine the effects of a variety of optogenetic manipulations in terms of firing rates, mostly at the population level. Focal inhibition of CA3 using both an optical fiber and uLED illumination produced heterogeneous interneuron responses at all distances from the site of illumination. As distance from the light source increased, so did the proportion of interneurons with increased firing. At all distances from the light source a proportion of pyramidal cells also showed increased firing in response to photoinhibition. In optrode recordings, at distances greater than or equal to 200 μm a higher proportion of excitatory cells showed increases in firing. The spatial range of our recordings were limited to the span of our high-density electrode array, though data from *in vitro* hippocampal recordings indicated field potentials generated by a single interneuron can be detected at multiple sites over distances of more than 800 μm along the stratum pyramidale (Bazelot et al., 2010). This suggests local changes in interneuron firing can produce responses along the lateral axis far beyond the area of illumination. We can conclude that somatic targeted photoinhibition of CA3 produces widespread heterogenous responses across the network, potentially favoring excitation over inhibition at sites away from illumination (Figure 13c). Our recordings from CA1 while silencing CA3 are then likely capturing an increase in excitation inherited from CA3.

One unresolved question relates to the underlying circuit mechanisms that give rise to increases in pyramidal cell and interneuron firing under direct illumination in CA3 but not

CA1. Population responses to inhibitory drive in both CA3 and CA1 showed paradoxical increases in firing at mid-range intensity levels, so differences in response to focal perturbations are likely the result of either differences in local circuitry or differences in synaptic strength from excitatory to inhibitory cells. Local excitatory-inhibitory interactions may differ between CA3 and CA1 and can be determined by measuring the responses of subpopulations of interneurons in both regions. Classification of CA1 interneurons are well characterized and can be achieved through a combination of anatomical location and modulation with respect to theta oscillations and SWRs (Klausberger and Somogyi, 2008; Royer et al., 2012). Less is known about the functional connectivity in CA3 compared to CA1, though most perisomatic cells show stereotyped behavior with respect to ongoing oscillations. PV+ basket cells form synapses on the proximal dendrites of pyramidal cells and, like CA1, control the precise timing of firing of pyramidal cell assemblies (Beyeler et al., 2013). During sharp wave events, PV+ basket cells are the most active while AACs were silent (Hájos et al., 2013). Classifcation of interneurons in CA1 and CA3 can help determine whether the responses of cells to perturbations can be mapped on to various cell types and whether that mapping differs between hippocampal region.

Differences in responses between CA3 and CA1 to focal optogenetic perturbations could also be due to differences in synaptic strength from excitatory to inhibitory cells between regions. This hypothesis, laid out in Section 4.3.1 proposes strong synaptic weights between pyramidal cells and interneurons in CA3 as an underlying mechanism for increased firing responses. We can test this hypothesis by measuring spike transmission probabilities between excitatory-inhibitory cells pairs. Measuring the distribution of connection probability and strength between regions could reveal differences in functional connectivity between CA3 and CA1 and help further elucidate the local network responses to optogenetic perturbations.

4.2 Disentangling primary and secondary effects of optogenetics

Optogenetics provides neuroscientists with a toolkit to investigate whether specific cells, regions and pathways contribute to brain function and explain roles of distinct circuit elements. However, like any experimental method, use of optogenetic techniques can result in side effects that complicate experimental design and interpretation. These undesired effects can arise from variance in protein expression, circuit response to heat and light, channel kinetics, and network level side effects. In order to design interpretable experiments it is important to control for confounds that arise from optogenetic side effects.

Protein expression

For viral delivery of opsin to neurons, expression levels are regulated by virus sterotype, dosage, and promoter choice and can further depend on factors including species, brain region and cell type. Some classes of cells may express optogenetic proteins better or worse than other cell classes even in the same species (Watakabe et al., 2015). Different AAV sterotypes express preferentially in specific cell types, for example AAV1/2 are reported to preferentially target inhibitory neurons (Nathanson et al., 2009). Viral spread and cell specific transduction depend on AAV choice and can be optimized through empirical testing. Testing different AAV sterotypes with varying concentrations can identify a viral dose that maximizes the number of target neurons infected and isolate expression to region of interest. For ArchT silencing experiments, AAV2 was selected for optimal focal expression limited to CA3b. In comparison, infusions of AAV5-CamKIIα to CA3b were more diffuse with expression often spreading to the dentate gyrus. These results were in line with other experiments that found AAV5 exhibits strong retrograde expression (Aschauer et al., 2013). In cases of experiments with CamKIIα-stGtACR2 and hSyn-oCHIEF, selection of AAV was not available, however testing viral concentration and volume prior to experiments allowed for well controlled expression limited to CA3b (Figure 6 for examples of CamKIIα-stGtACR2 and CamKIIα-ArchT expression in CA1 and CA3).

Classically CamKIIα was selected as a promoter to restrict expression to cortical excitatory neurons. However, immunocytochemistry imaging has indicated "leaky" opsin expression by CamKIIα, expressing not only in excitatory cells but various inhibitory cell classes in both the cortex and hippocampus (Nathanson et al., 2009; Watakabe et al., 2015; Schoenenberger et al., 2016). Currently, there are no better options for selectively targeting excitatory cells in non-transgenic rats. As a result, the effects of a leaky promoter must be considered when interpreting results. The degree of CamKIIα-driven expression in interneurons is dependent on both the targeted brain region and dilution of the viral vector, with lower concentrations shifting expression towards inhibitory neurons (Nathanson et al., 2009). In cortical regions with a viral concentration of 2.6×10^{11}, CamKIIα-driven expression is around 20% in interneurons, but is layer-dependent, with maximal interneuron expression in layer 4. In hippocampal region CA1, AAV2/CamKIIα-eNpHR2.0-YFP (concentration: 1.6×10^{13}) expressed in interneurons at levels between 65% and 76% in CA1 SOM+ and PV+ interneurons respectively (Schoenenberger et al., 2016). While immunocytochemistry was not performed in our own experiments, the similarity of stereotype, promoter, concentration, and brain region suggest a high proportion of inhibitory cells likely expressed opsins. When interpreting the results from our CamKIIα experiments, we can assume that the primary effect of illumination is changes in excitatory response since the majority of opsin expressing cells are excitatory pyramidal neurons, but also need to take into account direct photomanipulation in a subset of interneurons.

Heat and light

Light intensities commonly used in optogenetics may result in increases in brain tissue temperature, even with more modest pulse durations and frequencies (Stujenske et al., 2015; Arias-Gil et al., 2016). Increases in tissue temperature can result in changes in resting membrane potential, input resistance, and membrane time constant, all affecting the excitability of neurons (Kim and Connors, 2012). Temperature related changes in activity have

been observed in the hippocampus, which is important to consider when using firing rate changes as the primary measure of changes due to acute light-induced circuit manipulations. Temperature-dependent changes in hippocampal slices have shown contradictory results, but seem to be dependent on the age of the animal. In adult mice, temperature increases caused modest firing depression (Wu and Fisher, 2000), while in young mice hyperthermia increased intrinsic excitability in both excitatory and inhibitory neurons of the hippocampus and was most prominent in CA3 pyramidal cells (Kim and Connors, 2012). These data were all collected *in vitro* and it is unknown how they translate to physiological changes in the intact brain. In recent *in vivo* studies, cooling of the medial septum reduced theta frequency and power, but did not affect spatial attributes of place cells in CA1 (Petersen and Buzsáki, 2020). Since our experiments were performed in adult rats, temperature-dependent firing suppression is more likely, however, several factors make it improbable our results could be accounted for by temperature-dependent factors. Our parameters for intensity and duration were below those that found significant temperature changes (Arias-Gil et al., 2016). Furthermore, the strongest response in our network was a paradoxical increase in firing which counters the physiological response to hyperthermia. Changes in brain tissue temperature would be gradual and increase over prolonged exposure to illumination. Therefore, we would expect the temporal response of cell firing to temperature to be relatively slow compared to responses induced by light-activated opsins. Temperature related changes would be reflected in a change in firing rate of units across the experiment, rather than in the relative difference in firing rate between stimulation and baseline epochs. One solution to control for temperature dependent changes is to decrease light intensity though our experiments, although studies in cortical circuits show this modification does not come without other confounding factors, which were discussed in Section 4.1.1.

Channel and pump activity

Expression of various opsins and illumination location both influence cell responsivity, often in unintuitive ways. Prolonged ChR-stimulation can result in depolarization blocks where the repetitive stimulation does not allow for repolarization of the cell, resulting in an unintentional inhibition of firing (Herman et al., 2014). In contrast, prolonged suppression can engage hyperpolarization activated channels, resulting in rebound action potentials upon release of inhibition (Allen et al., 2015). While the duration of illumination in our experiments was short (max 2 sec), rebound activity was still observed and increased as a function of intensity of illumination. All comparison in these experiments was restricted to responses occurring during the stimulation window and baseline activity. The OFF widows were sufficiently long to allow firing to return to normal levels between photoillumination epochs guaranteeing our results were not biased by rebound firing. However, in future experiments it is worth considering how increases in cell synchrony through either stimulation or release from inhibition can lead to long term plastic changes in a circuit or downstream targets (Zhang and Oertner, 2007).

Cell responses can also depend on which cell compartment was illuminated. For example, both light-activated proton pumps archaerhodopsin and halorhodopsin as well as the light-activated chloride conducting channel GtACR2 show transient excitation when illumination is focused on axonal segments (Mahn et al., 2016; Malyshev et al., 2017). It is worth noting that work by El-Gaby et al. (2016) found prolonged (2-min) illumination of ArchT-expressing synaptic terminals resulted in rapid and reversible silencing. Both studies found that modulation of ArchT-mediated synaptic transmission was the result of changes in pH rather than hyperpolarization. ArchT silences cells by actively transporting one H+ proton during each photocycle against the H+ gradient. This results in both a decrease in extracellular pH and hyperpolarization of the cell (Yamanashi et al., 2019). Though previous studies found no significant change in pH at the soma during ArchT-mediated silencing (Chow et al., 2010), increases in pH at the synaptic terminal are likely due to a higher plasma membrane surface-

area-to-volume ratio (El-Gaby et al., 2016). Calcium currents are bidirectionally modulated by intracellular shifts in pH and can result in Ca^{2+}-dependent changes in NMDA responses (Tombaugh and Somjen, 1997; Chen et al., 1998). The conditions under which activation of ArchT at synaptic terminals results in activation or silencing is still unclear since both studies used similar illumination duration and light intensity. Differences in calcium channel type and properties of NMDA receptors at the synaptic terminal are a possible explanation since experiments were performed in different brain regions.

In our experiments unpredictable responses to synaptic terminal illumination was controlled for by focusing illumination on the cell bodies. Downstream disinhibition in CA1 when silencing CA3 is not likely the result of unintentional synaptic excitation. Local circuit manipulation in CA1 and CA3, especially under ArchT expression, could inadvertently excite axons passing through the cell layer and synapsing on nearby cells. This could result in primary inhibition of cells at the soma and secondary activation of synaptic terminals. This is especially true of CA3, which is composed of dense recurrent excitatory circuitry. However, two factors make this interpretation unlikely: 1) the temporal response of cells in both CA1 and CA3 were aligned to the laser. Synaptic excitation has a slower temporal response compared to somatic inhibition. If synaptic excitation were occurring in our experiments, the response of neurons to photoinhibition would reflect the dynamics of both inhibition and excitation. Cell responses in CA3 were tightly aligned to laser onset and offset suggesting the primary effect of our manipulations was ArchT-mediated inhibition (Figure 13a). 2) Cell responses to ArchT-mediated inhibition in CA3 can be compared to responses from cells expressing the somatic-targeting inhibitory opsin stGtARC2 (Figure 14). Expression of stGtACR2 is restricted to the soma and proximal dendrites, effectively eliminating the confound of synaptic excitation. Similar responses were observed in cells expressing ArchT and stGtACR2 suggesting cell responses to optical manipulations were almost certainly due to somatic inhibition rather than axonal excitation.

Network level side effects

The previous sections have explored confounding effects of optogenetics, however optogenetics can also be used to assess the contribution of a cell type or brain region to network function. Manipulation of a single cell or a specific subset of cells can cause "off-target" responses which can cause a ripple effect and influence activity in downstream regions. Brief inactivation of the sensorimotor nucleus Nif disrupts vocal behavior by acutely suppressing activity in the downstream premotor region HVC, which controls the temporal progression of song. However, when Nif is permanently lesioned the function of HVC recovers and is able to produce songs (Otchy et al., 2015). In the rodent hippocampus, contextual fear memories are thought to initially rely on the hippocampus, but over time retrieval of remote memories is unaffected by hippocampal lesions. Brief inactivation of hippocampal CA1 during remote memory retrieval abolishes the contextual fear memory recall suggesting long-term memory retrieval normally depends on the hippocampus but can shift to alternative structures in the absence of prolonged hippocampal inactivation (Goshen et al., 2011). These studies highlight the disparities observed between acute inactivation and chronic lesion studies. Lesion studies measure function once the brain has reached a post-lesion equilibrium while acute manipulations do not allow for compensation to occur.

Since neural circuits are complex nonlinear systems, network responses to sudden and unnatural perturbations can be difficult to interpret (Phillips and Hasenstaub, 2016). Perturbation can impact the response of cells within a circuit or the activity of downstream neurons. A main network level side effect of optogenetic perturbation is through excitatory-inhibitory circuits. Activating excitatory cells can recruit inhibitory cells that feedforward and shunt the activity of the excitatory cells initially activated. Conversely, silencing excitatory neurons that drive interneurons can result in disinhibition of downstream targets regulated by the inhibitory population (Allen et al., 2015). Similar responses can arise from networks with diverse connectivity patterns. Paradoxical interneuron responses can arise from disinhibitory loops or through networks operating in an ISN-regime. How to control

for, or interpret non-intuitive responses depends on the mechanisms by which those responses occur. In our own experiments, disinhibition of CA1 interneurons during windows of CA3 silencing could emerge through local disinhibitory loops within CA1 or could be inherited from CA3. If the observed increase in CA1 interneuron firing is due to increased excitation in CA3, is that due to local disinhibitory circuits in CA3 or because CA3 is an ISN responding paradoxically to external input? Tackling this question required probing local CA3 and CA1 circuitry under a multitude of experimental parameters and the interpretation of the functional role of disinhibition in CA1 depends largely on the circuit mechanics driving the response.

Several studies report unexpected responses to acute optogenetic perturbations but do not investigate whether the effects relate to network function or are an optogenetic artifact. Optogenetic silencing of cells in the PFC under the nonspecific neuronal promoter CAG and expression of ArchT, revealed the majority (44.6%) of cells exhibited a significant decrease in activity however a subset (23%) of neurons increased firing during photoinhibition epochs (Gilmartin et al., 2013). In this study, simultaneous recording and silencing was achieved using an integrated opto-electrode similar to the design described in Methods Section 2.3 (Royer et al., 2010). The majority of disinhibited neurons were recorded from the probe shank furthest away from the optic fiber, suggesting that disinhibition was an off-target response to focal silencing. Similarly, Do-Monte et al. (2015) employed an optogenetic approach to activate (with channelrhodopsin, CamKIIα-ChR) or silence (with halorhodopsin, CamKIIα-eNpHR) glutamatergic neurons in the infralimbic subregion on the medial prefrontal cortex. Activation of ChR-expressing neurons resulted in a 72% increase and 2% decrease in firing while inactivation of eNpHR-expressing neurons resulted in a 47% decrease and 17% increase in firing. These data suggest an asymmetric response of cortical cells to stimulation and silencing, with silencing resulting in an paradoxical increase in firing (Phillips and Hasenstaub, 2016).

Identification of optogenetic confounds is necessary to identify underlying circuit re-

sponses to acute manipulations. Off-target responses due to optogenetic manipulations have been observed in hippocampal area CA1. eNpHR-mediated photoinhibition driven by the CamKIIα promoter resulted in 34% suppression and 21% activation of pyramidal cells (Schoenenberger et al., 2016). In addition to suppression of pyramidal cells, the authors found 77% of interneurons exhibited firing rate suppression which was the due to non-specificity of the CamKIIα promoter and subsequent opsin expression in interneurons. In this case, fluorescent imaging in combination with cell labeling allowed the authors to determine that the confounding factor in their technique was non-specific opsin expression which resulted in subsequent suppression of local interneurons and disinhibition of pyramidal cells. In a study by Trouche et al. (2016) photosilencing previously active place cells resulted in suppression of 12% and activation of 31% of all recorded pyramidal cells. Silencing a subset of place fields facilitated the disinhibition of previously quiet neurons resulting in the emergence of an alternative place field map. Circuit modification through acute changes in excitation and inhibition can have important functional implications such as the reorganization of cell ensembles representing a previously learned environment.

4.3 Strategies for disrupting network activities

Optogenetics is not the only tool available to modulate neurons in a cell- and region-specific manner. While optogenetics allows for the precise temporal control of neuronal firing, several methods are available to modify circuits on longer timescales. Many tools are available for chronic modifications of neural circuits, including lesions, genetic knockout of cellular synaptic transmission and chemogenetic manipulations. Lesion studies have formed the basis of what we know about how neurological function is localized in the brain. However, removal of brain regions either surgically or through pharmacological methods lacks specificity since manipulated regions can consist of multiple cell types and circuits. Genetic targeting techniques provide a toolkit for dissecting neural circuits with cell-type specific resolution. Depending on the scientific question and chosen technique, circuit manipulations

can span from milliseconds to days.

Inducible tetanus neurotoxin blocks synaptic transmission through proteolytic cleavage of a synaptic vesicle protein (Link et al., 1992; Schiavo et al., 1992; Südhof, 1995). This technique has been briefly discussed in Section 4.1.2 as a method to block synaptic transmission between CA3 and CA1 (Nakashiba et al., 2008, 2009; Middleton and McHugh, 2016). Synaptic transmission is reversibly blocked through oral administration of the drug doxycycline, which induces the tetracycline responsive element and can be maintained for days to weeks. However, this system is based on protein expression following doxycycline treatment, which can take several days to reach maximum inactivation levels. This long latency period can allow other circuits to adapt to the loss of transmission within the targeted circuit. Use of inducible tetanus toxin to selectively silence synaptic transmission may be well suited to evaluate the long term functional reorganization of circuits.

Chemogenetics provides the ability to modulate neuronal firing over the span of several hours (Roth, 2016). This is most commonly accomplished using Designer Receptors Exclusively Activated by Designer Drugs (DREADDs) (Armbruster et al., 2007). DREADDs are modified G protein coupled "designer" receptors activated by chemically and pharmacologically distinct designer ligands. The result is a downstream signaling cascade leading to either enhanced excitability or silencing of targeted neurons (Armbruster et al., 2007; Urban and Roth, 2015). The effects of DREADDs-mediated neuronal changes emerge 10-15 minutes after injection, peak 45-50 min and slowly return to baseline over several hours (Alexander et al., 2009). DREADDs, in contrast to optogenetic interventions, do not offer temporal resolution but allow for sustained changes in excitability making it well suited to answer scientific questions related to neuronal mechanisms underlying homeostatic and compensatory mechanisms.

Combining electrophysiology with DREADDs techniques can allow for monitoring of circuits as they undergo homeostatic changes and may help resolve discrepancies between observations made with acute and chronic manipulations. Experiments described in Chapter

3 show acute silencing of CA3 elicits robust disinhibition of CA1 interneurons. Over longer windows of CA3 inactivation it is unlikely that CA1 interneurons would maintain the same degree of disinhibition, though how the network would respond is still unknown. Following long-term silencing of CA3 input, CA1 place fields are preserved but coordinating firing of cell ensembles is disrupted (Nakashiba et al., 2008). These results suggest compensatory mechanisms are capable of sustaining rate coding while temporal coding is disrupted implying dysregulation of inhibitory firing persists even as the circuit reaches a steady-state.

Acute, reversible silencing is a common optogenetic strategy to investigate the consequence of removing either a specific cell type or brain region from ongoing activity. Two methods are used to achieve region-specific silencing, 1) direct inactivation of a specific cell type, either at the cell body or at targeting fibers or 2) ChR-mediated activation of interneurons, resulting in indirect suppression of through increased inhibition. ChR-assisted photoinhibition is highly effective at low light intensities in suppressing local activity compared to direct photoinhibition using light-gated ion pumps (Li et al., 2019).

Reduced power has the advantage of limiting non-specific effects on neural activity, such as increased tissue temperature (Stujenske et al., 2015). However, ChR-assisted photoinhibition, even at light intensities as low as 2 mW, can cause spatially extensive inhibition extending beyond the targeted brain region (Babl et al., 2019; Lin et al., 2009). Stimulation of interneurons in hippocampal region CA1 can result in inhibition extending as far as the thalamus (Babl et al., 2019). The spatial extent of ChR-assisted photoinhibition is likely due to the both the range of interregional interneuron arborization (Fino and Yuste, 2011) and intraregional GABAergic long-range projections (Caputi et al., 2013; Melzer et al., 2012). Additionally, ChR-assisted photoinhibition lacks cell-type specificity, limiting scientific questions to the contribution of brain regions to neural activity and behavior. Virus-mediated expression of inhibitory opsins allows for targeted cell-type manipulations and for more restricted silencing (Li et al., 2019). However, off-target responses are also observed when using direct silencing methods. Choice of inhibitory opsin and light delivery method can

help alleviate some if the confounding effects of optogenetics.

4.4 Variability within and across sessions

Four sources of variability are worth noting when considering data collected across experiments: expression of opsin, recording location, brain state and depth of anesthesia, and non-stationary of background input to the network. The first source of variability is due to differences in opsin expression across animals. Since virus is introduced surgically, the exact location and quantity can vary slightly between animals. Small differences in the location and level of expression can result in differences in network responsiveness, even under exposure to the same laser intensities. Second, across sessions electrodes can capture neuronal activity at different radial and longitudinal locations within a given region adding variability in terms of both the connectivity and types of neurons sampled. Third, both brain state and depth of anesthesia can influences overall E/I balance which likely results in fluctuations in pyramidal cell and interneuron responses to optogenetic manipulations (Haider et al., 2013; Taub et al., 2013). Our data does not account for changes in brain state or depth of anesthesia, which varies across the recording window. Lastly, our optogenetic perturbations occurred on top of ongoing activity. Most of our conclusions made the assumption of a stationary background, with excitatory and inhibitory inputs driven exclusively by our manipulations. In reality, networks fluctuations shape ongoing activity patterns and are highly variable across multiple timescales, coordinating activity within multiple frequency bands. Similarly, models characterizing ISNs are often mean field, representing averages which are comprised of neurons with different connections, connectivity strength and consequently different levels of stabilizing behaviors. Since responses to the optogenetic illumination were captured across hundreds of presentations, our data measures the average response of a network regardless of these changes, which suggests these responses are robust to small fluctuations in both opsin expression and E/I balance.

4.5 Conclusions

This thesis provides one of the first studies to combine both electrophysiology and optogenetics to examine the effects of acute manipulations on different hippocampal circuits. The combined approach allowed us to characterize the response of CA3 and CA1 networks under a variety of parameters, including focal silencing and stimulation of pyramidal cells as well as to broad silencing of interneurons. In CA3, focal inhibition of pyramidal cells resulted in an unexpected activities of cells just 200 μm away from the site of illumination. Furthermore, large-scale silencing of CA3 resulted in a striking "off-target" responses in downstream CA1 that would not have been predicted based on the direction of manipulation and the functional connectivity between CA3 and CA1. Many experiments rely on optogenetic manipulations without monitoring the effect of these perturbations on network response. In our experiments, the responses of CA3 and CA1 networks to optogenetic manipulations were highly dependent on both the local circuitry and interregional connectivity and emphasize the need for simultaneous monitoring of cellular responses in order to properly characterize the effects of optogenetics on network activity patterns.

A combined technique of optogenetics and electrophysiology allowed us to answer the following questions, which were originally presented in Chapter 1 Section 1.6. The first asked, what was the role of CA3 in shaping spiking activity in downstream CA1? To address this question, we used optogentics to briefly silencing CA3 while recording neuronal responses in CA1. We found that silencing CA3 resulted in a consistent and robust increase in CA1 interneuron firing. This results was consistent across brain states as it was observed both during periods of quiet wakefulness and urethane anesthesia. Furthermore, dysregulation of perisomatic CA1 interneurons, as detailed in our findings can explain the previous accounts that silencing CA3 results in a disruption of both rate and temporal coding in CA1. The second question asked, how do excitatory and inhibitory populations respond to incoming signal? To address this questions we used integrated opto-electrode devices to simultaneously manipulate and measure the responses of CA3 and CA1 circuits. We found that focal

inhibition of CA3 resulted in a paradoxical increase in firing of both inhibitory and excitatory cells. At distances greater than 200 μm, from the site of illumination, net increases in firing were observed, even under conditions of strong photoinhibition. In contrast, CA1 cells responded in the direction of external drive. Silencing cells in CA1 resulted in nearly a 100% decrease in cell response at the site of illumination. These results were consistent when silencing was achieved through expression of light-activated opsins ArchT and stGtACR2. Broad illumination over a diameter of 600 μm and a range of laser intensities was used to assess whether inhibition-stabilization could account for differences observes in the response of CA3 and CA1 networks to focal perturbations. External suppression (stimulation) of interneurons in inhibitory-stabilized networks respond with paradoxically increases (decreases) in firing that is out of phase with the external drive. This response profile can be used to identify networks stabilized through inhibition. Our results found that interneurons in CA1, and to a lesser extent, CA3 increased firing in response photoinhibition suggesting both CA1 and CA3 operate as inhibitory-stabilized networks. Together these results suggest that inhibitory-stabilization cannot account for the differences observed between CA1 and CA3 in response to focal stimulation. In order to classify the network responses to external perturbation it is necessary to take into account both the anatomical and functional connectivity of a given region as well as the extent, both in terms of intensity and spatially, of illumination.

References

Ahmadian, Y., Rubin, D. B., and Miller, K. D. (2013). Analysis of the stabilized supralinear network. *Neural Computation*, 25(8):1994–2037.

Alexander, G. M., Rogan, S. C., Abbas, A. I., Armbruster, B. N., Pei, Y., Allen, J. A., Nonneman, R. J., Hartmann, J., Moy, S. S., Nicolelis, M. A., et al. (2009). Remote control of neuronal activity in transgenic mice expressing evolved g protein-coupled receptors. *Neuron*, 63(1):27–39.

Allen, B. D., Singer, A. C., and Boyden, E. S. (2015). Principles of designing interpretable optogenetic behavior experiments. *Learning & Memory*, 22(4):232–238.

Amaral, D. and Witter, M. (1989). The three-dimensional organization of the hippocampal formation: a review of anatomical data. *Neuroscience*, 31(3):571–591.

Andersen, P., Eccles, J., and Løyning, Y. (1963). Hippocampus of the brain: Recurrent inhibition in the hippocampus with identification of the inhibitory cell and its synapses. *Nature*, 198(4880):540.

Arias-Gil, G., Ohl, F. W., Takagaki, K., and Lippert, M. T. (2016). Measurement, modeling, and prediction of temperature rise due to optogenetic brain stimulation. *Neurophotonics*, 3(4):045007.

Armbruster, B. N., Li, X., Pausch, M. H., Herlitze, S., and Roth, B. L. (2007). Evolving the lock to fit the key to create a family of g protein-coupled receptors potently activated by an inert ligand. *Proceedings of the National Academy of Sciences*, 104(12):5163–5168.

Aschauer, D. F., Kreuz, S., and Rumpel, S. (2013). Analysis of transduction efficiency, tropism and axonal transport of aav serotypes 1, 2, 5, 6, 8 and 9 in the mouse brain. *PloS One*, 8(9):e76310.

Atallah, B. V., Bruns, W., Carandini, M., and Scanziani, M. (2012). Parvalbumin-expressing interneurons linearly transform cortical responses to visual stimuli. *Neuron*, 73(1):159–170.

Babl, S. S., Rummell, B. P., and Sigurdsson, T. (2019). The spatial extent of optogenetic silencing in transgenic mice expressing channelrhodopsin in inhibitory interneurons. *Cell Reports*, 29(5):1381–1395.

Basu, J., Srinivas, K. V., Cheung, S. K., Taniguchi, H., Huang, Z. J., and Siegelbaum, S. A. (2013). A cortico-hippocampal learning rule shapes inhibitory microcircuit activity to enhance hippocampal information flow. *Neuron*, 79(6):1208–1221.

Basu, J., Zaremba, J. D., Cheung, S. K., Hitti, F. L., Zemelman, B. V., Losonczy, A., and Siegelbaum, S. A. (2016). Gating of hippocampal activity, plasticity, and memory by entorhinal cortex long-range inhibition. *Science*, 351(6269):aaa5694.

Bazelot, M., Dinocourt, C., Cohen, I., and Miles, R. (2010). Unitary inhibitory field potentials in the CA3 region of rat hippocampus. *The Journal of physiology*, 588(12):2077–2090.

Beer, Z., Vavra, P., Atucha, E., Rentzing, K., Heinze, H.-J., and Sauvage, M. M. (2018). The memory for time and space differentially engages the proximal and distal parts of the hippocampal subfields CA1 and CA3. *PLoS Biology*, 16(8):e2006100.

Belluscio, M. A., Mizuseki, K., Schmidt, R., Kempter, R., and Buzsáki, G. (2012). Cross-frequency phase–phase coupling between theta and gamma oscillations in the hippocampus. *Journal of Neuroscience*, 32(2):423–435.

Bernard, C. and Wheal, H. V. (1994). Model of local connectivity patterns in CA3 and CA1 areas of the hippocampus. *Hippocampus*, 4(5):497–529.

Beyeler, A., Retailleau, A., Molter, C., Mehidi, A., Szabadics, J., and Leinekugel, X. (2013). Recruitment of perisomatic inhibition during spontaneous hippocampal activity in vitro. *PLoS One*, 8(6):e66509.

Bezaire, M. J. and Soltesz, I. (2013). Quantitative assessment of CA1 local circuits: knowledge base for interneuron-pyramidal cell connectivity. *Hippocampus*, 23(9):751–785.

Bittner, K. C., Grienberger, C., Vaidya, S. P., Milstein, A. D., Macklin, J. J., Suh, J., Tonegawa, S., and Magee, J. C. (2015). Conjunctive input processing drives feature selectivity in hippocampal CA1 neurons. *Nature Neuroscience*, 18(8):1133.

Bock, D. D., Lee, W.-C. A., Kerlin, A. M., Andermann, M. L., Hood, G., Wetzel, A. W., Yurgenson, S., Soucy, E. R., Kim, H. S., and Reid, R. C. (2011). Network anatomy and in vivo physiology of visual cortical neurons. *Nature*, 471(7337):177–182.

Bostock, E., Muller, R. U., and Kubie, J. L. (1991). Experience-dependent modifications of hippocampal place cell firing. *Hippocampus*, 1(2):193–205.

Boyden, E. S., Zhang, F., Bamberg, E., Nagel, G., and Deisseroth, K. (2005). Millisecond-timescale, genetically targeted optical control of neural activity. *Nature Neuroscience*, 8(9):1263–1268.

Brun, V. H., Leutgeb, S., Wu, H.-Q., Schwarcz, R., Witter, M. P., Moser, E. I., and Moser, M.-B. (2008). Impaired spatial representation in CA1 after lesion of direct input from entorhinal cortex. *Neuron*, 57(2):290–302.

Butovas, S. and Schwarz, C. (2003). Spatiotemporal effects of microstimulation in rat neocortex: a parametric study using multielectrode recordings. *Journal of Neurophysiology*, 90(5):3024–3039.

Buzsáki, G. (1984). Feed-forward inhibition in the hippocampal formation. *Progress in Neurobiology*, 22(2):131–153.

Buzsáki, G. (2001). Hippocampal gabaergic interneurons: a physiological perspective. *Neurochemical Research*, 26(8-9):899–905.

Buzsáki, G. (2010). Neural syntax: cell assemblies, synapsembles, and readers. *Neuron*, 68(3):362–385.

Buzsáki, G. (2015). Hippocampal sharp wave-ripple: A cognitive biomarker for episodic memory and planning. *Hippocampus*, 25(10):1073–1188.

Buzsáki, G., Geisler, C., Henze, D. A., and Wang, X.-J. (2004). Interneuron diversity series: circuit complexity and axon wiring economy of cortical interneurons. *Trends in Neurosciences*, 27(4):186–193.

Buzsáki, G., Vanderwolf, C. H., et al. (1983). Cellular bases of hippocampal eeg in the behaving rat. *Brain Research Reviews*, 6(2):139–171.

Campagna, J. A., Miller, K. W., and Forman, S. A. (2003). Mechanisms of actions of inhaled anesthetics. *New England Journal of Medicine*, 348(21):2110–2124.

Caputi, A., Melzer, S., Michael, M., and Monyer, H. (2013). The long and short of gabaergic neurons. *Current Opinion in Neurobiology*, 23(2):179–186.

Chen, Y.-H., Wu, M.-L., and Fu, W.-M. (1998). Regulation of presynaptic nmda responses by external and intracellular ph changes at developing neuromuscular synapses. *Journal of Neuroscience*, 18(8):2982–2990.

Chow, B. Y., Han, X., Dobry, A. S., Qian, X., Chuong, A. S., Li, M., Henninger, M. A., Belfort, G. M., Lin, Y., Monahan, P. E., et al. (2010). High-performance genetically targetable optical neural silencing by light-driven proton pumps. *Nature*, 463(7277):98–102.

Chrobak, J. J. and Buzsáki, G. (1996). High-frequency oscillations in the output networks of the hippocampal–entorhinal axis of the freely behaving rat. *Journal of Neuroscience*, 16(9):3056–3066.

Chrobak, J. J. and Buzsáki, G. (1998). Operational dynamics in the hippocampal-entorhinal axis. *Neuroscience & Biobehavioral Reviews*, 22(2):303–310.

Chung, J., Sharif, F., Jung, D., Kim, S., and Royer, S. (2017). Micro-drive and headgear for chronic implant and recovery of optoelectronic probes. *Scientific Reports*, 7(1):2773.

Colgin, L. L., Denninger, T., Fyhn, M., Hafting, T., Bonnevie, T., Jensen, O., Moser, M.-B., and Moser, E. I. (2009). Frequency of gamma oscillations routes flow of information in the hippocampus. *Nature*, 462(7271):353.

Cope, D., Maccaferri, G., Marton, L., Roberts, J., Cobden, P., and Somogyi, P. (2002). Cholecystokinin-immunopositive basket and schaffer collateral-associated interneurones target different domains of pyramidal cells in the CA1 area of the rat hippocampus. *Neuroscience*, 109(1):63–80.

Davidson, T. J., Kloosterman, F., and Wilson, M. A. (2009). Hippocampal replay of extended experience. *Neuron*, 63(4):497–507.

Davoudi, H. and Foster, D. J. (2019). Acute silencing of hippocampal CA3 reveals a dominant role in place field responses. *Nature Neuroscience*, 22(3):337–342.

de la Prida, L. M. (2020). Potential factors influencing replay across CA1 during sharp-wave ripples. *Philosophical Transactions of the Royal Society B*, 375(1799):20190236.

Deleuze, C., Pazienti, A., and Bacci, A. (2014). Autaptic self-inhibition of cortical gabaergic neurons: synaptic narcissism or useful introspection? *Current Opinion in Neurobiology*, 26:64–71.

Denève, S. and Machens, C. K. (2016). Efficient codes and balanced networks. *Nature Neuroscience*, 19(3):375–382.

Diba, K. and Buzsáki, G. (2007). Forward and reverse hippocampal place-cell sequences during ripples. *Nature Neuroscience*, 10(10):1241.

Dimidschstein, J., Chen, Q., Tremblay, R., Rogers, S. L., Saldi, G.-A., Guo, L., Xu, Q., Liu, R., Lu, C., Chu, J., et al. (2016). A viral strategy for targeting and manipulating interneurons across vertebrate species. *Nature Neuroscience*, 19(12):1743–1749.

Do-Monte, F. H., Manzano-Nieves, G., Quiñones-Laracuente, K., Ramos-Medina, L., and Quirk, G. J. (2015). Revisiting the role of infralimbic cortex in fear extinction with optogenetics. *Journal of Neuroscience*, 35(8):3607–3615.

Dong, S., Rogan, S. C., and Roth, B. L. (2010). Directed molecular evolution of dreadds: a generic approach to creating next-generation rassls. *Nature Protocols*, 5(3):561.

Dragoi, G. and Buzsáki, G. (2006). Temporal encoding of place sequences by hippocampal cell assemblies. *Neuron*, 50(1):145–157.

Dragoi, G. and Tonegawa, S. (2011). Preplay of future place cell sequences by hippocampal cellular assemblies. *Nature*, 469(7330):397.

Dragoi, G. and Tonegawa, S. (2013). Distinct preplay of multiple novel spatial experiences in the rat. *Proceedings of the National Academy of Sciences*, 110(22):9100–9105.

Dudek, F. E. and Sutula, T. P. (2007). Epileptogenesis in the dentate gyrus: a critical perspective. *Progress in Brain Research*, 163:755–773.

Ego-Stengel, V. and Wilson, M. A. (2007). Spatial selectivity and theta phase precession in CA1 interneurons. *Hippocampus*, 17(2):161–174.

El-Gaby, M., Zhang, Y., Wolf, K., Schwiening, C. J., Paulsen, O., and Shipton, O. A. (2016). Archaerhodopsin selectively and reversibly silences synaptic transmission through altered ph. *Cell Reports*, 16(8):2259–2268.

Feng, T., Silva, D., and Foster, D. J. (2015). Dissociation between the experience-dependent development of hippocampal theta sequences and single-trial phase precession. *Journal of Neuroscience*, 35(12):4890–4902.

Fernández-Ruiz, A., Oliva, A., Nagy, G. A., Maurer, A. P., Berényi, A., and Buzsáki, G. (2017). Entorhinal-CA3 dual-input control of spike timing in the hippocampus by theta-gamma coupling. *Neuron*, 93(5):1213–1226.

Fino, E. and Yuste, R. (2011). Dense inhibitory connectivity in neocortex. *Neuron*, 69(6):1188–1203.

Foster, D. J. and Wilson, M. A. (2006). Reverse replay of behavioural sequences in hippocampal place cells during the awake state. *Nature*, 440(7084):680.

Foster, D. J. and Wilson, M. A. (2007). Hippocampal theta sequences. *Hippocampus*, 17(11):1093–1099.

Freund, T. F. and Buzsáki, G. (1996). Interneurons of the hippocampus. *Hippocampus*, 6(4):347–470.

Fröhlich, F., Sejnowski, T. J., and Bazhenov, M. (2010). Network bistability mediates spontaneous transitions between normal and pathological brain states. *Journal of Neuroscience*, 30(32):10734–10743.

Fu, Y., Tucciarone, J. M., Espinosa, J. S., Sheng, N., Darcy, D. P., Nicoll, R. A., Huang, Z. J., and Stryker, M. P. (2014). A cortical circuit for gain control by behavioral state. *Cell*, 156(6):1139–1152.

Fuchs, E. C., Neitz, A., Pinna, R., Melzer, S., Caputi, A., and Monyer, H. (2016). Local and distant input controlling excitation in layer ii of the medial entorhinal cortex. *Neuron*, 89(1):194–208.

Fyhn, M., Molden, S., Witter, M. P., Moser, E. I., and Moser, M.-B. (2004). Spatial representation in the entorhinal cortex. *Science*, 305(5688):1258–1264.

Germroth, P., Schwerdtfeger, W. K., and Buhl, E. H. (1989). Gabaergic neurons in the entorhinal cortex project to the hippocampus. *Brain Research*, 494(1):187–192.

Gil, M., Ancau, M., Schlesiger, M. I., Neitz, A., Allen, K., De Marco, R. J., and Monyer, H. (2018). Impaired path integration in mice with disrupted grid cell firing. *Nature Neuroscience*, 21(1):81–91.

Gilmartin, M. R., Miyawaki, H., Helmstetter, F. J., and Diba, K. (2013). Prefrontal activity links nonoverlapping events in memory. *Journal of Neuroscience*, 33(26):10910–10914.

Goshen, I., Brodsky, M., Prakash, R., Wallace, J., Gradinaru, V., Ramakrishnan, C., and Deisseroth, K. (2011). Dynamics of retrieval strategies for remote memories. *Cell*, 147(3):678–689.

Govorunova, E. G., Sineshchekov, O. A., Janz, R., Liu, X., and Spudich, J. L. (2015). Natural light-gated anion channels: A family of microbial rhodopsins for advanced optogenetics. *Science*, 349(6248):647–650.

Govorunova, E. G., Sineshchekov, O. A., Li, H., and Spudich, J. L. (2017). Microbial rhodopsins: diversity, mechanisms, and optogenetic applications. *Annual Review of Biochemistry*, 86:845–872.

Gradinaru, V., Thompson, K. R., and Deisseroth, K. (2008). enphr: a natronomonas halorhodopsin enhanced for optogenetic applications. *Brain cell biology*, 36(1-4):129–139.

Grosmark, A. D. and Buzsáki, G. (2016). Diversity in neural firing dynamics supports both rigid and learned hippocampal sequences. *Science*, 351(6280):1440–1443.

Gulyás, A. I., Hájos, N., and Freund, T. F. (1996). Interneurons containing calretinin are specialized to control other interneurons in the rat hippocampus. *Journal of Neuroscience*, 16(10):3397–3411.

Gupta, A. S., van der Meer, M. A., Touretzky, D. S., and Redish, A. D. (2010). Hippocampal replay is not a simple function of experience. *Neuron*, 65(5):695–705.

Guzowski, J. F., Knierim, J. J., and Moser, E. I. (2004). Ensemble dynamics of hippocampal regions CA3 and CA1. *Neuron*, 44(4):581–584.

Haider, B., Häusser, M., and Carandini, M. (2013). Inhibition dominates sensory responses in the awake cortex. *Nature*, 493(7430):97–100.

Hájos, N., Karlócai, M. R., Németh, B., Ulbert, I., Monyer, H., Szabó, G., Erdélyi, F., Freund, T. F., and Gulyás, A. I. (2013). Input-output features of anatomically identified CA3 neurons during hippocampal sharp wave/ripple oscillation in vitro. *Journal of Neuroscience*, 33(28):11677–11691.

Hales, J. B., Schlesiger, M. I., Leutgeb, J. K., Squire, L. R., Leutgeb, S., and Clark, R. E. (2014). Medial entorhinal cortex lesions only partially disrupt hippocampal place cells and hippocampus-dependent place memory. *Cell Reports*, 9(3):893–901.

Hangya, B., Li, Y., Muller, R. U., and Czurkó, A. (2010). Complementary spatial firing in place cell–interneuron pairs. *The Journal of Physiology*, 588(21):4165–4175.

Harris, K. D., Csicsvari, J., Hirase, H., Dragoi, G., and Buzsáki, G. (2003). Organization of cell assemblies in the hippocampus. *Nature*, 424(6948):552.

Hasselmo, M. E., Bodelón, C., and Wyble, B. P. (2002). A proposed function for hippocampal theta rhythm: separate phases of encoding and retrieval enhance reversal of prior learning. *Neural Computation*, 14(4):793–817.

Hazan, L., Zugaro, M., and Buzsáki, G. (2006). Klusters, neuroscope, ndmanager: a free software suite for neurophysiological data processing and visualization. *Journal of Neuroscience Methods*, 155(2):207–216.

Herman, A. M., Huang, L., Murphey, D. K., Garcia, I., and Arenkiel, B. R. (2014). Cell type-specific and time-dependent light exposure contribute to silencing in neurons expressing channelrhodopsin-2. *eLife*, 3:e01481.

Hunsaker, M. R., Tran, G. T., and Kesner, R. P. (2008). A double dissociation of subcortical hippocampal efferents for encoding and consolidation/retrieval of spatial information. *Hippocampus*, 18(7):699–709.

Huxter, J., Burgess, N., and O'Keefe, J. (2003). Independent rate and temporal coding in hippocampal pyramidal cells. *Nature*, 425(6960):828–832.

Igarashi, K. M., Lu, L., Colgin, L. L., Moser, M.-B., and Moser, E. I. (2014). Coordination of entorhinal–hippocampal ensemble activity during associative learning. *Nature*, 510(7503):143–147.

Isaacson, J. S. and Scanziani, M. (2011). How inhibition shapes cortical activity. *Neuron*, 72(2):231–243.

Jensen, O. and Lisman, J. E. (2000). Position reconstruction from an ensemble of hippocampal place cells: contribution of theta phase coding. *Journal of Neurophysiology*, 83(5):2602–2609.

Jinno, S., Klausberger, T., Marton, L. F., Dalezios, Y., Roberts, J. D. B., Fuentealba, P., Bushong, E. A., Henze, D., Buzsáki, G., and Somogyi, P. (2007). Neuronal diversity in gabaergic long-range projections from the hippocampus. *Journal of Neuroscience*, 27(33):8790–8804.

Kajiwara, R., Wouterlood, F. G., Sah, A., Boekel, A. J., Baks-te Bulte, L. T., and Witter, M. P. (2008). Convergence of entorhinal and CA3 inputs onto pyramidal neurons and interneurons in hippocampal area CA1 - an anatomical study in the rat. *Hippocampus*, 18(3):266–280.

Katona, I., Acsády, L., and Freund, T. F. (1999). Postsynaptic targets of somatostatin-immunoreactive interneurons in the rat hippocampus. *Neuroscience*, 88(1):37–55.

Kesner, R. P. and Rolls, E. T. (2015). A computational theory of hippocampal function, and tests of the theory: new developments. *Neuroscience & Biobehavioral Reviews*, 48:92–147.

Kim, J. and Connors, B. (2012). High temperatures alter physiological properties of pyramidal cells and inhibitory interneurons in hippocampus. *Frontiers in Cellular Neuroscience*, 6:27.

Kitamura, T., Pignatelli, M., Suh, J., Kohara, K., Yoshiki, A., Abe, K., and Tonegawa, S. (2014). Island cells control temporal association memory. *Science*, 343(6173):896–901.

Klausberger, T., Magill, P. J., Márton, L. F., Roberts, J. D. B., Cobden, P. M., Buzsáki, G., and Somogyi, P. (2003). Brain-state-and cell-type-specific firing of hippocampal interneurons in vivo. *Nature*, 421(6925):844.

Klausberger, T., Márton, L. F., Baude, A., Roberts, J. D. B., Magill, P. J., and Somogyi, P. (2004). Spike timing of dendrite-targeting bistratified cells during hippocampal network oscillations in vivo. *Nature Neuroscience*, 7(1):41.

Klausberger, T., Marton, L. F., O'Neill, J., Huck, J. H., Dalezios, Y., Fuentealba, P., Suen, W. Y., Papp, E., Kaneko, T., Watanabe, M., et al. (2005). Complementary roles of cholecystokinin-and parvalbumin-expressing gabaergic neurons in hippocampal network oscillations. *Journal of Neuroscience*, 25(42):9782–9793.

Klausberger, T. and Somogyi, P. (2008). Neuronal diversity and temporal dynamics: the unity of hippocampal circuit operations. *Science*, 321(5885):53–57.

Kubie, J. L. and Muller, R. U. (1991). Multiple representations in the hippocampus. *Hippocampus*, 1(3):240–242.

Leão, R. N., Mikulovic, S., Leão, K. E., Munguba, H., Gezelius, H., Enjin, A., Patra, K., Eriksson, A., Loew, L. M., Tort, A. B., et al. (2012). Olm interneurons differentially modulate CA3 and entorhinal inputs to hippocampal CA1 neurons. *Nature Neuroscience*, 15(11):1524.

Lee, H., GoodSmith, D., and Knierim, J. J. (2020). Parallel processing streams in the hippocampus. *Current Opinion in Neurobiology*, 64:127–134.

Lee, H., Wang, C., Deshmukh, S. S., and Knierim, J. J. (2015). Neural population evidence of functional heterogeneity along the CA3 transverse axis: pattern completion versus pattern separation. *Neuron*, 87(5):1093–1105.

Lee, I., Yoganarasimha, D., Rao, G., and Knierim, J. J. (2004). Comparison of population coherence of place cells in hippocampal subfields CA1 and CA3. *Nature*, 430(6998):456–459.

Leutgeb, S., Leutgeb, J. K., Treves, A., Moser, M.-B., and Moser, E. I. (2004). Distinct ensemble codes in hippocampal areas CA3 and CA1. *Science*, 305(5688):1295–1298.

Li, N., Chen, S., Guo, Z. V., Chen, H., Huo, Y., Inagaki, H. K., Chen, G., Davis, C., Hansel, D., Guo, C., et al. (2019). Spatiotemporal constraints on optogenetic inactivation in cortical circuits. *eLife*, 8:e48622.

Lin, J. Y., Lin, M. Z., Steinbach, P., and Tsien, R. Y. (2009). Characterization of engineered channelrhodopsin variants with improved properties and kinetics. *Biophysical Journal*, 96(5):1803–1814.

Link, E., Edelmann, L., Chou, J. H., Binz, T., Yamasaki, S., Eisel, U., Baumert, M., Südhof, T. C., Niemann, H., and Jahn, R. (1992). Tetanus toxin action: inhibition of neurotransmitter release linked to synaptobrevin proteolysis. *Biochemical and Biophysical Research Communications*, 189(2):1017–1023.

Litwin-Kumar, A., Rosenbaum, R., and Doiron, B. (2016). Inhibitory stabilization and visual coding in cortical circuits with multiple interneuron subtypes. *Journal of Neurophysiology*, 115(3):1399–1409.

Lorente de Nó, R. (1934). Studies on the structure of the cerebral cortex. ii. continuation of the study of the ammonic system. *Journal für Psychologie und Neurologie*, 46:113–177.

Losonczy, A., Zemelman, B. V., Vaziri, A., and Magee, J. C. (2010). Network mechanisms of theta related neuronal activity in hippocampal CA1 pyramidal neurons. *Nature Neuroscience*, 13(8):967.

Lu, L., Igarashi, K. M., Witter, M. P., Moser, E. I., and Moser, M.-B. (2015). Topography of place maps along the CA3-to-ca2 axis of the hippocampus. *Neuron*, 87(5):1078–1092.

Mahn, M., Gibor, L., Patil, P., Malina, K. C.-K., Oring, S., Printz, Y., Levy, R., Lampl, I., and Yizhar, O. (2018). High-efficiency optogenetic silencing with soma-targeted anion-conducting channelrhodopsins. *Nature Communications*, 9(1):1–15.

Mahn, M., Prigge, M., Ron, S., Levy, R., and Yizhar, O. (2016). Biophysical constraints of optogenetic inhibition at presynaptic terminals. *Nature Neuroscience*, 19(4):554–556.

Mahrach, A., Chen, G., Li, N., van Vreeswijk, C., and Hansel, D. (2020). Mechanisms underlying the response of mouse cortical networks to optogenetic manipulation. *eLife*, 9:e49967.

Malyshev, A., Roshchin, M., Smirnova, G., Dolgikh, D., Balaban, P., and Ostrovsky, M. (2017). Chloride conducting light activated channel gtacr2 can produce both cessation of firing and generation of action potentials in cortical neurons in response to light. *Neuroscience Letters*, 640:76–80.

Mann, E. O. and Paulsen, O. (2007). Role of gabaergic inhibition in hippocampal network oscillations. *Trends in Neurosciences*, 30(7):343–349.

Masurkar, A. V., Srinivas, K. V., Brann, D. H., Warren, R., Lowes, D. C., and Siegelbaum, S. A. (2017). Medial and lateral entorhinal cortex differentially excite deep versus superficial CA1 pyramidal neurons. *Cell Reports*, 18(1):148–160.

Mateo, C., Avermann, M., Gentet, L. J., Zhang, F., Deisseroth, K., and Petersen, C. C. (2011). In vivo optogenetic stimulation of neocortical excitatory neurons drives brain-state-dependent inhibition. *Current Biology*, 21(19):1593–1602.

McNaughton, B. L., Battaglia, F. P., Jensen, O., Moser, E. I., and Moser, M.-B. (2006). Path integration and the neural basis of the'cognitive map'. *Nature Reviews Neuroscience*, 7(8):663.

Mehta, M. R. (2015). From synaptic plasticity to spatial maps and sequence learning. *Hippocampus*, 25(6):756–762.

Melzer, S., Michael, M., Caputi, A., Eliava, M., Fuchs, E. C., Whittington, M. A., and Monyer, H. (2012). Long-range–projecting gabaergic neurons modulate inhibition in hippocampus and entorhinal cortex. *Science*, 335(6075):1506–1510.

Mercer Jr, L., Remley, N., and Gilman, D. (1978). Effects of urethane on hippocampal unit activity in the rat. *Brain Research Bulletin*, 3(5):567–570.

Miao, C., Cao, Q., Ito, H. T., Yamahachi, H., Witter, M. P., Moser, M.-B., and Moser, E. I. (2015). Hippocampal remapping after partial inactivation of the medial entorhinal cortex. *Neuron*, 88(3):590–603.

Middleton, S. J. and McHugh, T. J. (2016). Silencing CA3 disrupts temporal coding in the CA1 ensemble. *Nature Neuroscience*, 19(7):945.

Miles, R., Tóth, K., Gulyás, A. I., Hájos, N., and Freund, T. F. (1996). Differences between somatic and dendritic inhibition in the hippocampus. *Neuron*, 16(4):815–823.

Miller, K. D. (2016). Canonical computations of cerebral cortex. *Current Opinion in Neurobiology*, 37:75–84.

Milstein, A. D., Bloss, E. B., Apostolides, P. F., Vaidya, S. P., Dilly, G. A., Zemelman, B. V., and Magee, J. C. (2015). Inhibitory gating of input comparison in the CA1 microcircuit. *Neuron*, 87(6):1274–1289.

Mizuseki, K., Diba, K., Pastalkova, E., and Buzsáki, G. (2011). Hippocampal CA1 pyramidal cells form functionally distinct sublayers. *Nature Neuroscience*, 14(9):1174–1181.

Mizuseki, K., Sirota, A., Pastalkova, E., and Buzsáki, G. (2009). Theta oscillations provide temporal windows for local circuit computation in the entorhinal-hippocampal loop. *Neuron*, 64(2):267–280.

Moore, A. K., Weible, A. P., Balmer, T. S., Trussell, L. O., and Wehr, M. (2018). Rapid rebalancing of excitation and inhibition by cortical circuitry. *Neuron*, 97(6):1341–1355.

Muller, R. U. and Kubie, J. L. (1987). The effects of changes in the environment on the spatial firing of hippocampal complex-spike cells. *Journal of Neuroscience*, 7(7):1951–1968.

Murphy, B. K. and Miller, K. D. (2009). Balanced amplification: a new mechanism of selective amplification of neural activity patterns. *Neuron*, 61(4):635–648.

Nakamura, N. H., Flasbeck, V., Maingret, N., Kitsukawa, T., and Sauvage, M. M. (2013). Proximodistal segregation of nonspatial information in CA3: preferential recruitment of a proximal CA3-distal CA1 network in nonspatial recognition memory. *Journal of Neuroscience*, 33(28):11506–11514.

Nakashiba, T., Buhl, D. L., McHugh, T. J., and Tonegawa, S. (2009). Hippocampal CA3 output is crucial for ripple-associated reactivation and consolidation of memory. *Neuron*, 62(6):781–787.

Nakashiba, T., Young, J. Z., McHugh, T. J., Buhl, D. L., and Tonegawa, S. (2008). Transgenic inhibition of synaptic transmission reveals role of CA3 output in hippocampal learning. *Science*, 319(5867):1260–1264.

Nakazawa, K., Quirk, M. C., Chitwood, R. A., Watanabe, M., Yeckel, M. F., Sun, L. D., Kato, A., Carr, C. A., Johnston, D., Wilson, M. A., et al. (2002). Requirement for hippocampal CA3 nmda receptors in associative memory recall. *Science*, 297(5579):211–218.

Nakazawa, K., Sun, L. D., Quirk, M. C., Rondi-Reig, L., Wilson, M. A., and Tonegawa, S. (2003). Hippocampal CA3 nmda receptors are crucial for memory acquisition of one-time experience. *Neuron*, 38(2):305–315.

Nathanson, J. L., Yanagawa, Y., Obata, K., and Callaway, E. M. (2009). Preferential labeling of inhibitory and excitatory cortical neurons by endogenous tropism of adeno-associated virus and lentivirus vectors. *Neuroscience*, 161(2):441–450.

O'Keefe, J. (1976). Place units in the hippocampus of the freely moving rat. *Experimental Neurology*, 51(1):78–109.

O'Keefe, J. and Dostrovsky, J. (1971). The hippocampus as a spatial map: Preliminary evidence from unit activity in the freely-moving rat. *Brain Research*, 31(1):171–175.

O'Keefe, J. and Nadel, L. (1978). *The hippocampus as a cognitive map*. Oxford: Clarendon Press.

O'Keefe, J. and Recce, M. L. (1993). Phase relationship between hippocampal place units and the eeg theta rhythm. *Hippocampus*, 3(3):317–330.

Ólafsdóttir, H. F., Carpenter, F., and Barry, C. (2016). Coordinated grid and place cell replay during rest. *Nature Neuroscience*, 19(6):792.

Oliva, A., Fernández-Ruiz, A., Buzsáki, G., and Berényi, A. (2016). Role of hippocampal ca2 region in triggering sharp-wave ripples. *Neuron*, 91(6):1342–1355.

Otchy, T. M., Wolff, S. B., Rhee, J. Y., Pehlevan, C., Kawai, R., Kempf, A., Gobes, S. M., and Ölveczky, B. P. (2015). Acute off-target effects of neural circuit manipulations. *Nature*, 528(7582):358–363.

Owen, S. F., Liu, M. H., and Kreitzer, A. C. (2019). Thermal constraints on in vivo optogenetic manipulations. *Nature Neuroscience*, 22(7):1061–1065.

Ozeki, H., Finn, I. M., Schaffer, E. S., Miller, K. D., and Ferster, D. (2009). Inhibitory stabilization of the cortical network underlies visual surround suppression. *Neuron*, 62(4):578–592.

Packer, A. M. and Yuste, R. (2011). Dense, unspecific connectivity of neocortical parvalbumin-positive interneurons: a canonical microcircuit for inhibition? *Journal of Neuroscience*, 31(37):13260–13271.

Paxinos, G. and Watson, C. (1986). Atlas of the rat brain in stereotaxic coordinates. *Academic, New York*.

Pelkey, K. A., Chittajallu, R., Craig, M. T., Tricoire, L., Wester, J. C., and McBain, C. J. (2017). Hippocampal gabaergic inhibitory interneurons. *Physiological Reviews*, 97(4):1619–1747.

Petersen, P. C. and Buzsáki, G. (2020). Cooling of medial septum reveals theta phase lag coordination of hippocampal cell assemblies. *Neuron*.

Pfeffer, C. K., Xue, M., He, M., Huang, Z. J., and Scanziani, M. (2013). Inhibition of inhibition in visual cortex: the logic of connections between molecularly distinct interneurons. *Nature Neuroscience*, 16(8):1068–1076.

Phillips, E. A. and Hasenstaub, A. R. (2016). Asymmetric effects of activating and inactivating cortical interneurons. *eLife*, 5:e18383.

Pi, H.-J., Hangya, B., Kvitsiani, D., Sanders, J. I., Huang, Z. J., and Kepecs, A. (2013). Cortical interneurons that specialize in disinhibitory control. *Nature*, 503(7477):521.

Pouille, F. and Scanziani, M. (2001). Enforcement of temporal fidelity in pyramidal cells by somatic feed-forward inhibition. *Science*, 293(5532):1159–1163.

Pouille, F. and Scanziani, M. (2004). Routing of spike series by dynamic circuits in the hippocampus. *Nature*, 429(6993):717.

Raimondo, J. V., Kay, L., Ellender, T. J., and Akerman, C. J. (2012). Optogenetic silencing strategies differ in their effects on inhibitory synaptic transmission. *Nature Neuroscience*, 15(8):1102–1104.

Rao, S. G., Williams, G. V., and Goldman-Rakic, P. S. (2000). Destruction and creation of spatial tuning by disinhibition: Gabaa blockade of prefrontal cortical neurons engaged by working memory. *Journal of Neuroscience*, 20(1):485–494.

Rolls, E. (2013). The mechanisms for pattern completion and pattern separation in the hippocampus. *Frontiers in Systems Neuroscience*, 7:74.

Rossant, C., Kadir, S. N., Goodman, D. F., Schulman, J., Hunter, M. L., Saleem, A. B., Grosmark, A., Belluscio, M., Denfield, G. H., Ecker, A. S., et al. (2016). Spike sorting for large, dense electrode arrays. *Nature Neuroscience*, 19(4):634.

Roth, B. L. (2016). Dreadds for neuroscientists. *Neuron*, 89(4):683–694.

Roux, L. and Buzsáki, G. (2015). Tasks for inhibitory interneurons in intact brain circuits. *Neuropharmacology*, 88:10–23.

Royer, S., Zemelman, B. V., Barbic, M., Losonczy, A., Buzsáki, G., and Magee, J. C. (2010). Multi-array silicon probes with integrated optical fibers: light-assisted perturbation and recording of local neural circuits in the behaving animal. *European Journal of Neuroscience*, 31(12):2279–2291.

Royer, S., Zemelman, B. V., Losonczy, A., Kim, J., Chance, F., Magee, J. C., and Buzsáki, G. (2012). Control of timing, rate and bursts of hippocampal place cells by dendritic and somatic inhibition. *Nature Neuroscience*, 15(5):769.

Rubin, D. B., Van Hooser, S. D., and Miller, K. D. (2015). The stabilized supralinear network: a unifying circuit motif underlying multi-input integration in sensory cortex. *Neuron*, 85(2):402–417.

Rubin, R., Abbott, L., and Sompolinsky, H. (2017). Balanced excitation and inhibition are required for high-capacity, noise-robust neuronal selectivity. *Proceedings of the National Academy of Sciences*, 114(44):E9366–E9375.

Rudy, B., Fishell, G., Lee, S., and Hjerling-Leffler, J. (2011). Three groups of interneurons account for nearly 100% of neocortical gabaergic neurons. *Developmental Neurobiology*, 71(1):45–61.

Rueckemann, J. W., DiMauro, A. J., Rangel, L. M., Han, X., Boyden, E. S., and Eichenbaum, H. (2016). Transient optogenetic inactivation of the medial entorhinal cortex biases the active population of hippocampal neurons. *Hippocampus*, 26(2):246–260.

Sadeh, S. and Clopath, C. (2020). Patterned perturbation of inhibition can reveal the dynamical structure of neural processing. *eLife*, 9:e52757.

Sadeh, S., Silver, R. A., Mrsic-Flogel, T. D., and Muir, D. R. (2017). Assessing the role of inhibition in stabilizing neocortical networks requires large-scale perturbation of the inhibitory population. *Journal of Neuroscience*, 37(49):12050–12067.

Sanzeni, A., Akitake, B., Goldbach, H. C., Leedy, C. E., Brunel, N., and Histed, M. H. (2020). Inhibition stabilization is a widespread property of cortical networks. *eLife*, 9:e54875.

Sargolini, F., Fyhn, M., Hafting, T., McNaughton, B. L., Witter, M. P., Moser, M.-B., and Moser, E. I. (2006). Conjunctive representation of position, direction, and velocity in entorhinal cortex. *Science*, 312(5774):758–762.

Schiavo, G., Poulain, B., Rossetto, O., Benfenati, F., Tauc, L., and Montecucco, C. (1992). Tetanus toxin is a zinc protein and its inhibition of neurotransmitter release and protease activity depend on zinc. *The EMBO journal*, 11(10):3577–3583.

Schlesiger, M. I., Boublil, B. L., Hales, J. B., Leutgeb, J. K., and Leutgeb, S. (2018). Hippocampal global remapping can occur without input from the medial entorhinal cortex. *Cell Reports*, 22(12):3152–3159.

Schlesiger, M. I., Cannova, C. C., Boublil, B. L., Hales, J. B., Mankin, E. A., Brandon, M. P., Leutgeb, J. K., Leibold, C., and Leutgeb, S. (2015). The medial entorhinal cortex is necessary for temporal organization of hippocampal neuronal activity. *Nature Neuroscience*, 18(8):1123–1132.

Schoenenberger, P., O'Neill, J., and Csicsvari, J. (2016). Activity-dependent plasticity of hippocampal place maps. *Nature Communications*, 7:11824.

Schomburg, E. W., Fernández-Ruiz, A., Mizuseki, K., Berényi, A., Anastassiou, C. A., Koch, C., and Buzsáki, G. (2014). Theta phase segregation of input-specific gamma patterns in entorhinal-hippocampal networks. *Neuron*, 84(2):470–485.

Sharif, F., Tayebi, B., Buzsaki, G., Royer, S., and Fernandez-Ruiz, A. (2020). Subcircuits of deep and superficial CA1 place cells support efficient spatial coding across heterogeneous environments. *bioRxiv*.

Sharpe, M. J., Marchant, N. J., Whitaker, L. R., Richie, C. T., Zhang, Y. J., Campbell, E. J., Koivula, P. P., Necarsulmer, J. C., Mejias-Aponte, C., Morales, M., et al. (2017). Lateral hypothalamic gabaergic neurons encode reward predictions that are relayed to the ventral tegmental area to regulate learning. *Current Biology*, 27(14):2089–2100.

Shepherd, G. M. (2003). *The synaptic organization of the brain*. Oxford University Press.

Siegle, J. H., López, A. C., Patel, Y. A., Abramov, K., Ohayon, S., and Voigts, J. (2017). Open ephys: an open-source, plugin-based platform for multichannel electrophysiology. *Journal of Neural Engineering*, 14(4):045003.

Sik, A., Penttonen, M., Ylinen, A., and Buzsáki, G. (1995). Hippocampal CA1 interneurons: an in vivo intracellular labeling study. *Journal of Neuroscience*, 15(10):6651–6665.

Sik, A., Ylinen, A., Penttonen, M., and Buzsaki, G. (1994). Inhibitory CA1-CA3-hilar region feedback in the hippocampus. *Science*, 265(5179):1722–1724.

Skaggs, W. E., McNaughton, B. L., Wilson, M. A., and Barnes, C. A. (1996). Theta phase precession in hippocampal neuronal populations and the compression of temporal sequences. *Hippocampus*, 6(2):149–172.

Stark, E., Koos, T., and Buzsáki, G. (2012). Diode probes for spatiotemporal optical control of multiple neurons in freely moving animals. *Journal of Neurophysiology*, 108(1):349–363.

Stark, E., Roux, L., Eichler, R., Senzai, Y., Royer, S., and Buzsáki, G. (2014). Pyramidal cell-interneuron interactions underlie hippocampal ripple oscillations. *Neuron*, 83(2):467–480.

Stewart, M., Quirk, G., Barry, M., and Fox, S. (1992). Firing relations of medial entorhinal neurons to the hippocampal theta rhythm in urethane anesthetized and walking rats. *Experimental Brain Research*, 90(1):21–28.

Stujenske, J. M., Spellman, T., and Gordon, J. A. (2015). Modeling the spatiotemporal dynamics of light and heat propagation for in vivo optogenetics. *Cell Reports*, 12(3):525–534.

Südhof, T. C. (1995). The synaptic vesicle cycle: a cascade of protein–protein interactions. *Nature*, 375(6533):645–653.

Sun, Q., Sotayo, A., Cazzulino, A. S., Snyder, A. M., Denny, C. A., and Siegelbaum, S. A. (2017). Proximodistal heterogeneity of hippocampal CA3 pyramidal neuron intrinsic properties, connectivity, and reactivation during memory recall. *Neuron*, 95(3):656–672.

Suzuki, S. S. and Smith, G. K. (1988). Spontaneous eeg spikes in the normal hippocampus ii. relations to synchronous burst discharges. *Electroencephalography and Clinical Neurophysiology*, 69(6):532–540.

Tabarean, I., Conti, B., Behrens, M., Korn, H., and Bartfai, T. (2005). Electrophysiological properties and thermosensitivity of mouse preoptic and anterior hypothalamic neurons in culture. *Neuroscience*, 135(2):433–449.

Takács, V. T., Klausberger, T., Somogyi, P., Freund, T. F., and Gulyás, A. I. (2012). Extrinsic and local glutamatergic inputs of the rat hippocampal CA1 area differentially innervate pyramidal cells and interneurons. *Hippocampus*, 22(6):1379–1391.

Takahashi, H. and Magee, J. C. (2009). Pathway interactions and synaptic plasticity in the dendritic tuft regions of CA1 pyramidal neurons. *Neuron*, 62(1):102–111.

Taub, A. H., Katz, Y., and Lampl, I. (2013). Cortical balance of excitation and inhibition is regulated by the rate of synaptic activity. *Journal of Neuroscience*, 33(36):14359–14368.

Thiel, G., Greengard, P., and Südhof, T. (1991). Characterization of tissue-specific transcription by the human synapsin i gene promoter. *Proceedings of the National Academy of Sciences*, 88(8):3431–3435.

Thompson, C. L., Pathak, S. D., Jeromin, A., Ng, L. L., MacPherson, C. R., Mortrud, M. T., Cusick, A., Riley, Z. L., Sunkin, S. M., Bernard, A., et al. (2008). Genomic anatomy of the hippocampus. *Neuron*, 60(6):1010–1021.

Thompson, L. and Best, P. (1989). Place cells and silent cells in the hippocampus of freely-behaving rats. *Journal of Neuroscience*, 9(7):2382–2390.

Tombaugh, G. C. and Somjen, G. G. (1997). Differential sensitivity to intracellular ph among high-and low-threshold ca2+ currents in isolated rat ca1 neurons. *Journal of Neurophysiology*, 77(2):639–653.

Treves, A. and Rolls, E. T. (1994). Computational analysis of the role of the hippocampus in memory. *Hippocampus*, 4(3):374–391.

Tricoire, L., Pelkey, K. A., Erkkila, B. E., Jeffries, B. W., Yuan, X., and McBain, C. J. (2011). A blueprint for the spatiotemporal origins of mouse hippocampal interneuron diversity. *Journal of Neuroscience*, 31(30):10948–10970.

Trouche, S., Perestenko, P. V., van de Ven, G. M., Bratley, C. T., McNamara, C. G., Campo-Urriza, N., Black, S. L., Reijmers, L. G., and Dupret, D. (2016). Recoding a cocaine-place memory engram to a neutral engram in the hippocampus. *Nature Neuroscience*, 19(4):564.

Tsodyks, M. V., Skaggs, W. E., Sejnowski, T. J., and McNaughton, B. L. (1997). Paradoxical effects of external modulation of inhibitory interneurons. *Journal of Neuroscience*, 17(11):4382–4388.

Tukker, J. J., Fuentealba, P., Hartwich, K., Somogyi, P., and Klausberger, T. (2007). Cell type-specific tuning of hippocampal interneuron firing during gamma oscillations in vivo. *Journal of Neuroscience*, 27(31):8184–8189.

Tyan, L., Chamberland, S., Magnin, E., Camiré, O., Francavilla, R., David, L. S., Deisseroth, K., and Topolnik, L. (2014). Dendritic inhibition provided by interneuron-specific cells controls the firing rate and timing of the hippocampal feedback inhibitory circuitry. *Journal of Neuroscience*, 34(13):4534–4547.

Urban, D. J. and Roth, B. L. (2015). Dreadds (designer receptors exclusively activated by designer drugs): chemogenetic tools with therapeutic utility. *Annual Review of Pharmacology and Toxicology*, 55:399–417.

Van Cauter, T., Poucet, B., and Save, E. (2008). Unstable CA1 place cell representation in rats with entorhinal cortex lesions. *European Journal of Neuroscience*, 27(8):1933–1946.

Vanderwolf, C. H. (1969). Hippocampal electrical activity and voluntary movement in the rat. *Electroencephalography and Clinical Neurophysiology*, 26(4):407–418.

Vogels, T. P., Rajan, K., and Abbott, L. F. (2005). Neural network dynamics. *Annual Review of Neuroscience*, 28:357–376.

Voigts, J., Siegle, J. H., Pritchett, D. L., and Moore, C. I. (2013). The flexdrive: an ultra-light implant for optical control and highly parallel chronic recording of neuronal ensembles in freely moving mice. *Frontiers in Systems Neuroscience*, 7:8.

Watakabe, A., Ohtsuka, M., Kinoshita, M., Takaji, M., Isa, K., Mizukami, H., Ozawa, K., Isa, T., and Yamamori, T. (2015). Comparative analyses of adeno-associated viral vector serotypes 1, 2, 5, 8 and 9 in marmoset, mouse and macaque cerebral cortex. *Neuroscience Research*, 93:144–157.

Wierenga, C. J. and Wadman, W. J. (2003). Excitatory inputs to CA1 interneurons show selective synaptic dynamics. *Journal of Neurophysiology*, 90(2):811–821.

Wietek, J., Beltramo, R., Scanziani, M., Hegemann, P., Oertner, T. G., and Wiegert, J. S. (2015). An improved chloride-conducting channelrhodopsin for light-induced inhibition of neuronal activity in vivo. *Scientific Reports*, 5:14807.

Wilent, W. B. and Nitz, D. A. (2007). Discrete place fields of hippocampal formation interneurons. *Journal of Neurophysiology*, 97(6):4152–4161.

Wilson, M. A. and McNaughton, B. L. (1993). Dynamics of the hippocampal ensemble code for space. *Science*, 261(5124):1055–1058.

Wilson, M. A. and McNaughton, B. L. (1994). Reactivation of hippocampal ensemble memories during sleep. *Science*, 265(5172):676–679.

Witter, M. P. and Amaral, D. G. (2004). Hippocampal formation. In *The rat nervous system*, pages 635–704. Elsevier Inc.

Witter, M. P., Doan, T. P., Jacobsen, B., Nilssen, E. S., and Ohara, S. (2017). Architecture of the entorhinal cortex a review of entorhinal anatomy in rodents with some comparative notes. *Frontiers in Systems Neuroscience*, 11:46.

Witter, M. P., Groenewegen, H., Da Silva, F. L., and Lohman, A. (1989). Functional organization of the extrinsic and intrinsic circuitry of the parahippocampal region. *Progress in Neurobiology*, 33(3):161–253.

Wu, F., Stark, E., Ku, P.-C., Wise, K. D., Buzsáki, G., and Yoon, E. (2015). Monolithically integrated μleds on silicon neural probes for high-resolution optogenetic studies in behaving animals. *Neuron*, 88(6):1136–1148.

Wu, J. and Fisher, R. S. (2000). Hyperthermic spreading depressions in the immature rat hippocampal slice. *Journal of Neurophysiology*, 84(3):1355–1360.

Yamamoto, J. and Tonegawa, S. (2017). Direct medial entorhinal cortex input to hippocampal CA1 is crucial for extended quiet awake replay. *Neuron*, 96(1):217–227.

Yamanashi, T., Maki, M., Kojima, K., Shibukawa, A., Tsukamoto, T., Chowdhury, S., Yamanaka, A., Takagi, S., and Sudo, Y. (2019). Quantitation of the neural silencing activity of anion channelrhodopsins in caenorhabditis elegans and their applicability for long-term illumination. *Scientific Reports*, 9(1):1–11.

Yang, L., Lee, K., Villagracia, J., and Masmanidis, S. C. (2020). Open source silicon microprobes for high throughput neural recording. *Journal of Neural Rngineering*, 17(1):016036.

Zhang, K., Ginzburg, I., McNaughton, B. L., and Sejnowski, T. J. (1998). Interpreting neuronal population activity by reconstruction: unified framework with application to hippocampal place cells. *Journal of Neurophysiology*, 79(2):1017–1044.

Zhang, Y.-P. and Oertner, T. G. (2007). Optical induction of synaptic plasticity using a light-sensitive channel. *Nature Methods*, 4(2):139–141.

Laurel Watkins de Jong

Education

PhD, Psychology,
University of Wisconsin - Milwaukee ..... August 2020
Thesis: *Optogenetic Interrogation of Hippocampal Circuit Stabilization*
Advisor: Dr. Kamran Diba, Department of Anesthesiology (University of Michigan)

MS, Neuroscience, University of Arizona ..... August 2012
Thesis: *An ERP study of the monitoring of primary stop errors and secondary choice errors.*
Advisor: Dr. John Allen, Department of Psychology

BS, Physiology, University of Arizona ..... August 2010

Fellowships and Awards

AGSIP Travel Award (declined) ..... October 2018

Summer Graduate Research Fellowship (SGRF) ($3,218) ..... Summer 2017

UWM Graduate Student Travel Award ($500) ..... September 2012

NSF Graduate Research Fellowship ($132,000) ..... June 2011- May 2014

Science Foundation of Arizona Graduate Research Fellowship ($30,000) . June 2010 - May 2011

UBRP Travel Award to present poster at ASTMH ..... December 2009

Undergraduate Biology Research Program ..... Summer 2008 - May 2010

Publications

K. Maboudi, E. Ackermann, **L. Watkins de Jong**, B. Pfeiffer, D. Foster, K. Diba, C. Kemere. (2018) Uncovering temporal structure in hippocampal output patterns. *eLIFE* 7:e34467.

L. Watkins de Jong, B. Gereke, G.M Martin, J.M. Fellous. (2011) The Traveling Salesrat: Insights into the dynamics of efficient spatial navigation in the rodent. *Journal of Neural Engineering* 8(6): 065010.

V. Corby-Harris, A. Drexler, **L. Watkins de Jong** et. al. (2010) Activation of Akt signaling reduces the prevalence and intensity of malaria parasite infection and lifespan in *Anopheles stephensi* mosquitoes. *PLoS Pathogens* 6(7): e1001003s.

Manuscripts in Preparation

L. Watkins de Jong, K. Diba. Optogenetic probe of inhibition stabilization in hippocampal networks. *In preparation.*

Poster Presentations

L. Watkins de Jong, D. Lyttle, K. Diba. Paradoxical response of hippocampal interneurons in optogenetic perturbation. Poster session presented at: *The International Conference for Advanced Neurotechnology*; May 19-20, 2019; Seoul, KOR

L. Watkins de Jong, D. Lyttle, K. Diba. Paradoxical response of interneurons in both CA3 and CA1 to optogenetic inactivation of CA3. Poster session presented at: *48th Annual Meeting for the Society of Neuroscience*; November 3-7, 2018; San Diego, CA

L. Watkins de Jong, J. J. B. Allen. If I can't stop myself does it matter what I do next?: An ERP study of the monitoring of primary stop errors and secondary choice errors. Poster session presented at: *42nd Annual Meeting for the Society of Neuroscience*; October 13-17, 2012; New Orleans, LA

L. Watkins de Jong, B Gereke, N.S. Corral-Frias, K. Scott, G.M. Martin, J.M. Fellous. The Traveling Salesrat: Learning efficitent spatial navigation. Poster session presented at: *40th Annual Meeting for the Society of Neuroscience*; November 13-17, 2010; San Diego, CA

L. Watkins de Jong, B. Gereke, G.M. Martin, J.M. Fellous. The Traveling Salesrat: Insights into optimal spatial navigation in a rat model. Poster session presented at: *21th Annual Undergraduate Biology Research Conference*; January 23, 2010; Tucson, AZ.

L. Watkins de Jong, G.M. Martin, J.M. Fellous. The Traveling Salesrat: Insights into optimal spatial navigation and the role of the dopaminergic system. Poster session presented at: *39th Annual Meeting for the Society of Neuroscience*; October 17-21, 2009; Chicago, IL.

L. Watkins de Jong, M.A. Riehle. The Aging Mosquito: Increased insulin signaling in the midgut of *An. Stephensi* reduces lifespan. Poster session presented at: *20th Annual Undergraduate Biology Research Conference*; January 23, 2009; Tucson, AZ.

L. Watkins de Jong, M.A. Riehle. The Aging Mosquito: Increased insulin signaling in the midgut of *An. Stephensi* reduces lifespan. Poster session presented at: *57th Annual Meeting of the Society for Tropical Medicine and Hygiene (ASTMH)*; December 7-11, 2008; New Orleans, LA.

Presentations

L. Watkins de Jong. *Paradoxical response of interneurons in both CA3 and CA1 during optogenetic inactivation of CA3.* Talk presented at: *Neural Networks Seminar Series*; November 30, 2018; Ann Arbor, MI.

L. Watkins de Jong. *Optogenetic disruption of CA3 input to CA1 during hippocampal oscillations.* Talk presented at: *Neuroscience Seminar Series*; April 24, 2015; Milwaukee, WI.

L. Watkins de Jong. *The network origins of hippocampal activity patterns: An optogenetic approach.* Talk presented at: *Neuroscience Seminar Series*; January 24, 2014; Milwaukee, WI.

Related Work Experience

Graduate Rotation, University of Arizona ..... January 2011 - June 2011
Principle Investigator: Dr. John Allen, Psychology
Description: Technical rotation to learn EEG data analysis using the software, EEGlab. Simple analysis was performed on a group of 40 participants in a No/No-Go flanker task to assess the biomarkers (measured event-related potentials) following a incorrect 'No-Go' response.

Graduate Rotation, University of Arizona ..... August 2010 - December 2010
Principle Investigator: Dr. Kevin Lin, Mathematics
Description: Studied a broad range of dynamical systems applications in neuroscience focusing primarily on cases of coupled oscillating systems.

Undergraduate Research Assistant, University of Arizona .. Jan 2009 - May 2010
Principle Investigator: Dr. Jean-Marc Fellous, Psychology and Applied Mathematics
Description: Designed and implemented a rat model with the goal of understanding the relationship between reward centers and spatial navigation in decision-making processes.

Undergraduate Research Assistant University of Arizona May 2007 - January 2009
Principle Investigator: Dr. Michael Riehle, Entomology
Description: Designed a line of transgenic mosquitoes with over-activated insulin signaling in order to understand the role of blood metabolism and the related insulin signaling pathway in lifespan and fecundity.

Special Coursework

CAMP: Computational Approaches to Memory and Plasticity .... June 2014
Location: National Center for Biological Sciences, Bangalore, India
Description: 16-day summer school on the theory and simulation of learning, memory and plasticity in the brain.

Teaching Experience

MINT Workshop, University of Michigan ..... May, 2018-2019
Course: Optogenetic Experimentation Using a μLED Optoelectrode
Role: Assisted in the organization and teaching of a workshop designed to train participants in 1) optoelectrode preparation for chronic surgery (designing and using microdrives) and 2) hands-on surgical experience using a chronic μLED array with simultaneous multi-channel stimulation and recording.

Teaching Assistant, University of Wisconsin - Milwaukee ..... Spring 2015
Course: Psychological Statistics
Role: Ran three sections of a weekly discussion expanding on topics covered in the lecture and lab using the software SPSS. Curriculum, including worksheets for the discussion were designed weekly by me.

Teaching Assistant, University of Wisconsin - Milwaukee ..... Fall 2014

Course: Physiological Psychology
Role: Ran five sections of a weekly discussion expanding on topics covered in the lecture. The discussion included an end of the semester debate, designed and ran by me.

Teaching Assistant, University of Arizona ..... Spring 2012
Course: Introduction to Statistical Methods
Description: In Introduction to Statistical Methods, we shall be using your background in biology, economics, or engineering and your previous knowledge of calculus and differential equations to consider the issues of collection, model derivation and analysis, interpretation, explanation, and presentation of data.

Professional Affiliations

International Brain Research Organization 2015

Society of Neuroscience ..... 2009 - present

Technical Skills

Experimental Skill Set

Rodent training, hyperdrive construction, optrode construction, optogenetic techniques, rodent surgery/implantation, electrophysiological recording, spike cutting, analysis of spike trains, spectral analysis of EEG signal, PCR, western blots, immunocytochemistry

Computational Skill Set

Languages: Arduino, MATLAB, NEURON, PYTHON, R
Coursework: dynamical systems, mathematical modeling, probability, statistics, quantitative analysis of biological systems, fourier analysis, linear algebra, calculus